2011

The Effect of Ankle Joint Rotational Stiffness and Localized Muscle Fatigue on Tibial Response During Impact

Nikki Nolte
University of Windsor

THE EFFECT OF ANKLE JOINT ROTATIONAL STIFFNESS AND LOCALIZED MUSCLE FATIGUE ON TIBIAL RESPONSE DURING IMPACT

by

Nikki L. Nolte

A Thesis
Submitted to the Faculty of Graduate Studies
through the Faculty of Human Kinetics
in Partial Fulfillment of the Requirements for
the Degree of Master of Human Kinetics at the
University of Windsor

Windsor, Ontario, Canada

2010

AUTHOR'S DECLARATION OF ORIGINALITY

I hereby certify that I am the sole author of this thesis and that no part of this thesis has been published or submitted for publication.

I certify that, to the best of my knowledge, my thesis does not infringe upon anyone's copyright nor violate any proprietary rights and that any ideas, techniques, quotations, or any other material from the work of other people included in my thesis, published or otherwise, are fully acknowledged in accordance with the standard referencing practices. Furthermore, to the extent that I have included copyrighted material that surpasses the bounds of fair dealing within the meaning of the Canada Copyright Act, I certify that I have obtained a written permission from the copyright owner(s) to include such material(s) in my thesis and have included copies of such copyright clearances to my appendix.

I declare that this is a true copy of my thesis, including any final revisions, as approved by my thesis committee and the Graduate Studies office, and that this thesis has not been submitted for a higher degree to any other University or Institution.

ABSTRACT

The purpose of this study was to investigate the relationship between ankle joint rotational stiffness (AJRS) and localized muscle fatigue on tibial response parameters (TRPs): peak acceleration (PA), time to peak acceleration (TPA), and acceleration slope (AS). The right leg of 15 male and 11 female runners was impacted using a human pendulum apparatus in both non-fatigue and fatigue conditions across a range of ankle angles (0%, 20%, 40%, and 60% of maximum dorsiflexion angle). No differences in TRPs were found between non-fatigue and fatigue conditions, or between sexes. Overall, a positive relationship was found between AJRS and PA, as well as AJRS and AS, while a negative relationship existed between AJRS and TPA. It is proposed that an optimal amount of AJRS is needed when regulating the transmission of impact shock as a tradeoff between optimizing joint stability and possibly preventing injury resulting from impact.

ACKNOWLEDGEMENTS

Firstly, I would like to thank my advisor, Dr. David Andrews, for your guidance and support. Your ability to relate on a personal level and your incredibly helpful attitude are very much appreciated. Thank you for allowing me to take on a project that would satisfy my curiosity (and obsession) with running. I give my most sincere gratitude for accommodating my many other pursuits and interests during the course of my studies. The lessons and skills that I have learned extend far beyond the walls of HK.

Thank you to my committee members, Dr. Altenhof and Dr. Marino, for your involvement in this project. Your constructive criticism and suggestions have helped me produce something of which I am truly proud.

I would like to thank Professor Joel Cort for adapting your joint rotational stiffness (JRS) model for my study and your assistance with the facilitation of my data processing. Thank you for sharing your valuable time on this project.

Thank you to Don Clarke for your technical expertise, time, and willingness to help.

My sincere appreciation goes to Robyn Bertram for your unbelievable energy during data collection. Your positive attitude and desire to learn is inspiring.

Thank you to my lab mates, past and present, for your leadership, feedback and moral support.

Thank you to those who were always watching out for me over the years and offered kind words of encouragement when the going got tough. Kathy Harvie , Kenji Kenno, Wayne Marino, and Dennis Fairall, your belief in me when I needed it most is what will always make me remember Windsor as my home.

To my family and friends, thank you for always encouraging me to do my best and to pursue my dreams.

And finally to Nathan, your love and unconditional support is what helped me see this through to the end. I cannot thank you enough.

TABLE OF CONTENTS

AUTHOR'S DECLARATION OF ORIGINALITY iii
ABSTRACT iv
ACKNOWLEDGEMENTS v
LIST OF TABLES x
LIST OF FIGURES xi
LIST OF APPENDICES xv
GLOSSARY xvi
LIST OF ABBREVIATIONS xviii
CHAPTER I 1
INTRODUCTION 1
1.1 Statement of Purpose 7
1.2 Statement of Hypotheses 7
CHAPTER II 9
LITERATURE REVIEW 9
2.1 Impact Forces During Running 9
2.2 Impact Force Frequency Domain Considerations 12
2.3 Leg Properties Affecting Force Transmission 14
2.3.1 Cartilage and Bone 15
2.3.2 Heel Pad 16
2.3.3 Wobbling Mass 16
2.4 Mechanisms Affecting Force Transmission 18
2.4.1 Knee Angle 18
2.4.2 Ankle Angle 19
2.4.3 Muscle Tuning 19
2.5 Stiffness and Running 20
2.5.1 Defining Stiffness 20
2.5.2 Stiffness vs. Stability 21
2.5.3 Calculating Stiffness 22
2.5.4 Joint Rotational Stiffness 25
2.5.5 Passive Muscle Stiffness 26
2.5.6 Passive Joint Stiffness 27

2.5.7 Muscle Stiffness, Injury, and Performance 27
2.6 Fatigue 28
2.6.1 Whole Body Fatigue 29
2.6.2 Localized Muscle Fatigue 30
2.7 The Human Pendulum 32
2.7.1 Leg Geometry at Impact 33
2.7.2 Impact Intensity 33
2.7.3 Validity of the Human Pendulum Method 34
2.7.4 Limitations of the Human Pendulum Method 35
2.8 Instrumentation 36
2.8.1 Measuring Shank Acceleration 36
2.8.2 Electromyography (EMG) 37
2.9 Sex Differences 38
2.9.1 Stiffness 38
2.9.2 Fatigue 39
2.10 Joint Rotational Stiffness Model 40
2.11 Summary: Literature Review 41
CHAPTER III 43
METHODOLOGY 43
3.1 Participants 43
3.2 Experimental Equipment 44
3.2.1 Human Pendulum 44
3.2.2 Force Plate 45
3.2.3 Velocity Transducer 46
3.2.4 Accelerometer 47
3.2.5 Electrogoniometers 47
3.2.6 Electromyography (EMG) 48
3.3 Data Acquisition 49
3.4 Procedure 50
3.4.1 Measuring Maximum Voluntary Exertion (MVE) 52
3.4.2 Electrogoniometer and Accelerometer Setup 55
3.4.3 Impacts 56

3.4.4 Local Muscle Fatigue 57
3.5 Data Analysis 59
3.6 Study Design 67
3.7 Statistical Analysis 68
CHAPTER IV 70
RESULTS 70
4.1 Participant Details 70
4.2 Impact Parameters 70
4.3 Tibial Response 72
4.3.1 Peak Acceleration (PA) 72
4.3.2 Time to Peak Acceleration (TPA) 73
4.3.3 Acceleration Slope (AS) 73
4.4 Fatigue 74
4.4.1 Time to Fatigue and Mean Power Frequency 74
4.5 Electromyography (EMG) 74
4.5.1 Main Effect of Sex 75
4.5.2 Main Effect of Time Period 76
4.5.3 Main Effect of Fatigue 77
4.5.4 Main Effect of Ankle Angle at Impact 77
4.6 Individual Muscles' Contribution to Joint Rotational Stiffness (MJRS) 78
4.6.1 Main Effect of Sex 80
4.6.2 Main Effect of Fatigue 80
4.6.3 Time Period-Ankle Angle Interaction for Tibialis Anterior 80
4.7 Ankle Joint Rotational Stiffness (AJRS) 81
4.7.1 AJRS-Tibial Response Parameter Relationship 84
CHAPTER V 86
DISCUSSION 86
5.1 Participant Details 86
5.2 Impact Parameters 86
5.3 Tibial Response Parameters (TRPs) 87
5.3.1 Peak Acceleration (PA) 88
5.3.2 Time to Peak Acceleration (TPA) 89

5.3.3 Acceleration Slope (AS) ... 90
5.4 Fatigue ... 90
5.4.1 Time to Fatigue and Mean Power Frequency ... 90
5.4.2 Tibial Response to Fatigue ... 91
5.5 Electromyography (EMG) ... 93
5.5.1 Main Effect of Sex ... 93
5.5.2 Main Effect of Time Period ... 94
5.5.3 Main Effect of Fatigue ... 94
5.5.4 Main Effect of Ankle Angle at Impact ... 95
5.6 Individual Muscles' Contribution to Joint Rotational Stiffness (MJRS) ... 95
5.6.1 Main Effect of Sex ... 95
5.6.2 Main Effect of Fatigue ... 95
5.6.3 Time Period-Ankle Angle Interaction for Tibialis Anterior ... 96
5.7 Ankle Joint Rotational Stiffness (AJRS) ... 96
5.7.1 AJRS-Tibial Response Parameter Relationship ... 98
5.8 Functional Significance and Application ... 99
5.9 Limitations and Future Directions ... 100
CHAPTER VI ... 104
CONCLUSIONS ... 104
REFERENCES ... 105
APPENDICES ... 117
APPENDIX A ... 118
APPENDIX B ... 119
APPENDIX C ... 122
VITA AUCTORIS ... 123

LIST OF TABLES

Table 1. Filtering specifications used during analysis. 59

Table 2. Study design consists of one between-participant variable (sex: female/male) and two within- participant variables (fatigue: non-fatigue/fatigue and dorsiflexion angle: 0%, 20%, 40%, and 60% of maximum dorsiflexion angle (MDA)). 68

Table 3. Relationship classification based on correlation coefficient magnitude (effect size). (Cohen, 1988). 69

Table 4. Mean (SD) participant details (n = 26). * p < 0.05 70

Table 5. Mean (SD) values for TTF and MPF (n = 25). 74

Table 6. Correlation coefficients and coefficients of determination between peak acceleration (PA) and ankle joint rotational stiffness (AJRS) collapsed across a range of 0% to 60% of maximum dorsiflexion angle (n = 26). * p < 0.05 84

Table 7. Correlation coefficient and coefficients of determination between time to peak acceleration (TPA) and ankle joint rotational stiffness (AJRS) collapsed across a range of 0% to 60% of maximum dorsiflexion angle (n = 26). * p < 0.05.. 85

Table 8. Correlation coefficients and coefficients of determination between acceleration slope (AS) and ankle joint rotational stiffness (AJRS) collapsed across a range of 0% to 60% of maximum dorsiflexion angle (n = 26). * p < 0.05 85

Table 9. Comparison of the means (SD) of the tibial response parameters in the current study with previously reported results. † = Use of time instead of amplitude to calculate acceleration slope. 88

LIST OF FIGURES

Figure 1: Typical ground reaction force curve for heel-toe running (Modified from Cavanagh & Lafortune, 1980) ... 10

Figure 2: Tibial response parameters of the acceleration-time graph. Leg accelerations can be described in terms of the peak acceleration (PA), time to peak acceleration (TPA), and acceleration slope (AS). (From Holmes and Andrews, 2006) ... 12

Figure 3: The three-linked model with wobbling mass. The wobbling mass has been modeled as being attached to the skeletal frame via damped elastic connections, where 'r' is the radius of the axis of rotation, 'φ' is the joint angle, and 'F_G' is the ground reaction force. (From Gruber et al., 1998) ... 17

Figure 4: The whole leg is often represented as a spring supporting the body's mass (m), allowing for the vertical stiffness of the whole leg (k) to be calculated at ground contact when the leg is oriented vertically. Vertical stiffness of the whole leg can be calculated by dividing maximum vertical force by the maximum vertical displacement of the body's centre of mass ($F_{max}/\Delta y$). (Adapted from Butler et al., 2003) ... 23

Figure 5: Model for calculating lower leg stiffness when impacting the ground in a non-vertical position. Using the mass-spring system, leg length (L_O) and landing angle (Θ_O) allows for calculation of lower leg stiffness using the vertical displacement of the body's centre of mass (Δy). (From Butler et al., 2003) ... 24

Figure 6: Sagittal plane ankle joint stiffness. Torsional stiffness (K_{tors}) is calculated as the slope of the line through the moment-angle curve from the point of maximum knee flexion to maximum knee extension moment. (From Butler et al., 2003) ... 25

Figure 7. The human pendulum apparatus. Isolated heel impacts can be delivered at similar magnitudes and velocities as those in running. (From Lafortune & Lake, 1995) ... 33

Figure 8. Comparison of a ground reaction force (GRF) achieved during running with a wall reaction force curve achieved during a human pendulum impact. Participant mean wall reaction force curve (solid line) is compared with a typical GRF curve (dotted line). (Lafortune & Lake, 1995) ... 35

Figure 9. Superficial musculature of the shank contributing to ankle joint rotational stiffness ... 38

Figure 10. (a) Human pendulum apparatus in its rest position, suspended from the ceiling, (b) Participant instrumented in human pendulum. The participant's orientation represents the 0% maximum dorsiflexion angle of the ankle joint (see Section 3.4.2) ... 45

Figure 11. Steel grid incorporated into the building's wall to which the force plate was vertically mounted ... 46

Figure 12: Electrogoniometer and accelerometer placement. Two electrogoniometers, one on the medial side at the knee joint and the other on the lateral side at the ankle joint, were applied to monitor joint angles. An accelerometer was attached to the medial aspect of the tibial tuberosity. The Velcro® strap used to preload the accelerometer is not seen in the diagram. 48

Figure 13: Electromyography (EMG) electrode placement. Electrodes were placed on the following muscles: tibialis anterior (TA), fibularis longus (FL), lateral gastrocnemius (LG), medial gastrocnemius (MG), and soleus (SOL). Figure 13a, b and c depict anterior, lateral, and posterior views, respectively. 49

Figure 14. Flow diagram illustrating the experimental protocol. Abbreviations from the diagram are as follows: research ethics board (REB), general health questionnaire (GHQ), maximum voluntary exertion (MVE), lateral gastrocnemius (LG), medial gastrocnemius (MG), soleus (SOL), fibularis longus (FL), tibialis anterior (TA), range of motion (ROM), and maximum dorsiflexion angle (MDA)... 51

Figure 15: Maximum voluntary exertion (MVE) of the triceps surae group (lateral gastrocnemius (LG), medial gastrocnemius (MG), and soleus (SOL)) was taken by having the participant maximally plantarflex by performing a standing calf raise against padded shoulder straps.......... 53

Figure 16: The maximum voluntary exertion (MVE) of the fibularis longus (FL) was taken with the participant lying supine on the human pendulum apparatus. Manual resistance was provided by the investigator to prevent eversion and plantarflexion. 54

Figure 17. The maximum voluntary exertion (MVE) of the tibialis anterior (TA) was taken against unilateral manual resistance, whereby the foot was allowed to move against the resistance provided by the investigator.. 55

Figure 18. The target ankle angle was displayed on a computer monitor in the participants' field of view during each trial and was monitored throughout the impact. Participants were required to maintain 0%, 20%, 40%, and 60% of their maximum dorsiflexion by aligning the arrows represented on the computer monitor... 56

Figure 19. The fatigue apparatus, which consisted of a resistive rubber band with a hook at each end, was attached to the steel grid. Local muscle fatigue (LMF) of the tibialis anterior (TA) was achieved through isometric dorsiflexion against the rubber band.. 58

Figure 20. Free body diagram of the foot, oriented as the participant is lying on the pendulum in the supine position. Forces other than joint reaction forces on the leg (F_{Ax}, F_{Ay}) are not included, as the leg is assumed not to move. Coordinates for the knee joint centre (KJC), ankle joint centre (AJC), and toe (TTIP) were determined by digitization, while the centre of mass (COM) and radius of gyration were calculated using de Leva's (1996) segment parameters. The force applied by the perturbation (F_{app}) and the combined forces of the muscles crossing the ankle joint (F_{muscle}) contribute to the moment about the ankle (Mo_{Ankle}), which represent both the joint reaction moment and the EMG-derived moment, after the perturbation. 61

Figure 21. Flow diagram illustrating the model from which ankle joint rotational stiffness (AJRS) was obtained. Abbreviations from the diagram are as follows: physiological cross-sectional area (PCSA), moment arm (MA), muscle length (ℓ_{musc}), EMG-driven moment (Mo_{EMG}), joint reaction moment (Mo_{JtRxn}), electromechanical delay (EMD), ankle joint centre (AJC), knee joint centre (KJC), centre of mass (COM), distance from ankle to COM (d), distance from ankle to radius of gyration (r), joint rotational stiffness (JRS), and individual muscle JRS (MJRS). (Adapted from Cort & Potvin, 2008) 62

Figure 22. A typical trial of where the EMG-based moment (Mo_{EMG}) was matched to the joint reaction moment (Mo_{JtRxn}) curve using gain factors for both magnitude and in time. An average gain factor for each participant was used to match the magnitude of the two curves, while an individual gain factor was used to match the temporal aspect of the two curves. Baseline (BL), pre-impact (PRE) and post-impact (POST) time periods are labeled. 65

Figure 23. Mean (SD) ankle angle as a function of targeted dorsiflexion angle (% of maximum dorsiflexion angle). Mean ankle angles at all target angles were found to be significantly different from one another (n = 26). * $p < 0.05$ 71

Figure 24. Mean (SD) peak acceleration as a function of targeted dorsiflexion angle (% of maximum dorsiflexion angle) (n = 26). * $p < 0.05$ 73

Figure 25. Main effect of sex for EMG (n = 26). * $p < 0.05$ 75

Figure 26. Main effect of time period for EMG. Average EMG was measured for each muscle at baseline (BL), pre-impact (PRE), and post-impact (POST) intervals (n = 26). * $p < 0.05$........ 76

Figure 27. Main effect of fatigue for EMG. Average EMG was measured for each muscle in the non-fatigue (NF) and fatigue (F) conditions (n = 26). * $p < 0.05$ 77

Figure 28. Main effect of ankle angle for EMG. Average EMG was measured for each muscle at 0%, 20%, 40%, and 60% of maximum dorsiflexion angle (n = 26). * $p < 0.05$ 78

Figure 29. Changes in muscle joint rotational stiffness (MJRS) and ankle joint rotational stiffness (AJRS) with time. Note that the FL and LG appear very close together in the figure, but are distinguished by a thin solid line and a large dashed line. Baseline (BL), pre-impact (PRE) and post-impact (POST) time periods are labeled. 79

Figure 30. Main effect of fatigue for MJRS. Average MJRS was measured for each muscle in the non-fatigue (NF) and fatigue (F) conditions (n = 26). * $p < 0.05$ 80

Figure 31. MJRS interaction between time period and ankle angle for the tibialis anterior (TA). Average MJRS was measured for all muscles at baseline (BL), pre-impact (PRE), and post-impact (POST) intervals across 0%, 20%, 40%, and 60% of maximum dorsiflexion angle (MDA). All comparisons are significantly different ($p < 0.05$) except for the following % of maximum dorsiflexion pairs: 0% MDA BL/POST and 20% MDA POST/PRE (n = 26). 81

Figure 32. Main effect of sex for ankle joint rotational stiffness (AJRS) (n = 26). * $p < 0.05$ 82

Figure 33. Main effect of time period for ankle joint rotational stiffness (AJRS). AJRS was measured at baseline (BL), pre-impact (PRE), and post-impact (POST) intervals (n = 26). * p < 0.05 83

Figure 34. Main effect of fatigue for ankle joint rotational stiffness (AJRS). AJRS was measured in the non-fatigue (NF) and fatigue (F) conditions (n = 26). * p < 0.05 83

LIST OF APPENDICES

Appendix A: General Health Questionnaire (GHQ)...118

Appendix B: Consent to Participate in Research…..…………………………………...…119

Appendix C: Ethics Approval…………………………..……………………………….122

GLOSSARY

Acceleration slope (AS): the linear portion of the acceleration waveform, typically measured as 30%-70% of the rise in amplitude or time (units = g/s) between impact initiation and peak acceleration

Ankle joint rotational stiffness (AJRS): the ability of the muscles crossing the ankle joint to aid in maintaining ankle stability following a perturbation (units = Nm/rad)

Dorsiflexion: flexion at the ankle, whereby the toes move up towards the head

Eversion: movement of the foot whereby the bottom of the foot faces outwards

Extensor digitorum longus (EDL): deep muscle located within the anterior compartment of the shank; a dorsiflexor of the foot

Extensor hallucis longus (EHL): deep muscle located within the anterior compartment of the shank; a dorsiflexor of the foot

Fibularis longus (FL): superficial muscle on the lateral aspect of the shank; plantarflexor and evertor

Isometric: the contraction of a muscle that creates force without a change in joint angle or muscle length

Kinematics: the description of motion through examination of the position of body segments and joints, without regards to the cause of motion

Kinetics: the study of the causes and the loads that lead to motion

Lateral gastrocnemius (LG): largest and most superficial muscle within the posterior compartment of the shank; primary plantarflexor of the foot

Maximum dorsiflexion angle (MDA): the maximum angle that a participant can voluntarily achieve in dorsiflexion

Maximum voluntary exertion (MVE): the result of a maximum isometric contraction produced by a muscle

Mean ankle joint rotational stiffness (mAJRS): the mean (average) value of the time-varying AJRS curve, to be taken during the impact phases (pre-impact, at impact, and post-impact)

Mean power frequency (MPF): the mean (average) frequency of the power density spectrum (which describes how the power of a signal or time series is distributed with respect to frequency)

Medial gastrocnemius (MG): superficial muscle within the posterior compartment of the shank; primary plantarflexor of the foot

Muscle tuning: an alteration in the activation level of a muscle employed to minimize soft tissue vibrations

Peak acceleration (PA): the maximum value or point within the acceleration waveform (units = g)

Peak ankle joint rotational stiffness (pAJRS): the maximum value or point within the time-varying AJRS curve

Peak impact force: the highest peak force, within 50 ms after impact

Plantarflexion: flexion at the ankle, whereby the toes point toward the ground

Shock: the transient condition that occurs following a sudden change in force application, causing the disruption of a system's equilibrium

Shock wave: a stress wave through a medium

Soleus (SOL): superficial muscle within the posterior compartment of the shank acting as the primary plantarflexor; located deep and extending distal to the LG

Tibia: the 'shin bone'; the large medial, weight-bearing long bone of the leg

Tibialis anterior (TA): superficial muscle located within the anterior compartment of the shank; primary dorsiflexor of the foot

Time to peak acceleration (TPA): the time between the onset of the acceleration waveform and the peak acceleration (units = ms)

Recreational runner: participants who engage in running a weekly mileage in the range of 20-50 km

LIST OF ABBREVIATIONS

ℓ_{musc}: Muscle length

AJRS: Ankle joint rotational stiffness

AS: Acceleration slope

ATP: Adenosine triphosphate

BW: Body weight

COM: Centre of mass

EDL: Extensor digitorum longus

EHL: Extensor hallucis longus

EMD: Electromechanical delay

EMG: Electromyography

EVA: Ethylene and vinyl acetate

FL: Fibularis longus

GHQ: General health questionnaire

GRF: Ground reaction force

iEMG: Integrated electromyogram

JRS: Joint rotational stiffness

LG: Lateral gastrocnemius

LMF: Local muscle fatigue

MA: Moment arm

MG: Medial gastrocnemius

mAJRS: Mean ankle joint rotational stiffness

Mo_{EMG}: EMG-based moment

Mo_{JtRxn}: Joint reaction moment

MDA: Maximum dorsiflexion angle

MPF: Mean power frequency

MVE: Maximum voluntary exertion

PA: Peak acceleration

pAJRS: Peak ankle joint rotational stiffness

PCSA: Physiological cross-sectional area

PEC: Parallel elastic component

$PETCO_2$: End tidal carbon dioxide pressure

REB: Research Ethics Board

ROM: Range of motion

sEMG: Surface electromyogram

SOL: Soleus

TA: Tibialis anterior

TPA: Time to peak acceleration

TRP: Tibial response parameter

TTF: Time to fatigue

vGRF: Vertical ground reaction force

WBF: Whole body fatigue

CHAPTER I

INTRODUCTION

Running and jogging are popular forms of exercise characterized by relatively easy access for most people and few equipment requirements. The jogging boom of the 1970s introduced this new form of exercise to North America. According to Bowerman and Harris (1967), "jogging is a graduated program of moderate exercise which can be adapted to men and women of varying ages and levels of fitness" (p. 5). However, with the imposed stress to the body, the potential for injury is inevitable for some runners. Running injuries typically result from overuse, or they are attributed to training and biomechanical variables such as vertical force impact peak, maximal vertical loading rate, and increased maximal rates of rearfoot pronation and touchdown supination angles (Hreljac, Marshall & Hume, 2000). Typical running injuries are stress fractures, medial tibial stress syndrome (shin splints), chondromalacia patellae (runner's knee), plantar fasciitis, and Achilles tendinitis (Hreljac et al, 2000).

In running, the foot collides with the ground and a ground reaction force (GRF) is produced (Cavanagh & Lafortune, 1980). This GRF has an impact peak occurring within 50 ms (Cavanagh & Lafortune, 1980) and is transmitted as a shock wave that is dissipated through the human musculoskeletal system. These repetitive forces must be dissipated by the body in order to limit shock levels to the head (Hamill, Derrick & Holt, 1995). Shock dissipation is defined as the process of absorbing impact energy which results in the reduction of impact energy between the foot and head. Research has proposed that the intensity of impact and/or repetitive loading resulting from running constitute injury mechanisms (Buckwalter & Lane, 1997; Cole, Nigg, Fick & Morlock, 1995). However, it has been proposed that runners are no more at risk for degenerative joint disease than non-runners (Cole, Nigg, van den Bogert & Gerritsen, 1996), nor is impact peak associated with a higher incidence of running injury (Nigg, 1997).

The human musculoskeletal system consists of anatomical structures that passively aid in shock dissipation, including cartilage (Chu, Yazdani-Ardakani, Gradisar & Askew, 1986), bone (Radin, Paul & Lowy, 1970), the heel pad (Whittle, 1999) and the wobbling mass (Gruber, Denoth, Stuessi & Ruder, 1987). The wobbling mass is described as the non-rigid soft tissues of the human body, including muscles, fat, skin, internal organs and body fluids (Gruber et al., 1987; Gruber, Ruder, Denoth & Schneider, 1998), which move (translate and rotate) relative to the rigid skeleton.

In addition to passive shock attenuation, the body engages in active measures to dissipate shock waves. Muscles become stiffer as a result of increased muscle tension caused by an increase in muscle activation (Winter, 2005). Muscle tuning, described as an alteration in the activation level of a muscle in response to impact, is proposed to be employed in running situations to minimize soft tissue vibrations experienced after impact (Wakeling, Liphardt & Nigg, 2003; Wakeling & Nigg, 2001b; Wakeling, von Tscharner, Nigg & Stergiou, 2001). Changes in muscle activation can be monitored by electromyography (EMG) and the resulting changes in soft tissue vibrations can be measured by accelerometers placed over soft tissues (Wakeling & Nigg, 2001a, b).

Kinematic adaptations have been shown to alter the transmission of the shock waves through the body. Increases in knee and ankle angles alter the effective mass of the lower limb segments, and in turn, lower peak impact forces (Derrick, 2004; Gerritsen, van den Bogert & Nigg, 1995). In addition, the altered geometry of the body, by way of increased knee flexion, will decrease the effective stiffness of the body and therefore reduce peak impact forces (Derrick, 2004; McMahon, Valiant & Frederick, 1987). Conversely, increased stiffness has been proposed to improve performance by maximizing the use of the stretch-shortening cycle (Kubo, Kanehisa, Kawakami & Fukunaga, 2000). However, it is thought that an optimal level of stiffness may balance performance enhancement with the injury potential of exposing the body to increased peak impact forces (McMahon & Cheng, 1990).

Most researchers attribute sex differences in stiffness to anthropometrics, with increased stiffness in males being due to their increased muscle volume and mass. However, researchers have found that male musculature may be more effective at resisting changes in its length, and may therefore potentially result in greater joint stability (Blackburn, Padua, Weinhold & Guxkiewicz, 2006; Granata, Padua & Wilson, 2002). Sex differences are also proposed to be significant when investigating the effect of fatigue, as males have been shown to fatigue faster than females due to the increased metabolic demands of exerting additional force (Kent-Braun, Ng, Doyle & Towse, 2002). It is thought that fatigue could in turn reduce the stiffness levels of the individual muscles that contribute to rotational stiffness of the ankle joint, which is a reflection of how much the ankle angle changes in response to an applied moment.

Because of the link between leg stiffness and mechanical behaviour of the lower extremity (McMahon et al., 1987), it is speculated that the stiffness properties of the leg system may become altered as the system fatigues. Fatigue has been proposed to be a predecessor to running injuries due to its effect on running mechanics (Derrick, Dereu & Mclean, 2002) and shock absorbing capabilities of muscle (Mizrahi, Verbitsky & Isakov, 2000a; Voloshin, Mizrahi, Verbitsky & Isakov, 1998). In order to investigate the attenuation characteristics of individual fatigued muscles, Christina, White and Gilchrist (2001) examined how local muscle fatigue (LMF) affected the transmission of impact shock. Using a treadmill running protocol to induce fatigue, it was found that loading rate of peak force significantly increased, yet the peak magnitude of the impact force remained unchanged. A treadmill running protocol lacks control over the impacting conditions, as participants have been found to make kinematic adaptations in running mechanics in order to maintain impact shock below a tolerable threshold (Hamill et al., 1995). In order to specifically examine the effect of impact shocks on locally fatigued muscles, kinematic variables must be held constant; a feat not possible during treadmill running protocols.

The human pendulum method (Lafortune & Lake, 1995) has been shown to deliver controlled impacts to the heel, such as those seen in heel-toe running. Using the human pendulum, LMF has been found to decrease impact transmission and cause a decrease in acceleration slope (AS) and peak acceleration (PA) after impact (Flynn, Holmes & Andrews, 2006; Duquette & Andrews, 2010a). This is in opposition to the study by Christina et al. (2001), where impact conditions were not controlled.

Holmes and Andrews (2006) investigated the tibial response parameters (TRPs) of PA, AS, and time to peak acceleration (TPA) while voluntarily manipulating muscle activation level by varying the amount of dorsiflexion at the ankle when the heel impacted the force plate. It was found that with LMF of the leg muscles, decreased impact transmission could be seen through a decrease in AS and PA, and an increase in TPA. This is suggested to be a protective mechanism against impact shock when the muscle is in a fatigued state. The increased muscle activation through dorsiflexion is thought to increase ankle joint stiffness, as the prime dorsiflexion muscle (tibialis anterior) crosses the ankle joint. Using a LMF protocol, Kellis and Liassou (2009) suggested that during fatigue, the body compensates by altering joint movement to protect the knee (through increased flexion) and ankle (through decreased dorsiflexion) at initial impact.

In 2010a, Duquette and Andrews controlled for dorsiflexion angle during impact, and again found that LMF reduced the transmission of impact forces. This suggests that the muscles of the lower extremity and ankle joint may become less stiff when the muscles are fatigued, thereby increasing impact attenuation capability. Whether this is a function of changes in the rotational stiffness of the ankle joint or of the stiffness of the wobbling mass of the shank, has yet to be determined.

Cort and Potvin (2008) modeled the individual muscle contributions to joint rotational stiffness (JRS) at the knee in response to a perturbation. Using this same approach at the ankle, the contribution of individual muscles to JRS (MJRS) will lead to a total JRS value at the ankle (AJRS). The importance of this model lies in its ability to quantify JRS, not only in a static state prior to perturbation, but also dynamically during the kinematic disturbance as well. A potentially significant relationship between AJRS and tibial acceleration parameters (PA, AS, and TPA) could possibly explain whether the degree of ankle joint stiffness (also referred to as its ‘robustness’) alters impact acceleration transmission prior to and after LMF. These findings may have practical relevance to the kinematic adaptations that runners make in response to a change in surface stiffness (Boyer & Nigg, 2006; Ferris, Liang & Farley, 1999), shod versus unshod conditions (Clarke, Frederick & Cooper, 1983), or alteration in stride frequency (Ferris & Farley, 1997).

Knowing individual muscle contributions to AJRS may highlight protective and/or compensatory mechanisms in which the human body engages to maintain safe accelerations to the body when impacted in a fatigued state. Since fatigue results in a reduction of a muscle's force generating capabilities (Kent-Braun et al., 2002), it is thought that fatigue will in turn reduce the stiffness levels of the individual muscles that contribute to AJRS; this will possibly occur at varying rates, due to the different sizes and fibre type composition of the contributing muscles. The varying rates of fatigue could result in altered kinematic adjustments by the body, which may change the impact acceleration transmission through the body, such as that described previously by Lafortune, Hennig, and Lake (1996a), Lafortune, Lake, and Hennig (1996b), McMahon et al. (1987), and Milliron and Cavanagh (1990). Identifying the stabilizing potential of individual ankle muscles could then prove useful in injury prevention and rehabilitation, as strengthening treatments and training protocols could be applied to targeted muscles.

1.1 Statement of Purpose

The purpose of this study is fourfold:

i) To determine the relationship between ankle joint rotational stiffness (AJRS) and the tibial response parameters (TRPs) of peak acceleration (PA), time to peak acceleration (TPA), and acceleration slope (AS) across a range of ankle dorsiflexion angles.

ii) To determine the effect of tibialis anterior (TA) fatigue on the relationship of AJRS and the TRPs, across a range of ankle dorsiflexion angles.

iii) To quantify the relative contribution of each muscle's JRS (MJRS) during impact, before and after TA fatigue. The MJRS will be determined for the following muscles: TA, lateral gastrocnemius (LG), medial gastrocnemius (MG), soleus (SOL), and fibularis longus (FL).

iv) To determine if MJRS and AJRS values prior to and after fatigue will differ as a function of the sex of the participant.

1.2 Statement of Hypotheses

It is hypothesized that:

i) AJRS will increase as the dorsiflexion angle increases. The resulting effect at the tibia will be an increase in PA and AS, and a decrease in TPA, all reflecting decreased attenuation ability by the ankle joint.

ii) A decrease in AJRS will occur as TA fatigues. This decrease in AJRS will be associated with greater attenuation of impact shock, which will be reflected in decreases in PA and AS, and an increase in TPA, compared to baseline values.

iii) After fatigue, the contribution of the TA to AJRS will decrease, leading to an overall decrease in AJRS.

iv) Males will exhibit greater MJRS and AJRS prior to and after fatigue, relative to females. Also, it is thought that males will fatigue at a faster rate than females.

CHAPTER II

LITERATURE REVIEW

2.1 Impact Forces During Running

During heel-toe running, two impact peaks occur (Figure 1) (Cavanagh & Lafortune, 1980). The first is the impact peak that occurs within 50 ms after initial contact (Gruber et al., 1987; Nigg, 1997) at a force between one and three times that of body weight (BW) (Cavanagh & Lafortune, 1980). It is referred to as the passive impact peak because, although the leg muscles are active through the initial 30-50 ms of ground contact, they are unable to react this quickly to the increased force imposed on them (Bobbert, Yeadon & Nigg, 1992; Chavet, Lafortune & Gray, 1997; Nigg & Liu, 1999). In the short duration of the impact phase, runners do not have the opportunity to achieve neuromuscular control over the rotations of body segments other than by controlling the geometry and muscular activation levels prior to touchdown (Bobbert et al., 1992).

The second peak is the active force peak, so-named because of the active contribution of the musculoskeletal system to the impact forces (Cavanagh & Lafortune, 1980). It also occurs during the time period when force is being actively applied to propel the runner forward (Clarke et al, 1983).

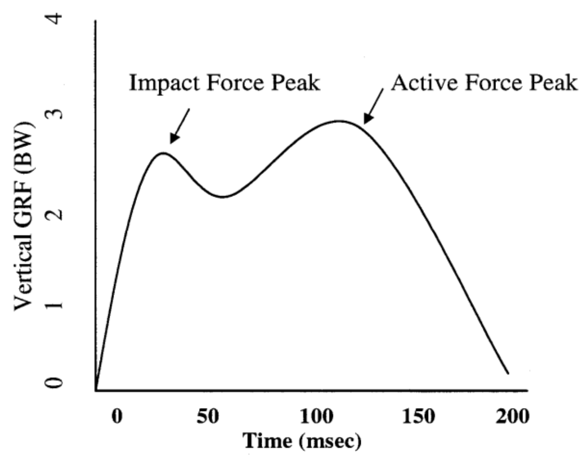

Figure 1: Typical ground reaction force curve for heel-toe running (Modified from Cavanagh & Lafortune, 1980).

When the foot impacts the ground during running, an impact reaction force equal in magnitude but opposite in direction to the imposing foot-strike occurs; it is named the ground reaction force (GRF). A shock wave is produced from the rapid deceleration of the lower extremity upon collision of the foot with the ground, and travels through the body from foot to head (Cavanagh & Lafortune, 1980; Whittle, 1999). ‘Shock wave’ is a term commonly used in the biomechanics literature to describe the propagation of a stress wave, as initiated by an impact force, through the body’s tissues (Derrick, Hamill & Caldwell, 1998; Duquette & Andrews, 2010a; Flynn et al., 2004; Hamill et al., 1995; Holmes & Andrews, 2006; Lafortune et al., 1995, 1996a, b; McMahon et al., 1987; Mercer, Bates, Dufek & Hreljac, 2003; Milner, Ferber, Pollard, Hamill & Davis, 2006; Verbitsky, Mizrahi, Voloshin, Treiger & Isakov, 1998; Voloshin et al., 1998; Whittle, 1999). While it has been observed that up to 70% of runners suffer overuse injuries on an annual basis (Hreljac et al., 2000), there is little epidemiological evidence to support the foot-ground impact as the root cause.

Nigg and Wakeling (2001) reviewed and summarized findings of studies investigating potential relationships between impact forces and injury. Although there are a great number of impacts that occur over the period of a run, it is suggested that repetitive impact forces are not central to running injuries. In fact, it is highlighted that a certain degree of repetitive loading can have a positive effect on bone tissue formation (Nigg & Wakeling, 2001; Wolff, van Croonenborg, Kemper, Kostense & Twisk, 1999). However, injury may occur when impact loading exceeds the tissue's tolerance, and when appropriate recovery is not provided. Over longer distances, runners may function near the limit of the healthy loading/recovery cycle, lending speculation that impacts in a fatigued state may result in injury. Although impact forces are not thought to be the sole cause of injuries, research also suggests a pattern related to impact forces, such that injury-free runners exhibit lower vertical impact-induced peak forces and maximal vertical loading rates than an injury-prone group (Hreljac et al., 2000; Milner et al., 2006).

The rate at which the impact peak is reached is termed the loading rate, which is related to the frequency of the impact peak (Wakeling et al., 2001) and is thought to be an indicator of potential injury (Lafortune et al., 1996b; Voloshin et al., 1998). However, much of the literature presents the idea that injury is due to training errors, where increases in mileage and intensity result in the body being unable to accommodate the imposed forces (Nigg, 1997). Specific tibial response parameters (TRPs) can be investigated to highlight the stresses of impact accelerations on the human musculoskeletal system; they include peak acceleration (PA), time to peak acceleration (TPA) and the acceleration slope (AS) (Holmes & Andrews, 2006) (Figure 2).

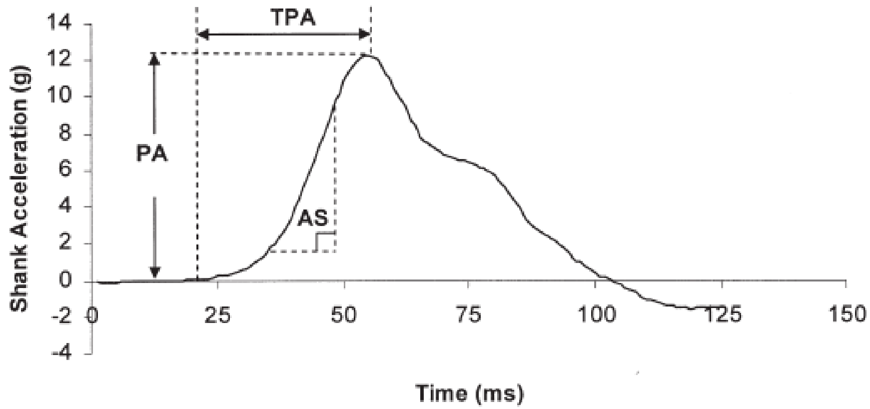

Figure 2: Tibial response parameters of the acceleration-time graph. Leg accelerations can be described in terms of the peak acceleration (PA), time to peak acceleration (TPA), and acceleration slope (AS). (From Holmes and Andrews, 2006)

2.2 Impact Force Frequency Domain Considerations

Impact shock peaks measured in the time domain, such as in acceleration-time signals from skin-mounted accelerometers, offer information about the shock wave. However, they also include additional, often unwanted components such as accelerations of limb motion and noise from resonant vibrations of the accelerometer (Shorten & Winslow, 1992). Examining the impact shock wave in the spectral, or frequency domain, via a Fourier Transformation, provides more information about the frequency content of the signal, such as the effect of acceleration components of muscle action and accelerometer noise (Shorten & Winslow, 1992).

The soft-tissue packages of the lower extremity have natural frequencies in the range of 10-60 Hz, which can depend on the activation, length, and contraction velocity of the major muscles involved (Wakeling & Nigg, 2001b). It has been found that the first impact region (passive) of the frequency-time curve oscillates at frequencies in the range of 10-20 Hz (Nigg & Wakeling, 2001), while the second active region includes low frequency motion in the range of 5-8 Hz (Hamill et al., 1995; Shorten & Winslow, 1992).

The impact region creates an overlap with the natural frequency of the lower extremity during heel-toe running, which could possibly lead to vibrations within the soft-tissue packages of the leg. However, Wakeling and Nigg (2001b) determined that although these ranges coincided, soft tissue vibrations are minimal during running. This is thought to be due to increases in muscle activity in order to move the frequency and damping characteristics of the soft tissue away from those induced by the impact force (Wakeling et al., 2003). In fact, altering muscle activation has been shown to change the natural frequency of the soft tissue packages (Pain & Challis, 2002; Wakeling & Nigg, 2003). Conversely, the natural frequencies of bone are rather high (200-900 Hz) and clearly lie outside the frequency range of the impact forces and the resulting shock wave that would induce resonance (Nigg & Wakeling, 2003).

The frequency components of these impact shock peaks are important to note due to the possibility of resonance being induced in the wobbling structures, should their natural frequencies match the frequency of the impacting force (Wakeling et al., 2003). Should resonance occur, the body tissues will experience excessive vibration, with potential damaging effects to the neuromuscular, endocrine and cardiovascular systems (Wakeling & Nigg, 2001b). Although minimizing vibrations is not necessary for maintaining basic running mechanics (Boyer & Nigg, 2006), it is important to minimize stress on the soft tissue, which could lead to discomfort or increased injury risk (Wakeling & Nigg, 2001b). Resonance can be avoided by changing the input signal characteristics or the mechanical properties of the system via muscle activation levels (Boyer & Nigg, 2007).

Specific properties of the musculoskeletal system aid in maintaining constant acceleration at the head when investigating unilateral impacts (Derrick et al., 2002; Hamill et al., 1995; Shorten & Winslow, 1992). Shorten and Winslow hypothesized that shock attenuation in the human body, is regulated by a responsive mechanism that maintains head shock below a sustainable threshold. At frequencies above 6 Hz, which correspond to the maximum frequency at which voluntary movements occur (Winter, 2005), the body attenuates the transmission of impact shock to the head. At frequencies above 12 Hz, no significant differences are found in accelerations to the head, indicating that despite large increases in the impact shock magnitude of the lower extremity with increases in running velocity, the body appears to engage an active, responsive mechanism that maintains a certain allowable shock level to the head (Hamill et al., 1995; Shorten & Winslow, 1992).

2.3 Leg Properties Affecting Force Transmission

The human musculoskeletal system plays an important role in the attenuation and dissipation of shock waves, such as those initiated as the foot contacts the ground during running (Lafortune et al., 1996a, b; Verbitsky et al., 1998). It has been shown that by the time the shock wave reaches the head, its magnitude is greatly attenuated (Hamill et al., 1995; McMahon et al., 1987; Shorten & Winslow, 1992), either actively by joint positioning (Bobbert et al., 1992) and muscle activity (Christina et al., 2001), or passively by cartilage, bone, the heel pad, and wobbling mass (Gruber et al., 1987, 1998) of the human leg.

2.3.1 Cartilage and Bone

Bone is the primary structure responsible for the transmission of shock waves through the body during running (Valiant, 1990). Cartilage has been shown to provide some force attenuation capabilities by aiding in shock dissipation and protecting against trabecular micro-fracture (Radin et al., 1970).

Chu et al. (1986) determined that a disruption in articular cartilage between joints (at the knee) resulted in an increase in the forces transmitted upwards through the body. Radin et al. (1970) suggested that cancellous bone can attenuate peak forces to an equal or greater extent than articular cartilage, due to its relative thickness. Very thick layers of relatively rigid materials can be more effective in attenuating forces than thin layers of very soft materials, because in a thin layer, little deformation can occur (Radin et al., 1970). However, due to its deformation and damping properties, cartilage is an important structure for decreasing the peak load transmitted during impact (Radin et al., 1970).

There are implications for injury when recovery between cyclic loads is not adequate. Fracture has been shown to occur should the magnitude and frequency of an applied load damage the bone beyond its rate of remodelling (Schaffler & Jepsen, 2000). For example, osteoarthritis (a degenerative joint disease) is thought to be a result of micro-fractures of the osseous tissue caused by repetitive impact loading (Voloshin, 1988). As a response to impulsive loading, bone remodelling occurs which results in stiffening of the underlying subchondral bone and a decrease in its ability to absorb shock (Voloshin, 1988). Joint pathology is associated with a decreased shock-absorbing capacity of that joint (Voloshin, 1988), which may expose the articular cartilage overlying the bone to increased stress, ultimately resulting in the degeneration of the cartilage and the joint itself.

2.3.2 Heel Pad

The human heel pad is comprised of uncompressed adipose tissue under the calcaneus, and is thought to help lower the impact force the foot experiences upon impact. Similar to the thickness of the foam material in the heel of most running shoes (Cavanagh, Valiant & Misevich, 1984), the adult male heel pad is about 18 mm thick, (although it is highly variable between individuals) (Gefen, Megido-Ravid & Itzchak, 2001). At heel strike, the calcaneus decelerates by traveling into the intermediate heel pad that exists between the calcaneus and the ground (Whittle, 1999). The further the calcaneus is able to travel in coming to a stop, the longer it takes to arrest its motion, leading to decreased momentum and associated force of impact (Whittle, 1999).

Gefen et al. (2001) found that the in-vivo heel pad can absorb 17-19% of the energy initiated from heel strike. The heel pad's overlying skin, composed of fat and tough fibrous tissues bound firmly to the underlying bone structure of the foot, contributes to its overall stiffness during an applied perturbation (Valiant, 1990). While the heel pad has a low initial stiffness, it can deform rapidly (by about 40%) (Gefen et al, 2001). However, after a perturbation, the viscoelastic tissue of the heel pad takes time to return to its original shape (Valiant, 1990).

2.3.3 Wobbling Mass

Simplified biomechanical modelling is used to measure the effect of impacts on the human body, such that injuries and/or discomfort may ultimately be reduced or prevented. However, traditional rigid segment biomechanical models do not account for soft tissue movement relative to bone that occurs during impacts (Pain & Challis, 2001; Yue & Mester, 2001), such as those experienced during running and landing. Gruber et al. (1987) addressed this limitation by developing a 'wobbling mass model' that incorporates the rotational and translational movement of soft tissues, representing the wobbling mass about the rigid skeleton. The wobbling mass consists of all non-rigid parts of the body, including muscles, soft tissues, internal organs and fluids in the body that move relative to the rigid skeleton (Gruber et al, 1987; Yue & Mester, 2001). The wobbling mass has been modeled as being attached to the skeletal frame via damped elastic connections (Gruber et al., 1998) (Figure 3).

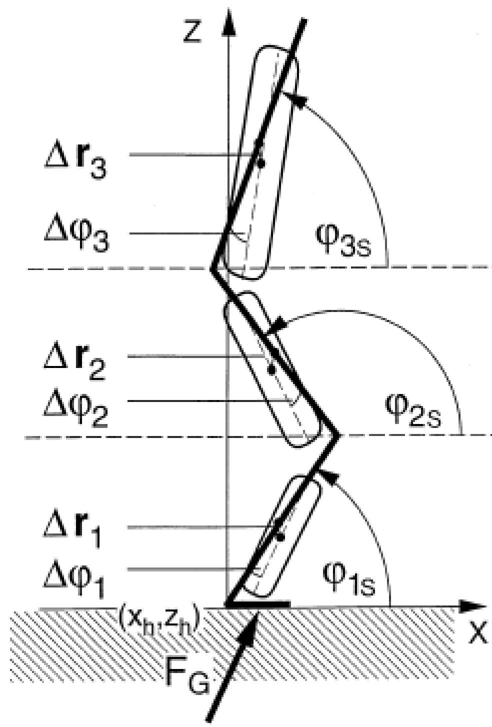

Figure 3: The three-linked model with wobbling mass. The wobbling mass has been modeled as being attached to the skeletal frame via damped elastic connections, where 'r' is the radius of the axis of rotation, 'φ' is the joint angle, and 'F_G' is the ground reaction force. (From Gruber et al., 1998)

During the first 10-30 ms after the foot impacts the ground, the soft tissues wobble in a complex damped manner for one to three oscillations (Gruber et al., 1998; Wakeling & Nigg, 2001a). While the wobbling mass is able to reduce the transmissibility of the impact shock wave (Yue & Mester, 2001), the response after the initial impact phase (~30 ms), as measured by accelerations at the knee, differs very little between the rigid skeleton and the wobbling mass (Gruber et al., 1998). Gerritsen et al. (1995) determined that a rigid model can overestimate the impact force peak by as much as 26% when compared to a musculoskeletal model that incorporates wobbling masses. In addition, they found that loading rate increased by 155% for a rigid-only model, suggesting that using a rigid segment only model is not acceptable for studying impacts.

2.4 Mechanisms Affecting Force Transmission

2.4.1 Knee Angle

Eccentric contraction during joint flexion is a mechanism by which the body absorbs impact energy following impact (Derrick et al., 1998). Active shock attenuation through eccentric muscle action is thought to be far more significant than the passive shock dissipating mechanisms of soft tissue and bone (Mizrahi & Susak, 1982).

Knee angle at impact has been found to be a highly effective regulator of shock transmission through the body. Milliron and Cavanagh (1990) introduced the term *cushioning flexion* to represent the role of knee flexion in attenuating impact forces. Increased knee flexion at ground contact has been found to result in decreased effective axial stiffness of the body (Lafortune et al., 1996b), leading to overall improved shock attenuation. In support of this, Gerritsen et al. (1995) used a direct dynamics approach to simulate the impact phase in heel-toe running, and found that more extended knee postures at touchdown resulted in an increase of 68 N per degree of change in leg angle. However, exaggerated knee flexion, described by McMahon et al. (1987) as *groucho* running, comes at an increased physiological cost of 25% more oxygen consumption per 5 degrees change in knee angle in midstance (McMahon et al., 1987), despite the fact that it results in reduced shank and ankle shock exposure (Lafortune et al., 1996b).

2.4.2 Ankle Angle

Upon impact in heel-toe running, a quick plantarflexion movement occurs that causes rapid lengthening of the tibialis anterior (TA) in preparation for the eccentric absorption of the impact force (Gerritsen et al., 1995). Eccentric absorption occurs through the relative lengthening of the TA in response to shortening of the plantarflexors. In their lower extremity simulation, Gerritsen et al. (1995) determined that for every degree of increased plantarflexion at heel contact, impact force increased by 85 N. Therefore, a decreased ability to perform dorsiflexion, such as in fatigue, is associated with decreased energy absorption and larger impact peak forces (Gerritsen et al., 1995).

2.4.3 Muscle Tuning

Wakeling et al. (2001) defined muscle tuning as “the alteration of the mechanical properties of the leg due to changes in muscle activity, irrespective of any motion that occurs in the joints” (p. 1316). These changes are present in muscle activation patterns with respect to the timing, intensity and frequency content of the EMG signal during the 50 ms prior to and after heel strike. Due to the fact that the impact phase is very short (~50 ms), a runner is said to change muscle activity in anticipation of the next impact.

Impact forces are described as input signals that initiate vibrations of soft tissue compartments associated with major muscle groups (Nigg & Wakeling, 2001). The body tries to minimize these vibrations by changing the mechanical properties of the soft tissue compartments via a mechanical coupling strategy between rigid and wobbling masses (Nigg & Liu, 1999). This coupling strategy is thought to minimize soft tissue vibrations experienced upon impact by changing the leg's natural frequency and damping characteristics (Wakeling et al., 2003). It is suggested that muscle activity increases as the frequency of the input signal approaches the natural frequency of the soft tissue compartment (Wakeling et al., 2003).

2.5 Stiffness and Running

Runners analyze feedback from a variety of environmental factors to find an optimal tradeoff between safety and performance. The dominant factor in determining the amount of shock the body experiences is the apparent stiffness of the leg upon impact (McMahon et al., 1987). Researchers agree that the magnitude of leg stiffness is adjusted to accommodate changes in impact conditions to maintain the level of intensity of the shock wave that is allowed to reach the head (Farley & Morgenroth, 1999; Ferris & Farley, 1997; Hamill et al., 1995; Shorten & Winslow, 1992).

2.5.1 Defining Stiffness

Traditionally, stiffness has been defined in physics as a property of a deformable body that, under the influence of external forces, can store elastic energy; in the absence of external force, it will maintain a constant shape (Latash & Zatsiorsky, 1993). Muscles and joints in the human body do not function in this way, yet they can still generate a measure of stiffness if elastic energy can be stored and deformation can take place (Latash & Zatsiorsky, 1993).

Stiffness can be described at the single muscle fibre level or by modeling the entire body as a mass and spring system (Butler, Crowell & Davis, 2003). Because the human body does not necessarily store elastic energy as would a spring, the traditional definition of stiffness cannot be applied. Latash and Zatsiorsky (1993) proposed a definition for 'quasi-stiffness', whereby requirements for the system being at equilibrium and the time course of displacement can both be disregarded. It is in the context of 'quasi-stiffness', calculated as a ratio of force applied to displace the limb (through leg compression upon impact) or rotation of the joint, that stiffness will be regarded in this document.

It is suggested that studies should clearly state their notion of stiffness, and to what extent the results are influenced by the system's properties or by the experimental procedure of obtaining a stiffness value. Since the literature presents many other definitions for stiffness and ways to quantify it, clarification of terms should be made in order to compare data across studies.

2.5.2 Stiffness vs. Stability

In order to quantify the amount of stiffness a joint experiences, it is important to clarify defining aspects related to joint stiffness and stability. Reeves, Narendra and Cholewicki (2007) reviewed the concept of stability as it relates to spine biomechanics in order to standardize the terms used in the literature. Although the review was specified for spine biomechanics, applying a common set of terms to all joints would be useful for future research. Reeves et al. (2007) suggest that the stability of an object is absolute, being either stable or not; it is either static, and in equilibrium, or dynamic and changing with time. The quantifiable amount of stability a joint can incur is described as its ‘robustness’ (Reeves et al., 2007). Robustness defines how well a system can deal with a disturbance; as such, a system that is stiffer is considered more robust than one that is less stiff. Increasing the degree of robustness occurs through increased muscle activation of the individual muscles that are contributing to the JRS. This will vary based on the joint position, as the musculature required to hold the joint in place must adapt to new positions by changing activation levels. In addition, the ankle gets its stability from the shape of the joints and support from ligaments and other deep muscles.

2.5.3 Calculating Stiffness

The whole leg (from hip to foot) is often represented as a spring supporting the mass of the body in a mass-spring model (Figure 4). Conceptually, this model demonstrates how, after the foot contacts the ground, joint motion at the ankle, knee and hip lowers the body’s centre of mass (COM), which represents absorption and compression of the spring (representing the leg). Limb extension is represented by recoil of the spring (Ferris & Farley, 1997). The stiffness of the whole leg spring then represents the average stiffness of the overall musculoskeletal system of the whole leg during the ground contact phase (Ferris & Farley, 1997; McMahon & Cheng, 1990).

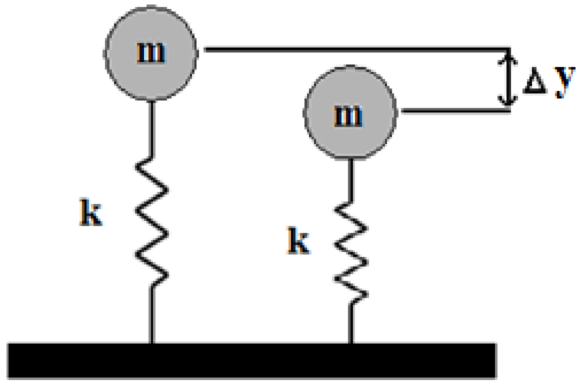

Figure 4: The whole leg is often represented as a spring supporting the body's mass (m), allowing for the vertical stiffness of the whole leg (k) to be calculated at ground contact when the leg is oriented vertically. Vertical stiffness of the whole leg can be calculated by dividing maximum vertical force by the maximum vertical displacement of the body's centre of mass ($F_{max}/\Delta y$).
(Adapted from Butler et al., 2003)

Vertical stiffness (k) is the simplest measure of the entire body's axial stiffness value. According to Butler et al. (2003), it can be calculated by dividing maximum vertical force, obtained from a force plate, by the maximum vertical displacement of the whole body COM (Δy), obtained through the double integration of the vertical acceleration. Lower leg (between knee and ankle) stiffness is calculated in a similar manner; however, leg length and leg landing angle are incorporated and maximum vertical displacement of the COM of the leg when it reaches its lowest point, i.e. the middle of the stance phase, is used (McMahon & Cheng, 1990) (Figure 5).

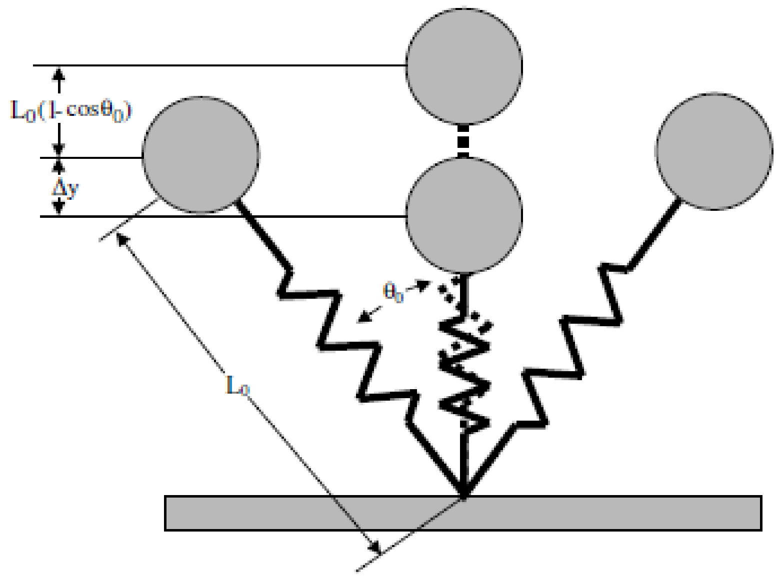

Figure 5: Model for calculating lower leg stiffness when impacting the ground in a non-vertical position. Using the mass-spring system, leg length (L_O) and landing angle (Θ_O) allows for calculation of lower leg stiffness using the vertical displacement of the body's centre of mass (Δy). (From Butler et al., 2003)

Whole leg stiffness is often measured during a hopping protocol, as impacts of similar magnitude to running can be achieved at landing (Farley & Morgenroth, 1999; Ferris & Farley, 1997). During *hopping*, whole leg stiffness accommodates differences in surface stiffness primarily by modulating ankle stiffness, and secondarily by modulating knee angle at touchdown (Farley, Houdijk, van Strien & Louie, 1998; Farley & Morgenroth, 1999). In contrast, it has been found that as *running* speed increases, ankle joint stiffness remains constant and knee joint stiffness increases, suggesting that knee joint stiffness regulates whole leg stiffness during running (Gunther & Blickhan, 2002; Kuitenen, Komi & Kyrolainen, 2002; Stefanyshyn & Nigg, 1998). A possible reason for this difference is due to the foot strike pattern during landing. In forefoot landings, such as those associated with hopping, the knee is stiffer than the ankle (Farley et al, 1998; Hamill, Derrick & McClay, 2000) and there is greater ankle flexion range (Mizrahi &

Susak, 1982). Rearfoot landings, such as those typically associated with running, have demonstrated a stiffer ankle than knee (Hamill et al., 2000).

2.5.4 Joint Rotational Stiffness

Joint rotational stiffness (JRS), or joint torsional stiffness, is considered the rotational correlate to vertical and linear stiffness; it is a reflection of how much an angle changes in response to an applied moment about the joint (Farley et al., 1998; Kuitunen et al., 2002; Milner et al., 2006) (Figure 6). JRS is difficult to quantify in the hip, knee and ankle joints due to the presence of multiple biarticular muscles crossing the joints. These muscles are important in leg stabilization and optimally maintaining leg stiffness (Nichols, 1987). The presence of biarticular muscles, however, creates a complex situation, as muscles are not able to work in isolation across an individual joint (Latash & Zatsiorsky, 1993).

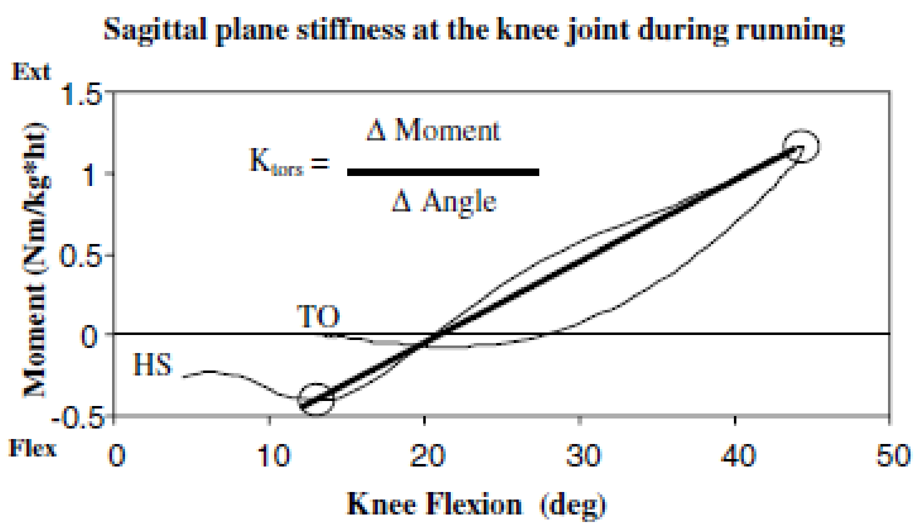

Figure 6: Sagittal plane ankle joint stiffness. Torsional stiffness (K_{tors}) is calculated as the slope of the line through the moment-angle curve from the point of maximum knee flexion to maximum knee extension moment.
(From Butler et al., 2003)

Joint stiffness is achieved by the contribution of individual muscles that cross the joint and their level of muscle activation, such that co-contraction of agonist and antagonist muscles is the main mechanism of stiffness control of a joint (Nichols, 1987). As the muscles that cross a joint generate more force, the joint is said to increase in stiffness, and undergo smaller angular displacement when a perturbation, such as a running impact, is applied. In running, muscle activity prior to landing is responsible for generating adequate joint stiffness, leg geometry and pre-activity for a safe landing (Nigg, 1997).

Since peak force has been shown to increase along a more rigid, stiffer segment (Pain & Challis, 2002), it is speculated that an increase in muscular co-activation is associated with an increase in joint stiffness, thereby increasing impact forces. It has been proposed that changes in joint stiffness may be the reason for changes in muscle pre-activation and may explain the surprising results of many studies which have not found differences in impact force magnitude for different shoe or surface interventions (Boyer & Nigg, 2007).

2.5.5 Passive Muscle Stiffness

Passive muscle stiffness is regulated by the number of cross-bridges that form spontaneously when a muscle is not in contraction (Hill, 1968). When a passive muscle exceeds its resting length, tension is generated by the parallel elastic component (PEC), that is, resistance is provided by the muscle membrane, lying parallel to the muscle fibre (Winter, 2005). The PEC is responsible for muscle stiffness when contractile components do not generate force. Passive stiffness is regulated by muscle mass, as greater muscle mass would imply a greater number of cross-bridges available for spontaneous reattachment. Additionally, greater muscle mass would incorporate a larger volume of passive connective tissues, components which contribute to passive stiffness (Winter, 2005).

2.5.6 Passive Joint Stiffness

Passive joint stiffness can be determined when all muscles crossing the joint are relaxed (Latash & Zatsiorsky, 1993). However, even at rest, the muscles acting around a joint are usually slightly stretched and generate a certain tension due to antagonistic muscle activity (Latash & Zatsiorsky, 1993). Gajdosik, Vander Linden, McNair, Williams and Riggin (2005) evaluated passive stiffness using an isokinetic dynamometer to measure passive resistance torque through a range of motion while participants did not actively resist; this is verified by the absence of muscle activity in EMG (Milliron & Cavanagh, 1990). Passive joint stiffness was then calculated as the ratio of passive resistance torque to angular displacement. Milliron and Cavanagh (1990) suggest that participants with tighter calf musculature, as a function of muscle and tendon stiffness, exhibit less range of motion in dorsiflexion than those who are more flexible.

2.5.7 Muscle Stiffness, Injury, and Performance

The literature supports the concept of optimizing performance and injury through lower extremity stiffness regulation. It appears that increased stiffness is beneficial to performance by improving the ability to efficiently store elastic potential energy through eccentric loading of the stretch-shortening cycle (Kubo et al., 2000). Adequate muscle stiffness is required to physically stop the downward progression of the body at impact. Inadequate muscle stiffness could potentially lead to a fall in extreme cases (Butler et al., 2003). Too little stiffness may also allow for excessive joint motion, leading to soft tissue injury (Granata et al., 2002).

McMahon et al. (1987) describe greater rates of oxygen consumption with increased compliance of the lower extremity. Gunther and Blickhan (2002) also suggest that a compromise between metabolic effort and material stress limitations dictate leg geometry and JRS at impact. It is suggested that an optimal stiffness level will balance the injury potential of stiff-legged running with the injury potential and reduced economy of high muscular loads in compliant running (Dutto & Smith, 2002; Kuitunen et al., 2002; McMahon & Cheng, 1990; Stefanyshyn & Nigg, 1998).

It has been found that vertical and joint stiffness increase with running speed (Gunther & Blickhan, 2002; Kuitunen et al., 2002). It is thought that as the velocity of activity increases, an increase in leg stiffness is necessary to resist collapse of the leg during landing and allow for maximum energy return for propulsion (Granata et al., 2002). Generally, it has been found that as the physical demands of the activity increases, leg stiffness also increases (Kuitenen et al., 2002; Stefanyshyn & Nigg, 1998).

2.6 Fatigue

Fatigue may be an important factor in the development of running injuries as it has been shown to decrease the ability of the musculoskeletal system to dissipate and attenuate impact shock (Mizrahi et al., 2000a; Verbitsky et al., 1998; Voloshin et al., 1998). Therefore, it is important to investigate the adjustments the body makes to protect itself from external forces in a fatigued state. Experimentally, the protocol for inducing fatigue may play a role in the measured response. The shock attenuation capability of the fatigued human shank has produced different results depending on the fatiguing protocol being used. Some researchers have used localized muscle fatigue (LMF), while others have used overall cardiovascular whole body fatigue (WBF). Individual differences in kinematic strategies in response to fatigue (e.g. an increase in step length with fatigue, an increased maximal knee flexion angle during swing, and an increased maximal thigh angle during hip flexion) may influence responses as well (Williams, Snow & Agruss, 1991).

2.6.1 Whole Body Fatigue

Whole body fatigue, such as that achieved through treadmill running protocols, is physiologically determined by a decrease in pressure of end tidal carbon dioxide pressure ($PETCO_2$) (Mizrahi et al., 2000a; Mizrahi, Verbitsky, Isakov & Daily, 2000b; Verbitsky et al., 1998; Voloshin et al., 1998). The use of $PETCO_2$ as a measure of fatigue represents the deterioration of muscle activity that is likened to running in a fatigued state. A decrease in $PETCO_2$ is due to the development of metabolic acidosis induced by exercise and is associated with a decrease in performance (Mizrahi et al., 2000a, b; Verbitsky et al., 2000b; Voloshin et al., 1998). This is commonly known as lactic acid production and signifies exceeding the anaerobic threshold.

As WBF is induced, the human musculoskeletal system is less capable of attenuating heel-strike induced shock waves (Christina et al., 2001; Mercer et al., 2003; Mizrahi et al., 2000a, 2000b; Verbitsky et al., 1998; Voloshin et al., 1998). Increases in loading rate (Mizrahi et al., 2000a) and acceleration values at the knee (Mizrahi et al., 2000a, 2000b; Verbitsky et al., 2000b; Voloshin et al., 1998) indicate a decreased ability of the leg muscles to attenuate the impact loading and accelerations when experiencing WBF. More specifically, Mizrahi et al. (2000a) found an imbalance in the rate of fatigue of the shank muscles, with the average integrated EMG (iEMG) and the mean power frequency (MPF) of the TA significantly decreasing through the running protocol. The gastrocnemius iEMG did not change, while its MPF increased, indicating that the muscle activity of the gastrocnemius increases as the TA fatigues. An increase in MPF, while maintaining a constant iEMG, is suggested to be due to an enhanced firing rate of the working motor units. The decrease in MPF and iEMG in the TA suggests that activity of this muscle is reduced due to fatigue. This is thought to have implications for injury, as excessive bending stresses to the tibia could occur due to the loading imbalance (Mizrahi et al., 2000a).

Biomechanically, treadmill-induced fatigue has been associated with a decrease in stride rate, an increase in knee angle at foot strike, and an increase in hip excursion angle (Mizrahi et al., 2000b). These kinematic changes have been found to be associated with higher impact accelerations, likely because knee angle affects impact attenuation via manipulation of the leg's vertical stiffness (McMahon et al., 1987). Mercer et al. (2003) suggest that when muscles are fatigued, bone and other structures are left to dissipate impact shock, and are placed under more stress during impact; this is subsequently thought to lead to an increased chance of injury to the musculoskeletal system (Verbitsky et al., 1998; Voloshin et al., 1998).

2.6.2 Localized Muscle Fatigue

While WBF has been shown to decrease the shock attenuation capabilities of the body, the associated fatiguing protocol does not necessarily result in fatigue of the individual muscles of the leg (Mizrahi et al., 2000a). Locally fatigued muscle has been shown to exhibit an increase in shock attenuation capabilities (Flynn et al., 2004; Holmes

& Andrews, 2006). According to Winter (2005), muscle fatigue is associated with a decrease in tension; if the muscle is less stiff, a more compliant lower extremity contacts the ground to attenuate force. This results in reduced PA and AS values (Duquette and Andrews, 2010a; Flynn et al., 2004; Holmes & Andrews, 2006).

Some researchers have found that LMF has led to increases in impact forces (Christina et al., 2001) and impact accelerations measured at the distal aspect of the tibia (Teramoto, Dufek & Mercer, 2006). However, both of these aforementioned studies had runners being tested on a treadmill, which may have led to kinematic adaptations in response to fatigue. A decrease in force production with the onset of fatigue (Kent-Braun et al., 2002) is thought to be associated with an inability of the leg system to maintain its stiffness level (Dutto & Smith, 2002). Because of the link between leg stiffness and mechanical behaviour of the lower extremity (McMahon et al., 1987), it is speculated that the stiffness properties of the leg system may become altered as the system fatigues. In order to specifically examine the effect of impact shocks on locally fatigued muscles, kinematic variables must be held constant, which is not possible during treadmill running protocols.

In experiments involving exhaustive running, a decrease in dorsiflexion at heel contact has been noted (Dutto, Levy, Lee, Sidthalaw & Smith, 1997). It is speculated that the inability to sustain initial dorsiflexion is likely a result of the smaller physiological cross-sectional area (PCSA) of the TA in comparison to the plantarflexors. As previously mentioned, a decreased ability to dorsiflex with fatigue would result in a decreased ability of the TA to eccentrically absorb impact energy (Gerritsen et al., 1995).

Duquette and Andrews (2010a) investigated the effect of dorsiflexion angle on tibial response during localized fatigue of the shank. Isometrically-induced LMF of the TA led to a reduction in such tibial parameters as PA and AS, as well as an increase in TPA, regardless of ankle angle. It is thought that the reduced stiffness of the wobbling mass, as a function of localized fatigue, or that a reduced AJRS contribute to the dampening of the shock wave caused by impact. This concept is supported by research by Pain and Challis (2002), who determined that a softer structure (i.e. wobbling mass) attenuates more impact force than a rigid structure. Since the differences in the TRPs by Duquette and Andrews (2010a) were seen between the fatigued and non-fatigued states while at the same joint angle, it is suggested that ankle angle alone does not entirely account for the differences seen in tibial response during LMF of the dorsiflexors.

2.7 The Human Pendulum

The human pendulum apparatus allows for the examination of the response of the lower limb to an impact orientation similar to that experienced during running (Lafortune & Lake, 1995). This method is characterized by the participant lying supine on a lightweight bed, with one leg extended over the edge of the bed closest to the impacting wall where a force plate is vertically mounted (Figure 7). Participants are required to resist the motion of the pendulum that is moving at a velocity that mimics impact velocity during heel-strike. At the moment of impact of the heel with the wall, the pendulum is at its lowest point and travelling horizontally (Lafortune & Lake, 1995).

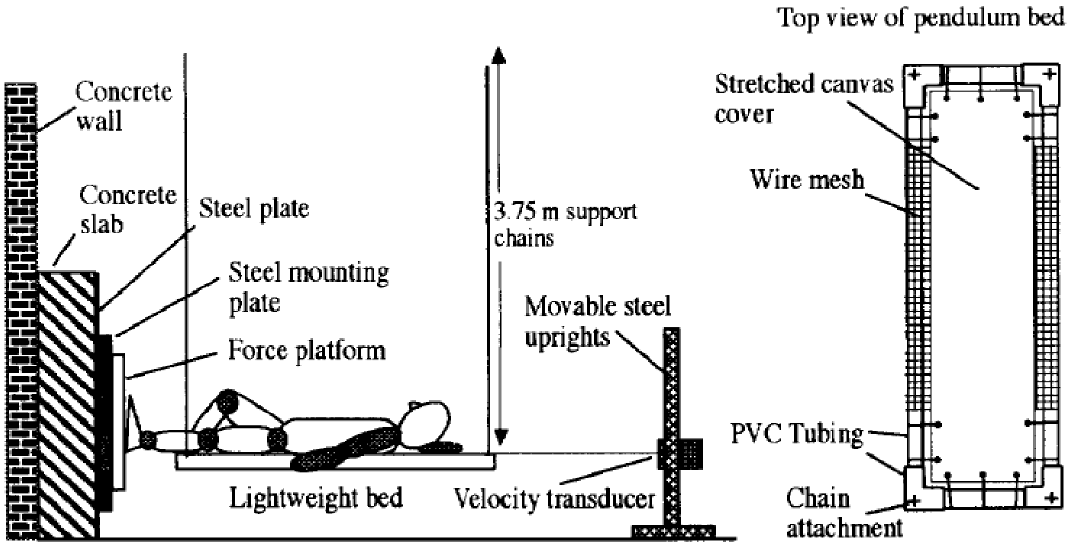

Figure 7. The human pendulum apparatus. Isolated heel impacts can be delivered at similar magnitudes and velocities as those in running. (From Lafortune & Lake, 1995)

2.7.1 Leg Geometry at Impact

Some previous studies have used a straight-legged impact to minimize the cushioning effect introduced by knee flexion (Duquette & Andrews, 2010a; Flynn et al., 2004; Fong, Hong & Li, 2007; Holmes & Andrews, 2006; Lafortune & Lake, 1995; Schinkel-Ivy, Burkhart & Andrews, 2010 in press) in addition to eliminating the effect that a changing knee angle has on proximal and distal joint kinematics, leg muscular activity and impact loading severity. Admittedly, this orientation reduces the outcome's relevance to running; however, it can eliminate certain external and inter-participant sources of variability in kinematic adaptations.

2.7.2 Impact Intensity

The magnitudes of impact forces are dependent on the velocity and leg geometry at impact. Investigators have used horizontal impact velocities in the range of 3.57-4.08 ms^{-1}, with an average velocity of 3.83 ms^{-1} (7 minute miles), as a standard in distance running studies (Milliron & Cavanagh, 1990). Different impact velocities can be achieved using the pendulum apparatus by releasing the bed from various distances away from the force plate. For example, an impact velocity of 1.15 ms^{-1} has been achieved by pulling straight-legged participants a distance of 0.71 m away from the force plate; initial conditions which emulate heel-strike impacts when running at a horizontal velocity of 3.6 ms^{-1} (Cavanagh et al., 1984).

2.7.3 Validity of the Human Pendulum Method

The magnitude of the impact force at foot strike depends upon leg geometry, impact velocity, and the material properties of the surface, the shoe sole and the human heel (Whittle, 1999). Due to the many cofounding kinematic adaptations that are possible, isolation and manipulation of these mechanical inputs are difficult to assess (Lake & Lafortune, 1998). It is therefore imperative to systematically control and change the mechanical inputs to the body. It has been suggested that once factors have been established in a controlled manner, experimentation in a more realistic locomotor manner can then be explored (Lake & Lafortune, 1998).

In addition, muscles are used to both move limbs and provide joint stiffness required for a locomotor task, making it difficult to determine which tasks are contributing to the EMG signal. By supporting the leg, muscle motion can be attributed to the joint stiffness required to withstand the impact, in addition to that necessary to minimize soft tissue vibrations (Wakeling et al., 2001).

To further support the validity of using the human pendulum, force and acceleration curves generated from pendulum impacts to a wall-mounted force plate have been shown to display similar characteristics to those exhibited during running (Figure 8).

For example, PA and TPA on a pendulum were 6.4 (0.7) g and 16.1 (3) ms, respectively, which fall close to acceptable ranges presented by multiple running studies (Cavanagh & Lafortune, 1980; Munro, Miller & Fuglevand, 1987; Nigg, 1997; Valiant, 1990).

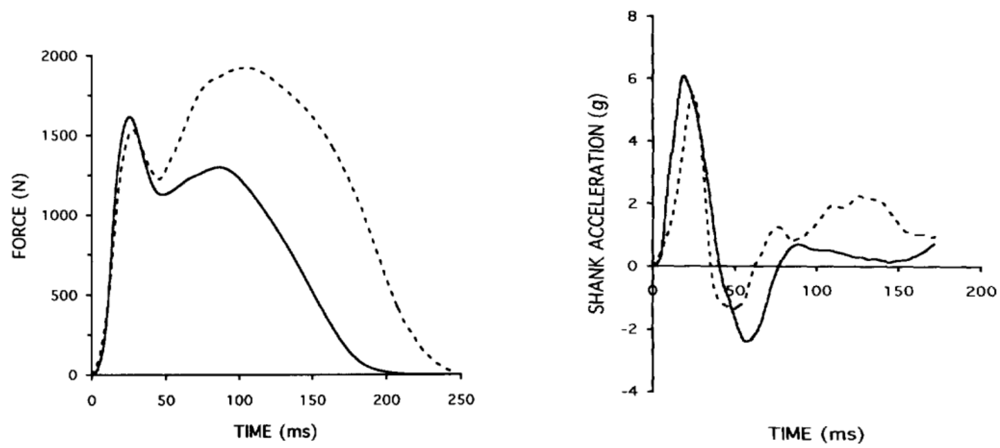

Figure 8. Comparison of a ground reaction force (GRF) achieved during running with a wall reaction force curve achieved during a human pendulum impact. Participant mean wall reaction force curve (solid line) is compared with a typical GRF curve (dotted line). (Lafortune & Lake, 1995)

2.7.4 Limitations of the Human Pendulum Method

Due to the horizontal orientation of the pendulum at impact, the human pendulum approach is limited to measuring the body's resultant axial component (along the length of the tibia) of reaction force (Lafortune & Lake, 1995). However, Cavanagh and Lafortune (1980) have shown that in running, the vertical component that acts along the axial component of the leg accounts for more than 95% of the initial impact peak force, making the axial component a fair representation of what is transmitted to the body during impact.

In addition, the human pendulum fails to allow the body's natural response that would typically occur during a running impact. Increased knee flexion has been shown to decrease the transmission of running impacts upwards through the body (Derrick 2004;

McMahon et al., 1987); thus, by having the leg oriented in a straight-legged locked knee position, the human pendulum method limits one of the body's major natural mechanisms for shock dissipation.

2.8 Instrumentation

2.8.1 Measuring Shank Acceleration

Shock waves initiated during running induce bone vibration that can be quantified using accelerometers. Hennig, Milani, and Lafortune (1993) reported that vertical ground reaction force (vGRF) loading rates were significantly and positively correlated to PA during running, suggesting that as tibial shock increases, so does loading rate. Clarke et al. (1983) explained that the measurement of accelerations can imply stress levels through the musculoskeletal system.

Acceleration of the shank has been measured using bone-mounted (Lafortune, Henning & Valiant, 1995) or preloaded skin-mounted accelerometers (Flynn et al., 2004; Hamill et al., 1995; Holmes & Andrews, 2006; Lafortune et al.; Mizrahi et al., 2000a, 2000b; Verbitsky et al., 1998; Voloshin et al., 1998). Bone-mounted accelerometers provide an accurate measure of the tibial shock that travels along the skeletal system of the body, but are invasive as they require implantation of the device into the bone. As an alternative, skin-mounted transducers have been found to measure bone vibrations fairly accurately, when little soft tissue exists between the bone and skin (Valiant, 1990). Cavanagh and Lafortune (1980) have shown that the axial tibial component of impact shock accounts for more than 95% of the initial impact peak force. Due to the fact that the resultant GRF in running acts along the shank during initial loading (Bobbert et al., 1992), investigating tibial acceleration along the shank allows for a good representation of the transmission of shock.

Skin-mounted accelerometers are limited by the low frequency response of accelerometer attachments; specifically, resonant vibrations of the accelerometer and limb motion contribute to gain or attenuation of the peak impact shock values in the acceleration-time domain (Shorten & Winslow, 1992). However, spectral analysis has been shown to separate spectral peaks due to limb motion and attachment resonance from impact shock waves (Shorten & Winslow, 1992). Care must be taken with skin-mounted accelerometers because they have been shown to overestimate peak accelerations to a degree, depending on the mass of the accelerometer and the firmness and location of the attachment (Valiant, 1990). Movement of the soft tissue between the accelerometer and the tibia can be minimized by using a low-mass accelerometer and preloading it (i.e. a normal force is applied to the accelerometer via a strap affixed around the segment) to the skin surface (Flynn et al., 2004; Holmes & Andrews, 2006; Valiant et al., 1987).

2.8.2 Electromyography (EMG)

In the current study, surface EMG (sEMG) of the musculature surrounding the ankle was used in order to determine the contribution of the superficial muscles to the AJRS. sEMG was used to gain information from the following superficial muscles: tibialis anterior (TA), fibularis longus (FL), lateral gastrocnemius (LG), medial gastrocnemius (MG), and soleus (SOL).

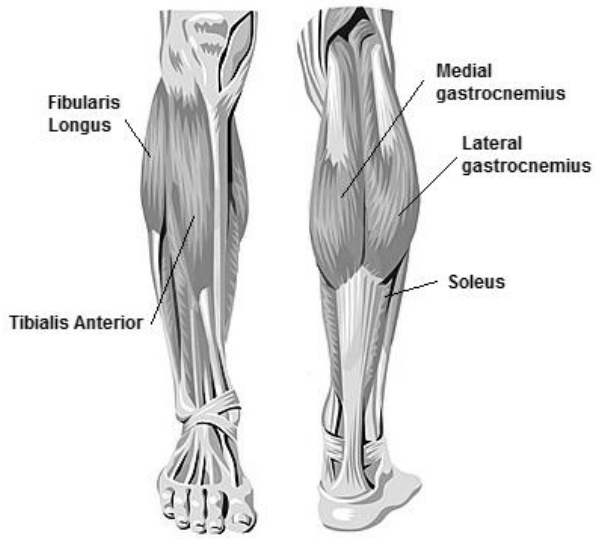

Figure 9. Superficial musculature of the shank contributing to ankle joint rotational stiffness.

2.9 Sex Differences

It has been reported that female runners are twice as likely to sustain common running injuries such as patellofemoral pain syndrome, iliotibial band friction syndrome, and tibial stress fractures, compared to their male counterparts (Taunton, Ryan, Clement, McKenzie, Lloyd-Smith & Zumbo, 2002). In addition, Ferber, McClay Davis, and Williams (2003) determined that female recreational runners exhibit significantly different lower extremity mechanics in the frontal and transverse planes at the hip and knee during running compared to male recreational runners. Although the aforementioned injuries and biomechanical variables will not be investigated, it is worthwhile to note that for some unknown reason, female runners may be more predisposed to injury.

2.9.1 Stiffness

Greater structural musculotendinous stiffness, due to tendon stiffness and muscle architecture, has been identified in males compared to females, with researchers attributing sex differences to anthropometrics. It is thought that increased structural stiffness in males is due to their increased muscle volume and mass, as greater force output and PCSA have been observed in males compared to females, for muscles of the lower extremities (Staron et al., 2000). Greater force capacity as a function of greater muscle mass likely plays an important role in the active resistive capabilities of the musculotendinous unit. However, in a study by Blackburn et al. (2006), it was found that greater values for structural stiffness and material modulus (ratio of stress to strain) occur in males in comparison to females, independent of anthropometric factors.

Granata et al. (2002) examined leg stiffness in males and females during a hopping task at controlled and preferred frequencies. During both the controlled and preferred frequency hopping task trials, they found a relationship between body mass and leg stiffness, as the male participants had to generate greater leg stiffness to ‘drive’ their greater body mass at the same frequency as the lighter female participants. This indicates that male musculature may be more effective at resisting changes in its length, and may therefore potentially result in greater joint stability.

2.9.2 Fatigue

Kent-Braun et al. (2002) found that isometric fatigue rates of the TA muscle did not differ between sexes. However, they found that men exhibited a greater dependence on anaerobic pathways (non-oxidative sources) for ATP, as indicated by higher intracellular concentrations of inorganic phosphate and hydrogen phosphates. It is suggested that males exhibit larger absolute forces generated from larger muscle mass; according to Hicks, Kent-Braun, & Ditor (2001), this would consequently increase metabolic demand, leading to a shorter time to fatigue in males when the same relative force (as a percentage of maximal force) was exerted.

While investigating sustained isometric fatigue of the elbow flexors at mild to moderate intensities (20% of the participant's maximum voluntary exertion (MVE)), Hunter and Enoka (2001) found that females were able to exhibit longer endurance times over their male counterparts. Females were able to sustain their endurance times 118% longer than males. This study also found that endurance time was inversely related to absolute force, whereby enhanced rate of motor unit recruitment (and thus increased EMG) was shown as the target force increased. The difference in endurance time, as demonstrated by increased EMG activity, shows that stronger individuals (males) have shorter endurance times.

2.10 Joint Rotational Stiffness Model

A model by Cort and Potvin (2008) allows for the quantification of the relative contributions of individual muscles surrounding a joint to its joint rotational stiffness (JRS), and can be applied to the ankle to determine ankle JRS (AJRS). Analyzing JRS provides understanding of the changes that occur in musculature surrounding a joint in various situations, such as with the progression of fatigue or during a perturbation. While joint systems have typically been examined in static states pre- and post-perturbation, this model provides knowledge about individual muscle contributions to JRS prior to and during a perturbation, which can be delivered via controlled impacts to the lower extremity.

The rotational stiffness of a joint is its resistance to angular motion and is determined by the change in moment (ΔMo) divided by the change in angular displacement ($\Delta\Theta$). To calculate JRS, muscle length and moment data are typically derived from kinematic data using inverse dynamics. However, the model by Cort and Potvin (2008) describes a forward dynamics approach to determine individual muscle contributions to joint stability in a static and dynamic context. This model is based on a simplified equation by Potvin and Brown (2005) that uses the energy approach (as opposed to the moment approach) to determine the individual muscle contributions to a joint's mechanical stability, based on EMG data and changes in joint position. Also, the use of the anatomical muscle origin and insertion data of the lower extremity, as well as the three-dimensional path of the muscle movement put forth by Delp et al. (1990), is used for calculating changes in muscle lengths and velocities during a perturbation. The model by Cort and Potvin (2008) allows individual muscle contributions to be quantified through individual muscle JRS (MJRS) values, which are calculated for each muscle crossing a joint, as well as an overall JRS value for the joint. JRS is then determined by summing the contribution of each individual muscle's MJRS.

2.11 Summary: Literature Review

Running presents an opportunity for injury, although the causes of running-related injuries are not fully understood. In running, the foot impacts the ground, which initiates a shock wave that travels through the human musculoskeletal system and is thought to have a positive relationship with injury (Buckwalter & Lane, 1997; Cole et al., 1995). The shock wave can be represented by an acceleration waveform (Hennig et al., 1993), whose characteristics (e.g. PA, TPA, and AS) have been investigated in terms of their potential relationship with injury (Milner et al., 2006).

The body dissipates impact forces, such as those incurred in running, through changes in joint angle (Derrick et al., 2002) and LMF (Christina et al., 2001). When impact conditions are controlled, such as with the human pendulum apparatus (Flynn et al., 2004; Holmes & Andrews, 2006; Duquette & Andrews, 2010a), it has been found that LMF of the TA helps dissipate the impact shock. In fact, even when holding all joints constant in a non-fatigue and a LMF protocol involving the TA, Duquette & Andrews (2010a) found an increased ability of the leg to dissipate shock in the fatigued condition. This finding suggests that there is a change in the stiffness of the wobbling masses about the shank, or perhaps changes in the rotational stiffness of the ankle joint, when TA fatigues.

Knowing how individual muscles contribute to AJRS may highlight protective and/or compensatory mechanisms in which the human body engages to maintain safe acceleration levels when impacted in a fatigued state. Identifying the stabilizing potential of individual ankle muscles in a dynamic context could prove useful in rehabilitation. By knowing which muscles are most important in maintaining joint stability during impact, strengthening of the identified muscles that experience excessive fatigue may help prevent ankle injuries that may occur as a result of decreased AJRS.

CHAPTER III

METHODOLOGY

3.1 Participants

Thirty (15 female, 15 male) recreational runners in the age range of 17-30 years were recruited from the university and running communities (see Table 3 in Results for specific participant details). Four participants were later removed from the study, as their data were consistent outliers, which resulted in a sample of 26 runners (11 female, 15 male). Participants were free from lower limb injury and other conditions that would limit their participation, as outlined in a General Health Questionnaire (GHQ) (Appendix A).

'Recreational' individuals were defined as those engaged in weekly running mileage of 20-50 km. Using participants who were routinely exposed to repetitive impact forces ensured their safety when exposed to the pendulum impacts.

Participants' age, sex, height, weight, and anthropometric measurements of the foot were recorded, and activity level confirmed by noting the participant's weekly running mileage. Anyone who answered 'yes' to any of the GHQ questions were excluded from the study. In addition, participants did not engage in impact activities in the 24 hours prior to data collection, as residual fatigue effects could have potentially influenced muscular contributions to AJRS. Participants were informed of the study's procedures and signed an informed consent form, as approved by the University of Windsor's Research Ethics Board (REB).

3.2 Experimental Equipment

3.2.1 Human Pendulum

A human pendulum apparatus similar to that used by Flynn et al. (2004) and Holmes and Andrews (2006) was used in the study. The pendulum consisted of a rectangular frame (190.5 cm x 52.5 cm) constructed from 3.5 cm diameter steel pipe. A stiff canvas sheet (176.5 cm x 41 cm) was attached to the frame by nylon rope, which in turn strengthened the structure. The pendulum was then suspended from the ceiling at each of the four corners of the frame by aircraft cable and tensioners, making the pendulum height adjustable (Figure 10a). The total mass of the frame and suspension apparatus was approximately13 kg.

Participants lay supine on the pendulum with the joint space of the right knee aligned with the leading edge of the pendulum frame (leg completely extended). The impacting leg was secured using a nylon strap positioned just proximal to the knee, while another nylon strap was placed over the hips, securing them to the pendulum firmly (Figure 10b) to prevent any appreciable movement of the body relative to the pendulum during impact. The left leg was flexed in order to prevent any contact with the force plate (see Section 3.2.2) at impact.

A sheet of ethylene and vinyl acetate (EVA) foam was placed over the force plate to simulate the effect of a shod impact condition while maintaining full ankle range of motion. Most running shoe midsoles are made from EVA foam, with a durometer rating in the range of 40 Asker C (soft) to 60 Asker C (hard) (Lafortune et al., 1996a; MacLean, Davis & Hamill, 2009). A 9 mm thick sheet of approximately 55 Asker C (medium) was used (EvaLite EVA 35 Shore A Durometer, National Shoe, Scarborough, Ontario, Canada). This thickness was used as it is a standard thickness manufactured by EvaLite.

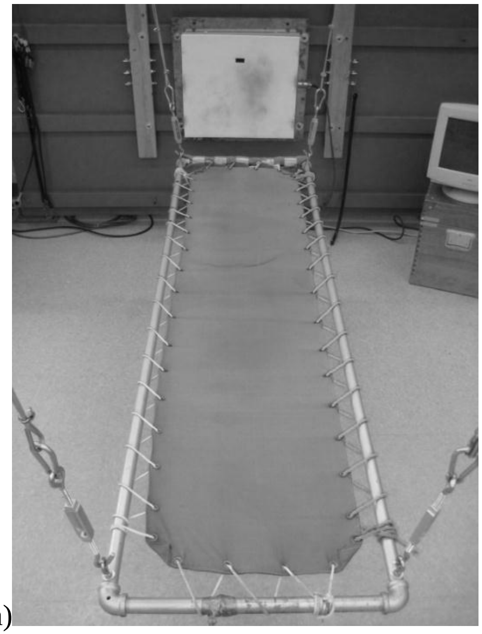
(a)

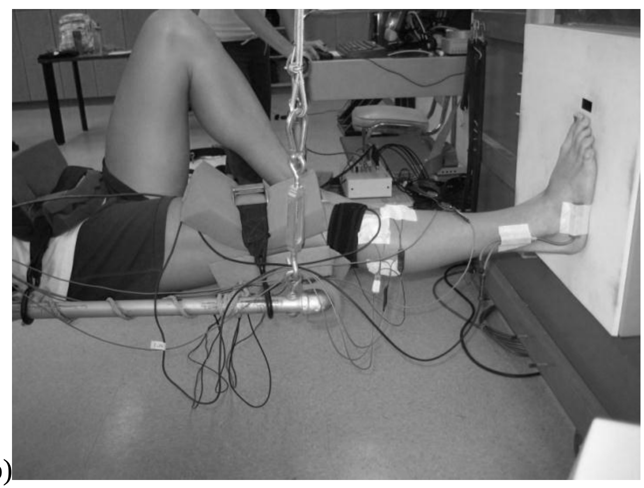
(b)

Figure 10. (a) Human pendulum apparatus in its rest position, suspended from the ceiling, (b) Participant instrumented in human pendulum. The participant's orientation represents the 0% maximum dorsiflexion angle of the ankle joint (see Section 3.4.2)

3.2.2 Force Plate

A force plate (AMTI-OR6-6-1000, A-Tech Instruments Ltd., Scarborough, ON, Canada, natural frequency of 1000 Hz) was used to measure impact forces; it was vertically mounted to the wall, so that it faced the incoming pendulum and was perpendicular to the floor. The plate was rigidly secured to a steel grid frame incorporated into the structure of the building itself (Figure 11). The grid was designed so that the force plate could be moved to accommodate different impacting heights and alignments, although the position of the plate remained constant in the study.

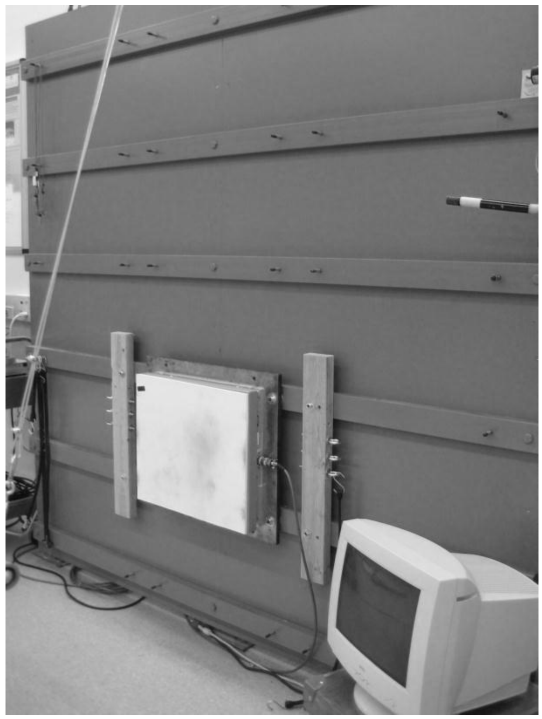

Figure 11. Steel grid incorporated into the building's wall to which the force plate was vertically mounted.

3.2.3 Velocity Transducer

A consistent impact velocity between 1.00-1.15 ms (Flynn et al., 2004; Holmes & Andrews, 2006) was required to control impact conditions. Velocity of the pendulum was monitored by a linear velocity/displacement transducer (Celesco DV301, Don Mills, ON, Canada), which was attached to its trailing edge. The velocity transducer is a permanent magnet generator that will have essentially instantaneous response to any pulling force that does not break the cable that is turning it.

3.2.4 Accelerometer

A custom made surface mounted tri-axial accelerometer (two accelerometer chips MMA1213D and MMA3201D, Freescale Semiconductor Inc., Ottawa, ON, Canada; frequency response range of +/- 50 G and +/- 40 G, respectively), was used to measure acceleration of the shank. The accelerometer was attached directly to the skin with double sided tape on the medial aspect of the tibial tuberosity. It was oriented such that the x-axis was parallel to the long axis of the tibia, which was the only channel analyzed. A knee strap (Tensor Brand, Oakville, ON, Canada) was then used to preload the accelerometer with a force of approximately 45 N (Flynn et al., 2004; Holmes & Andrews, 2006) (Figure 12).

3.2.5 Electrogoniometers

Two electrogoniometers (Biometrics SG110, Biometrics Ltd., Gwent, UK) were used to monitor joint angle over time; they were attached to clean, shaven skin across the knee and ankle joints using double sided tape (Figure 12). The electrogoniometers were attached to the lateral aspect of the ankle and medial aspect of knee joint of the right limb, in order to avoid other instrumentation. At the ankle, the fixed end-block of the electrogoniometer was placed in parallel to the fibula, while the telescopic block was placed in parallel to the fifth metatarsal. At the knee, the telescopic block was placed in parallel to an imaginary line between the medial condyle of the tibia and the medial malleolus, while the fixed end-block was placed in parallel to an imaginary line between the medial condyle of the femur and the inseam of the leg. The electrogoniometer affixed to the knee was used to measure the amount of knee angular movement resulting from impact.

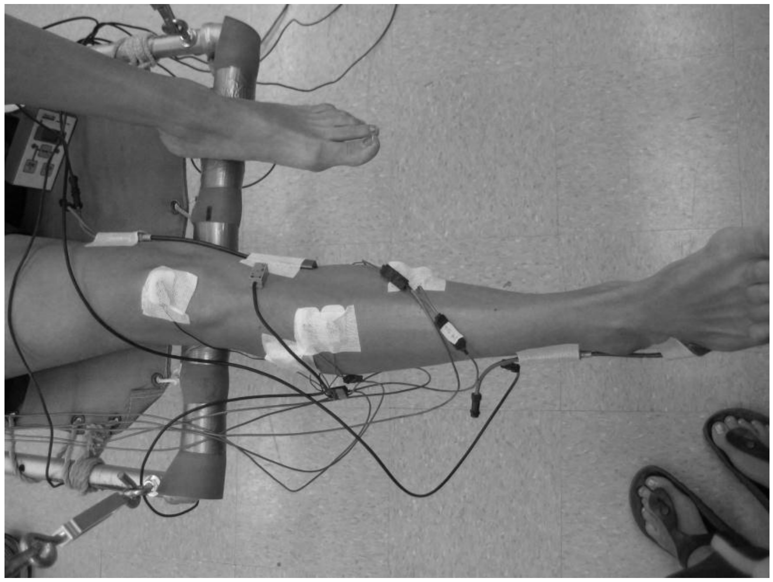

Figure 12: Electrogoniometer and accelerometer placement. Two electrogoniometers, one on the medial side at the knee joint and the other on the lateral side at the ankle joint, were applied to monitor joint angles. An accelerometer was attached to the medial aspect of the tibial tuberosity. The Velcro® strap used to preload the accelerometer is not seen in the diagram.

3.2.6 Electromyography (EMG)

Surface electromyography (sEMG) recordings were taken from the following muscles that cross the ankle joint: tibialis anterior (TA), fibularis longus (FL), lateral gastrocnemius (LG), medial gastrocnemius (MG), and soleus (SOL). Two Kendall bipolar disposable Ag/AgCl surface electrodes (23 mm x 33 mm: Tyco Healthcare, Chicopee, MA) were placed over the belly of each the aforementioned muscles, oriented parallel to the muscle fibres, with an inter-electrode distance of 2 cm (SENIAM, 1996). A ground electrode was placed over the surface of the patella (Figure 13a). To secure connecting wires and electrodes, a Hypafix dressing retention sheet (100 mm x 100 mm: BSN Medical, Hamburg, Germany) was applied over each set of electrodes.

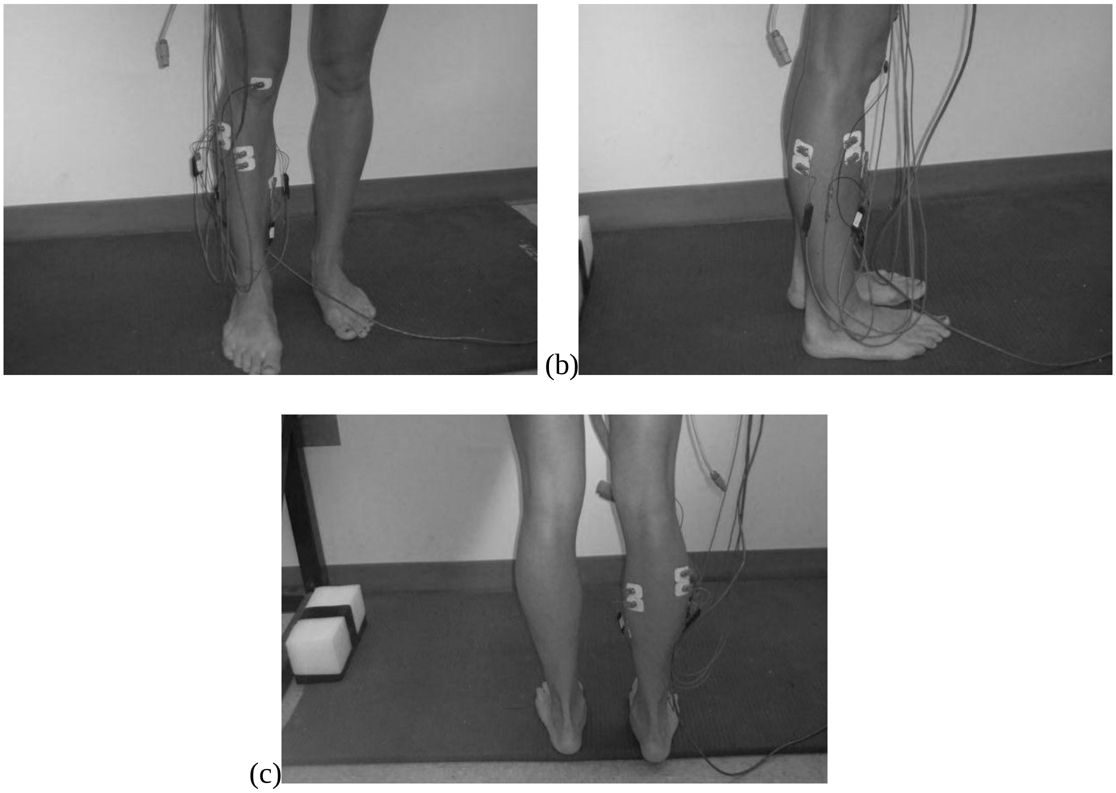

(a) (b) (c)

Figure 13: Electromyography (EMG) electrode placement. Electrodes were placed on the following muscles: tibialis anterior (TA), fibularis longus (FL), lateral gastrocnemius (LG), medial gastrocnemius (MG), and soleus (SOL). Figure 13a, b and c depict anterior, lateral, and posterior views, respectively.

3.3 Data Acquisition

Custom designed LabVIEW® software (Version 8.6, National Instruments, Austin, Texas) was used to acquire and process all collected data. All data were sampled at 4096 Hz. Raw data were output to Microsoft Excel 2007® files to be analyzed.

During the MVE trials, sEMG data were filtered online by full-wave rectification and then low pass filtered using a 2nd order Butterworth filter with a frequency cut-off of 1.5 Hz, and then normalized to each participant's maximal voluntary exertion (see Section 3.4.1). This provided a filtered value for the MVE trials to which sEMG data would be compared.

In the fatigue protocol (see Section 3.4.4), Mean Power Frequency (MPF) of the TA EMG was monitored in real time to indicate to the investigator when fatigue had been achieved. To do so, a Fast Fourier Transform Function was used to obtain the frequency characteristics of the signal, which was updated every second. The data were output to Microsoft Excel 2007® files to determine the time to fatigue (TTF) and change in the MPF over the fatigue protocol.

3.4 Procedure

Data collection was completed in one session, and is summarized in Figure 14. Participants were briefed on the purpose of the study and were required to read and sign the 'GHQ' (Appendix A) and the 'Consent to Participate in Research' form (Appendix B) approved by the University of Windsor's Research Ethics Board (Appendix C). Participant-specific information, including age, sex, and weekly mileage was recorded. Anthropometric measurements, including participant height, mass, and length of the foot segment were also taken. Foot segment length was taken from the centre of the lateral malleolus to the centre of the head of the second metatarsal. A digital picture of the participant's right leg was taken against a ruler which was positioned in the same plane; digitization of the picture provided coordinates to estimate the inertial components of the leg required for the JRS model (see Section 3.5) (Cort & Potvin, 2008).

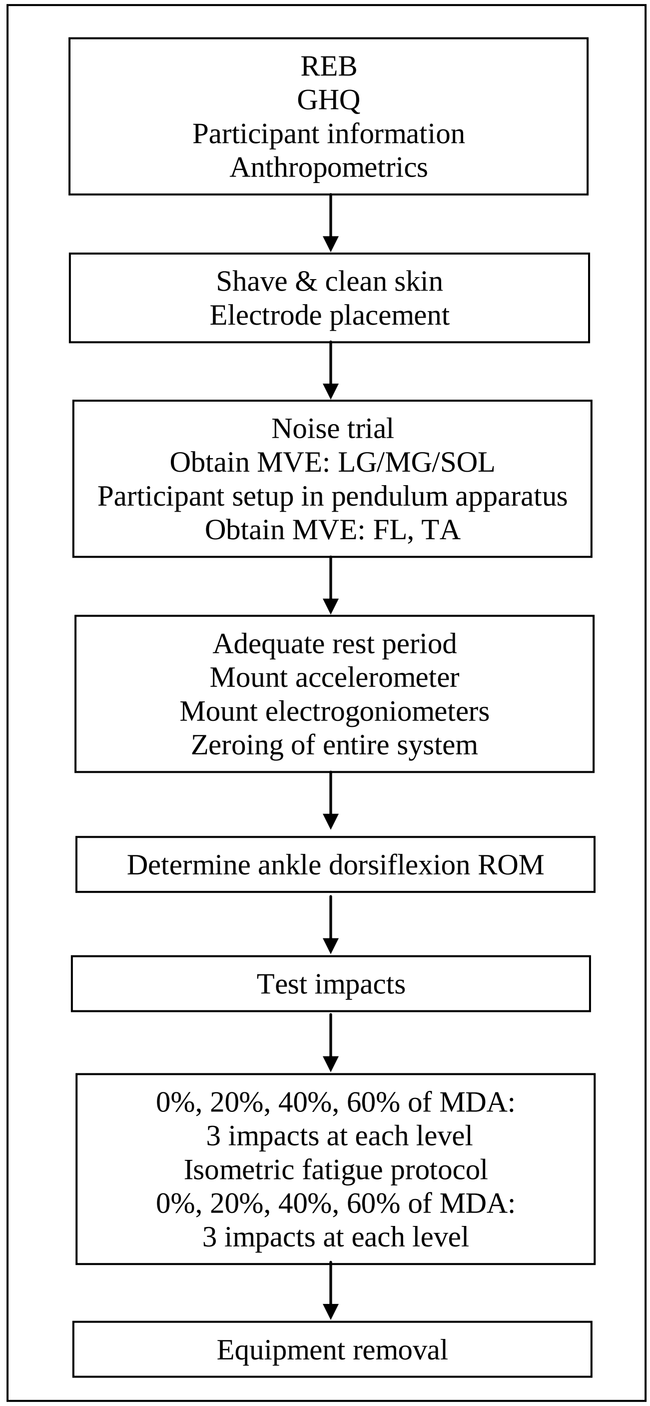

Figure 14. Flow diagram illustrating the experimental protocol. Abbreviations from the diagram are as follows: research ethics board (REB), general health questionnaire (GHQ), maximum voluntary exertion (MVE), lateral gastrocnemius (LG), medial gastrocnemius (MG), soleus (SOL), fibularis longus (FL), tibialis anterior (TA), range of motion (ROM), and maximum dorsiflexion angle (MDA).

3.4.1 Measuring Maximum Voluntary Exertion (MVE)

sEMG of the superficial muscles that cross the ankle joint was recorded throughout the impact trial to quantify muscular electrical activity. In preparation for electrode placement, areas of skin were shaved (if needed) and then cleaned with an isopropyl alcohol pad. Electrodes were placed on the skin overlying the TA, FL, LG, MG, and SOL muscles of the right (dominant) leg. Prior to taking MVEs, participants were placed in a relaxed position so that baseline muscle activity could be collected.

A measure of MVE for each muscle was taken in order to normalize the sEMG data generated during the impacting conditions. Participants were asked to exert a maximal contraction against dynamic resistance by ramping up the force exerted and attempting to hold it for three seconds, and then releasing. Dynamic resistance allowed the participant to exert maximal force by finding the optimal muscle length through the muscle's natural range of motion (ROM). Three trials for each MVE were taken, and adequate rest of about one to two minutes (adequate rest was confirmed by the participant) was given between trials. Verbal encouragement was given to participants to motivate them to contract maximally. The maximal EMG amplitude achieved during the three trials was used to represent the MVE.

The MVEs for the gastrocnemius and soleus muscles were taken while the participant was in a standing position. The LG, MG, and SOL muscles are often grouped together under the name of 'triceps surae' due to their similar function of plantarflexion. First, the participants were asked to do a standing calf raise in order to demonstrate the location of the muscle belly. Electrodes were then placed on the muscle belly of the LG and MG. Secondly, the muscle belly of the SOL was determined by having the participant plantarflex while sitting on the floor with the knee bent at 90°. The electrodes for the SOL were placed on the medial aspect of the SOL, distal to the LG (Figure 13c). Once electrodes were in place, the participant stood on a wood platform, where two straps of 5 cm wide nylon webbing were secured to a wood platform under the participant's feet, and placed over the participants' shoulders (Figure 15). The straps were adjustable and were tightened down so that the participant could stand in an upright position with minimal flexion. To limit shoulder contribution to vertical force production, participants' arms were folded across their chest while they maximally plantarflexed both feet at the ankles against the resistance of the shoulder straps, and held the contraction for three seconds. The shoulder straps had two additional adjustable straps across both the chest and back that ensured the straps going over the shoulders did not slip off laterally.

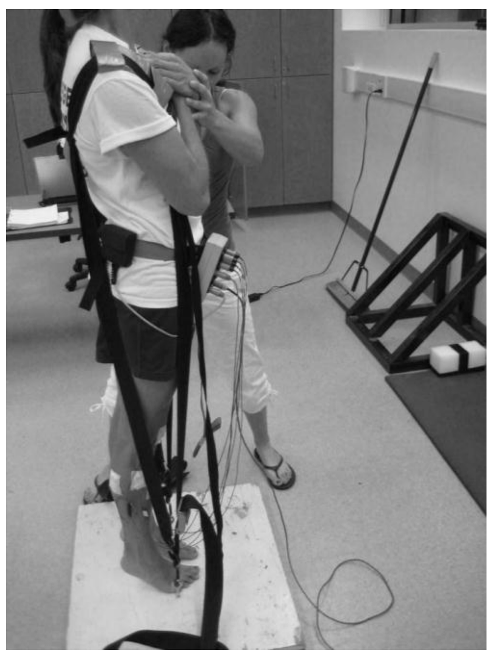

Figure 15: Maximum voluntary exertion (MVE) of the triceps surae group (lateral gastrocnemius (LG), medial gastrocnemius (MG), and soleus (SOL)) was taken by having the participant maximally plantarflex by performing a standing calf raise against padded shoulder straps.

Electrode location for the FL was determined by having the participant plantarflex and evert, while following the landmark of the muscle's origin (the head of the fibula) to the muscle belly (Figure 13a). Prior to obtaining the MVE of the FL, the participant was positioned in the pendulum apparatus (see Section 3.2.1). While lying supine on the pendulum (Figure 10b), manual resistance was provided by the investigator's assistant (Figure 16). Using their hands, the assistant resisted the eversion and plantarflexion movement caused by the FL muscle when the participants contracted.

Figure 16: The maximum voluntary exertion (MVE) of the fibularis longus (FL) was taken with the participant lying supine on the human pendulum apparatus. Manual resistance was provided by the investigator to prevent eversion and plantarflexion.

The MVE of the TA was taken against manual resistance, provided by the assistant (Figure 17). While lying supine on the pendulum apparatus (Figure 10), the assistant applied resistance to the dorsal surface of the foot with their left hand (the right hand supported the participant's heel), while the participant contracted against it.

Figure 17. The maximum voluntary exertion (MVE) of the tibialis anterior (TA) was taken against unilateral manual resistance, whereby the foot was allowed to move against the resistance provided by the investigator.

3.4.2 Electrogoniometer and Accelerometer Setup

While lying supine on the pendulum apparatus, the electrogoniometers were mounted (as described in Section 3.2.5), and zeroed as the participant remained still with the leg extended in the impact position. Dorsiflexion range of motion (ROM) of the ankle joint was then assessed. Baseline (zero dorsiflexion) was considered the neutral position where the ankle was flexed just enough for the plantar aspect of the foot to touch the force plate softly. While still lying supine on the pendulum apparatus, maximum dorsiflexion angle (MDA) (100%) was determined as the maximum angle that could be generated during voluntary dorsiflexion. Three trials were performed and the greatest angle achieved was taken as the MDA, a value from which subsequent target dorsiflexion angles were calculated.

Participants were then familiarized with the target ankle angles that were required to be achieved during the impacts (see section 3.5.3). The target ankle angle was displayed on a computer monitor (Figure 18) in the participants' field of view during each trial and was monitored throughout the impact. Participants were required to maintain 0%, 20%, 40%, and 60% of their MDA by aligning arrows representing their actual ankle angle and the target ankle angle on the computer monitor.

Figure 18. The target ankle angle was displayed on a computer monitor in the participants' field of view during each trial and was monitored throughout the impact. Participants were required to maintain 0%, 20%, 40%, and 60% of their maximum dorsiflexion by aligning the arrows represented on the computer monitor.

3.4.3 Impacts

Participants were instructed to lay supine on the pendulum apparatus with their right leg extended straight over the edge of the pendulum and their heel in slight contact with the force plate when the pendulum was at rest (Figure 10b). The pendulum was pulled back from the wall and released during several test trials in order to determine the pull-back distance required for each participant that would result in a target velocity of between 1.00 ms^{-1} and 1.15 ms^{-1} and impact force of between 1.8 and 2.8 times BW to be obtained (Flynn et al., 2004; Holmes & Andrews, 2006). The practice trials also helped to familiarize participants with the procedure and allowed the participants to achieve the muscle tuning effect (see section 2.4.3) in anticipation of the controlled impacts over the course of the session. Once impact conditions were determined, all transducers in system were zeroed with the participant and pendulum at rest. The force plate was zeroed by having the assistant hold the participant's foot in its rest position, just off the surface of the force plate.

Data collection was triggered manually by the investigator following an auditory queue presented by the data collection program. After the queue, the pendulum was released by the assistant. Data were recorded for a total of two seconds, which included the pendulum's swing phase (pre-impact), during the heel impact with the force plate (at impact), and after impact with the force plate (post-impact). When swung into the force plate, the participants were instructed to resist the forward motion of the pendulum at impact in order to maintain the impacting leg geometry. This was similar to what a runner would do during the heel-strike phase of running.

Participants were impacted three times at each of the dorsiflexion angles (0%, 20%, 40%, and 60% of MDA), with the trials presented in a randomized order. A fatiguing protocol then took place (see Section 3.5.4), after which participants were impacted three more times at each dorsiflexion angle (0%, 20%, 40%, and 60% of MDA). The order of these trials was also randomized.

3.4.4 Local Muscle Fatigue

A localized muscle fatigue (LMF) protocol was used to induce fatigue in the primary dorsiflexor, tibialis anterior (TA). The fatigue apparatus, which consisted of a resistive rubber band with a hook at each end, was stretched between steel eyebolts anchored in a wooden support structure, which was attached to the steel impact frame (Figure 19). The pendulum was held steady by the assistant with the participant's foot placed flat against the force plate such that the forefoot was located under the rubber band. The participant was instructed to dorsiflex against this resistance at a level of 50% of their MVE, until fatigued. The level of muscle activity was monitored by the participant on a video monitor placed in their visual field.

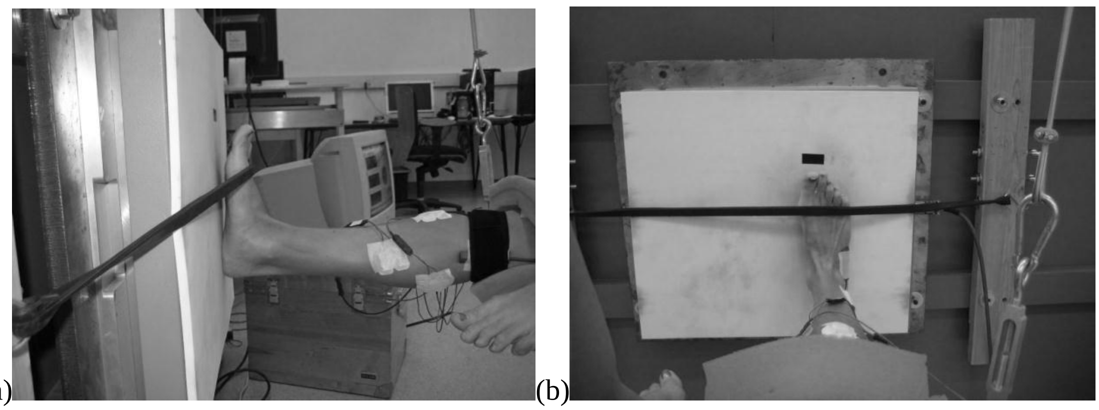

(a) (b)

Figure 19. The fatigue apparatus, which consisted of a resistive rubber band with a hook at each end, was attached to the steel grid. Local muscle fatigue (LMF) of the tibialis anterior (TA) was achieved through isometric dorsiflexion against the rubber band.

During the fatiguing condition, the frequency and amplitude of the TA's EMG signal were monitored online by the investigator. A decrease in MPF of at least 15% has been shown to be indicative of fatigue (Ament, Bonga, Hof & Verkerke, 1993); however, previous studies in our lab employing this measure have found drops much greater than 15% during this protocol (Flynn et al., 2004; Holmes & Andrews, 2006). Fatigue was also indicated by the inability of participants to maintain 50% MVE, and by muscle trembling and an inability to maintain ankle joint angle (Holmes & Andrews, 2006). A Fast Fourier Transform Function was used to obtain the frequency characteristics of the signal, and the MPF was assessed in real time and presented visually to the investigator on a computer monitor. The drop in MPF was later calculated using a four-point moving average of the start and end values of MPF. When fatigue was achieved, the fatigue apparatus was removed as quickly as possible (within ten seconds) from the pendulum apparatus and the fatigued impacts were performed.

3.5 Data Analysis

Custom designed LabVIEW® software (Version 8.6, National Instruments, Austin, Texas) was used to acquire and process all collected data, and then raw data were output to Microsoft Excel 2007® files to be manipulated. The cutoff frequency for each transducer (Table 1) was determined by performing residual analyses by hand (Winter, 2005) between the filtered and unfiltered signals over a range of cutoff frequencies.

Table 1. Filtering specifications used during analysis.

Transducer	Filter Used	Cutoff frequency (Hz)
Force plate	4th order Butterworth	115
Velocity transducer	4th order Butterworth	25
Accelerometer	4th order Butterworth	125
Electrogoniometer	Critically damped	5
EMG	2nd order Butterworth	2.5

Ankle angle at impact rarely matched the target angle exactly. The amount of permissible variation around the target was determined by first plotting the difference between the target and actual ankle angle at impact. It was then estimated, and confirmed by counting a significant number of trials, that a variation within 10% of target dorsiflexion angle would be used to indicate a ‘good’ trial. The criterion for selecting this amount of variation was based on having at least two, if not all three trials, available to use for analysis.

Knee angle was recorded to ensure that the leg remained straight during impact. The knee flexion angle in response to impact (or change in knee joint angle) was quantified as the difference between the knee angle at impact and the peak deflection of the knee angle curve following impact.

A custom LabVIEW® program was written to detect the point at which impact occurred in the force plate and accelerometer signals. Each signal was visually checked to verify the accuracy of impact determination by the program. The following dependent variables were then manually extracted from the filtered curves using Microsoft Excel 2007®: peak force, velocity at impact, ankle angle at impact, change in knee angle, PA, TPA, and AS, and placed in a spreadsheet to prepare for statistical analysis.

To determine the percent drop in TA mean power frequency (MPF), as a measure of fatigue, the MPF signal was graphed using Microsoft Excel 2007®, and a linear trend line was applied through the data that demonstrated a decrease in MPF. The equation of the line was used to determine the start and end values for the MPF signal. The y-intercept was used as the MPF start value, while the x-value was calculated using the sample point at which the MPF stopped decreasing. This sample point was selected visually as the point on the line graph at which MPF stopped decreasing. The point of interest was then confirmed by scanning the data set to determine the exact point in time at which MPF stopped decreasing. The difference between these points was used to calculate the percent drop in MPF.

The scaled photograph of each participant's leg was digitized. Digitization points were applied in Microsoft Powerpoint 2007®, saved in the '.gif' format, and opened in

Windows Vista Paint Application®. Using the drawing tool, coordinates were given when the tip was at the centre of the digitization point. Coordinates were converted from pixels to metres using a scale ruler taken in the photograph (Figure 20). This digitization allowed coordinates for the heel, toe (TTIP), ankle joint centre (AJC), and knee joint centre (KJC) to be determined, which were then input into the model (see below) as anthropometric factors. Coordinates for the centre of mass (COM) and radius of gyration (ROG) were calculated, based on de Leva's (1996) adjusted segment parameters.

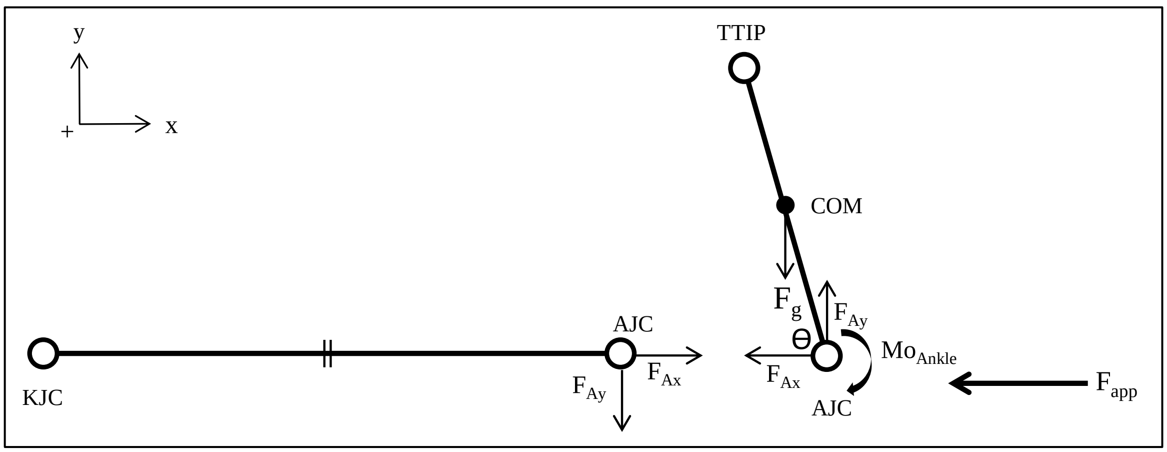

Figure 20. Free body diagram of the foot, oriented as the participant is lying on the pendulum in the supine position. Forces other than joint reaction forces on the leg (F_{Ax}, F_{Ay}) are not included, as the leg is assumed not to move. Coordinates for the knee joint centre (KJC), ankle joint centre (AJC), and toe (TTIP) were determined by digitization, while the centre of mass (COM) and radius of gyration were calculated using de Leva's (1996) segment parameters. The force applied by the perturbation (F_{app}) and the combined forces of the muscles crossing the ankle joint (F_{muscle} not shown) contribute to the moment about the ankle (Mo_{Ankle}), which represent both the joint reaction moment and the EMG-derived moment, after the perturbation.

The sEMG data were filtered using LabVIEW® software, and the mean EMG value of each of the three time periods of interest (see below) were placed in a Microsoft Excel 2007® spreadsheet to prepare for statistical analysis.

Joint rotational stiffness of the ankle (AJRS) was obtained from the JRS model by Cort and Potvin (2008) (Figure 21). Custom LabVIEW® software provided the necessary calculations to determine the individual muscle contributions to JRS (MRJS), which when summed, provided the AJRS in the sagittal plane.

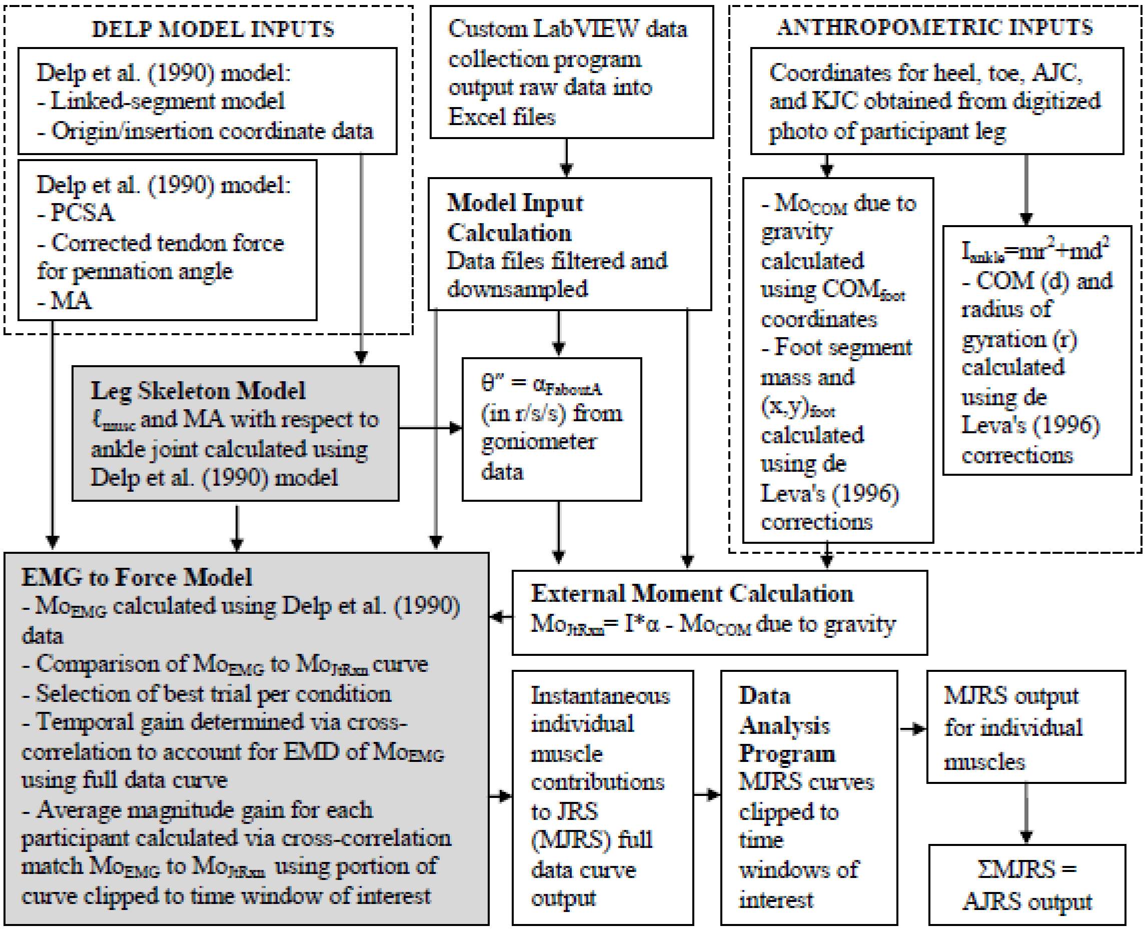

Figure 21. Flow diagram illustrating the model from which ankle joint rotational stiffness (AJRS) was obtained. Abbreviations from the diagram are as follows: physiological cross-sectional area (PCSA), moment arm (MA), muscle length (ℓ_{musc}), EMG-driven moment (Mo$_{EMG}$), joint reaction moment (Mo$_{JtRxn}$), electromechanical delay (EMD), ankle joint centre (AJC), knee joint centre (KJC), centre of mass (COM), distance from ankle to COM (d), distance from ankle to radius of gyration (r), joint rotational stiffness (JRS), and individual muscle JRS (MJRS).
(Adapted from Cort & Potvin, 2008)

The first part of the model, which consisted of the 'Leg Skeleton Model,' used the linked-segment model of the human lower extremity and origin and insertion coordinate data of the muscles and tendons of the lower extremity, as defined by Delp et al. (1990).

Muscles included in the full Delp et al. (1990) model consisted of those in the anterior compartment of the leg: TA, extensor digitorum longus (EDL), extensor hallucis longus (EHL), and fibularis tertius (FT), the posterior compartment of the leg: LG, MG, SOL, and the lateral component of the leg: FL and fibularis brevis (FB). Because of their common peroneal innervation, and thus common nervous drive, the EMG of the TA was used for the EDL and EHL in the model. However, the model outputs indicated that neither the EDL nor the EHL contributed significantly to the AJRS. The FB and FL share a common innervation (superficial fibular nerve), while the FT has a different innervation (deep fibular nerve). The EMG activity of the FB was thus taken from the most lateral of the three muscles, the FL, while no EMG data were available for the FT. Results of the model also indicated that the FB did not contribute significantly. The Delp et al. (1990) model provided the lines of action of the musculotendonous structures in relation to the joints of the lower extremity. It also allowed changes in musculoskeletal geometry to be biomechanically assessed, as musculoskeletal geometry determined the length of the musculotendinous unit (i.e. distance from origin to insertion). The inputs to the Leg Skeleton Model allowed muscle lengths (ℓ_{musc}) and moment arms (MA) of the muscles crossing the ankle joint to be calculated.

The external moment calculation required the joint angle time history as input, which was double differentiated using the central difference method, and then filtered, to produce the angular acceleration (α) of the foot about the COM. The moment of inertia (I_{ankle}) of the foot about the ankle, based on de Leva's (1996) segment inertia parameters, was then used with the angular acceleration to calculate the external moment ($Mo = I*\alpha$). Due to the straight-legged orientation of the human pendulum, the knee joint was assumed to be stationary at impact, and thus any slight motion of the knee that was measured by the other electroniometer was not incorporated into the model. Once acceleration due to gravity was incorporated, the calculation dictated force production and the resulting required moment about a joint (Mo_{JtRxn}).

Using the calculated ℓ_{musc} and MA data, the processed EMG data from the muscles crossing the ankle, and the muscle physiological cross-sectional area (PCSA) and pennation angle corrections (Delp et al., 1990), the 'EMG to Force Model' provided an EMG-based moment (Mo_{EMG}) and the instantaneous MJRS values for each muscle, which when summed produces the AJRS. PCSA is the area of a transverse section of muscle and reflects its ability to generate muscle force. The pennation angle dictates the line of action and direction in which a muscle generates force, and must be accounted for when describing force output of a muscle. Typically, a greater pennation angle results in a greater PCSA, and therefore higher force production. The Mo_{EMG} curve was calculated, which then allowed a comparison between the internal and external joint moments. The Mo_{EMG} counteracted the Mo_{JtRxn}, as shown by the muscles crossing the ankle joint (Figure 9), creating a moment equal in magnitude and opposite in direction to that generated by the joint reaction to external factors. The goal of this step was to match the Mo_{EMG} to the Mo_{JtRxn} curve to show that the moment achieved internally (Mo_{EMG}) matched what was being seen externally (Mo_{JtRxn}) (Figure 22).

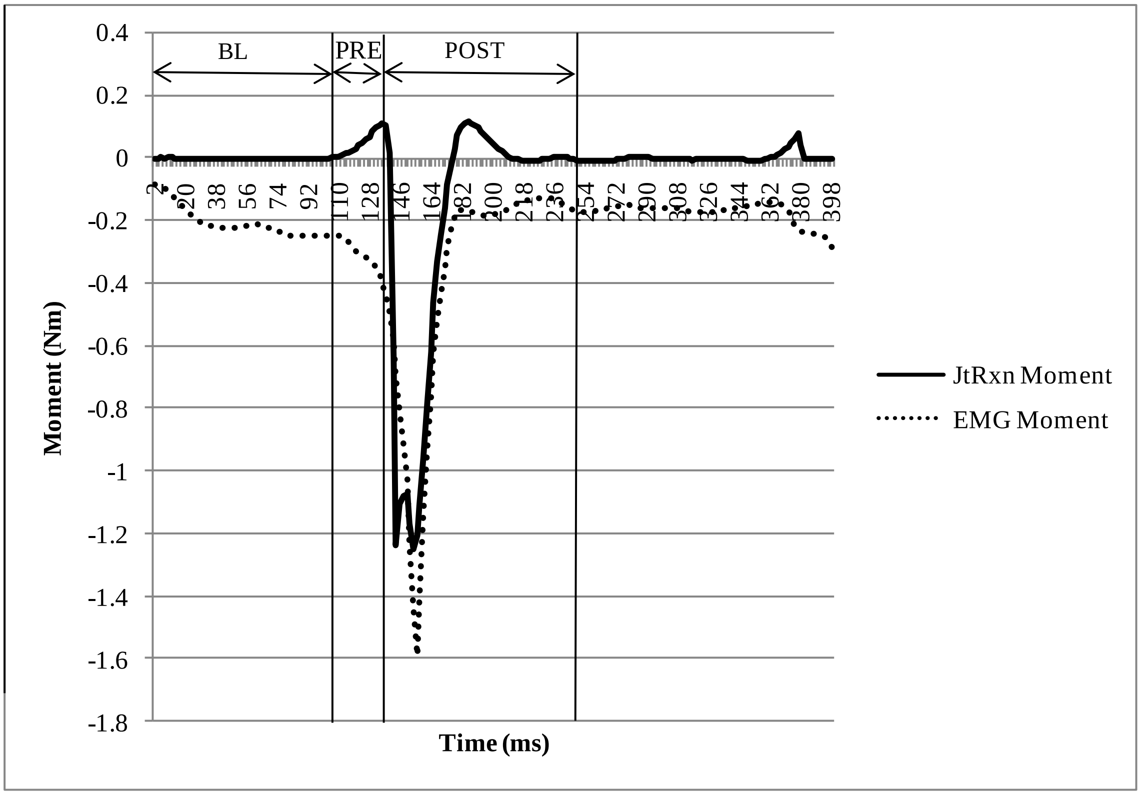

Figure 22. A typical trial of where the EMG-based moment (Mo_{EMG}) was matched to the joint reaction moment (Mo_{JtRxn}) curve using gain factors for both magnitude and in time. An average gain factor for each participant was used to match the magnitude of the two curves, while an individual gain factor was used to match the temporal aspect of the two curves. Baseline (BL), pre-impact (PRE) and post-impact (POST) time periods are labeled.

In order to compare the Mo_{EMG} and Mo_{JtRxn} curves, the Mo_{EMG} had to be gained (the application of an average ratio of the signal output to the signal input) both in time and magnitude to match the Mo_{JtRxn} curve as closely as possible. The Mo_{EMG} was treated with an electromechanical delay (EMD) factor in order to align the two curves in time. EMD is the delay between the brain's signal for the muscle to contract and the development of muscle tension and is known to vary between different muscles. The EMG to Force Model (Figure 21) incorporated nine different muscles, crossing the ankle joint, each with its own EMD. Due to the varying contributions of each muscle across ankle angles and fatigue conditions, the EMD changed with each trial. Correlation analysis revealed that using an individual EMD for each trial (r = 0.60 (0.13)) provided a better representation of the matching of the Mo_{EMG} and Mo_{JtRxn} curves than using a mean EMD for all trials (r = 0.36 (0.23)) of a participant. The Mo_{EMG} curve was also treated with a gain factor to match its magnitude to that of the Mo_{JtRxn} curve as closely as possible. An average gain factor for each participant was used in this case (as a function of PCSA), because the gain factor is based on the maximum output of tension possible for the muscles involved, which is a constant value within a person.

The pendulum impacts controlled many aspects of the applied perturbation, including joint orientation, velocity, and force of impact. However, the ability of the participant to maintain the same joint position and muscle activation for every trial, as instructed, was limited. When comparing the Mo_{EMG} to the Mo_{JtRxn} curves in the EMG to Force Model, it was obvious that some participants were not capable of activating their leg musculature in the same way for every impact. This in turn led to inconsistency in terms of how the Mo_{EMG} and Mo_{JtRxn} curves matched in time and amplitude. For this reason, one trial was chosen as a best representation of the Mo_{EMG} matching the Mo_{JtRxn} in order to generate one JRS value during each time period for every combination of fatigue and ankle angle conditions.

After filtering, the data were clipped into 400 ms intervals and normalized to the time of impact. This was done to decrease the time needed to process the signals. After the data were run through the model, they were then trimmed into the three time periods of interest surrounding impact (totaling 250 ms): -150 ms to -50 ms (baseline), -50 ms to 0 ms, or impact (pre-activation), and 0 ms to +100 ms (post-impact). These windows were chosen because 50 ms prior to impact has been shown to be the period where pre-activation, or muscle tuning, occurs (Wakeling et al., 2001), and 100 ms after impact was the average period of time for the tibial acceleration waveform to return to baseline. After the temporal gain was calculated to account for EMD using the entire curve, data were output based on the 250 ms samples of interest, and an appropriate gain factor was assigned to match the Mo_{EMG} to the Mo_{JtRxn} curve both in time and magnitude. Resulting MJRS and AJRS outputs were used for statistical analysis.

There were three other dependent variables that were obtained from the accelerometer data, which enabled the relationship between the ankle JRS (AJRS) and tibial response during impact to be quantified. The measures of peak acceleration (PA), time to peak acceleration (TPA), and acceleration slope (AS) were obtained, using LabVIEW® software, from the shank acceleration waveform. AS was measured from the linear portion of the acceleration waveform, recorded by the accelerometer at the tibial tuberosity, between 30%-70% of the rise in the amplitude between onset and peak acceleration (Duquette and Andrews, 2010a, b; Holmes &Andrews, 2006) (Figure 2).

3.6 Study Design

The dependent variables for this study were: peak acceleration (PA), time to peak acceleration (TPA), acceleration slope (AS), each individual muscles' contribution to JRS (MJRS), including LG, MG, SOL, FL, and TA, and the AJRS (calculated as the sum of the MJRS values). There was one between-participant variable (sex), consisting of two levels (female and male) and two within-participant variables: fatigue level (non-fatigue and fatigue) and dorsiflexion angle (0%, 20%, 40%, and 60% MDA). The study design is illustrated in Table 2.

Table 2. Study design consists of one between-participant variable (sex: female/male) and two within-participant variables (fatigue: non-fatigue/fatigue and dorsiflexion angle: 0%, 20%, 40%, and 60% of maximum dorsiflexion angle (MDA)).

	Within-Participant Variables: Fatigue (Non-Fatigue/Fatigue) Dorsiflexion Angle (% Maximum Dorsiflexion Angle)							
	Non-Fatigue				Fatigue			
	Dorsiflexion Angle				Dorsiflexion Angle			
Between-Participant Variable: Sex (M/F)	0%	20%	40%	60%	0%	20%	40%	60%
Female								
Male								

3.7 Statistical Analysis

Independent t-tests for age, height, mass, body mass index (BMI), foot segment length, maximum dorsiflexion angle (MDA) and weekly mileage were performed to determine if there were any differences in participant details between the sexes.

Impact trials were considered acceptable if the ankle angle at impact was within 10% of the target angle. Trials were excluded from analysis if they were found to be more than two standard deviations from the group mean value for ankle angle across all trials under the specific experimental condition. Missing data were filled by group mean substitution.

The value of PA, AS, and TPA associated with the trial selected in the JRS model was used for all analyses of tibial response variables. A repeated measures ANOVA (2 x 2 x 4: sex x fatigue level x ankle angle) was performed to detect any significant differences. The same repeated measures ANOVA was used to analyze knee angle data. The value of EMG for the LG, MG, SOL, FL, and TA associated with the trial selected in the JRS model was used to analyze the muscle activation in three time periods around the impact (baseline, pre-impact and post-impact). A mixed ANOVA (2 x 2 x 3 x 4: sex x fatigue level x time period x ankle angle) was performed to detect any significant differences. The same design was used to analyze AJRS and MJRS for each muscle. Alpha (α) was set at 0.05 for all comparisons. Any interactions arising from the ANOVA tests had to account for at least 1% of the total variance to be included in further analyses (Keppel, 1982). Tukey's HSD post hoc tests were performed on significant main effects and interactions.

Pearson product-moment correlations were performed between the overall AJRS values at baseline (-150 ms to -50 ms), pre-impact (-50 ms to impact), and after impact (impact to 100 ms), with each TRP (PA, AS, and TPA), to determine the magnitude and direction of the relationship between these variables as dorsiflexion angle increased. Relationships were classified according to the guidelines suggested by Cohen (1988) (Table 3). The correlation coefficient obtained was then squared (r^2=coefficient of determination) to quantify the amount of variance shared between the variables. This was performed separately for both the non-fatigue and fatigue conditions and for both male and female participants. In addition, correlation coefficients were calculated across time periods, while collapsing both across sex and then across fatigue.

Table 3. Relationship classification based on correlation coefficient magnitude (effect size). (Cohen, 1988).

Relationship Classification	Negative	Positive
None	-0.09 to 0.0	0.00 to 0.09
Small	-0.3 to -0.1	0.1 to 0.3
Medium	-0.5 to -0.3	0.3 to 0.5
Large	-1.0 to -0.5	0.5 to 1.0

CHAPTER IV

RESULTS

4.1 Participant Details

Male and female participants differed on average in three of the eight personal variables evaluated. Male participants (n=15) had significantly greater body mass [t (24) = -4.071, $p < 0.05$], height [t (24) = -3.879, $p < 0.05$], and foot length [t (24) = -3.066, $p < 0.05$] than females (n=11). The groups were statistically similar for all other personal variables (Table 4).

Table 4. Mean (SD) participant details (n = 26). * p < 0.05

Sex	# of participants	Age (years)	Mass (kg)	Height (m)	Body Mass Index (kg/m^2)	Foot segment length (cm)	km run per week (km/wk)	Max dorsi-flexion (deg)
Female	11	22.0 (2.9)	57.0* (6.3)	1.66* (0.05)	20.6 (1.9)	14.8* (0.7)	38.0 (12.9)	15.6 (2.9)
Male	15	23.3 (3.4)	66.6* (5.7)	1.76* (0.07)	21.5 (1.6)	15.7* (0.8)	33.7 (13.2)	17.1 (3.8)
Overall	26	22.7 (3.2)	62.5 (7.6)	1.72 (0.08)	21.1 (1.7)	15.3 (0.9)	35.5 (13.0)	16.5 (3.4)

4.2 Impact Parameters

Impact force and velocity were controlled to create impact conditions that were as similar as possible across participants. Mean (SD) impact force for all participants was 2.2 (0.3) times body weight (BW), falling within the target range of 1.8 – 2.8 BW. The mean (SD) impact velocity was 1.03 (0.04) ms^{-1}. Only two participants had mean impact velocities (0.97 (0.01) ms^{-1} and 0.96 (0.02) ms^{-1}) that fell outside the target range of between1.00 ms^{-1} and 1.15 ms^{-1}.

Participants were generally able to successfully impact the force plate within 10% of the target ankle angle, with only two participants missing data for two trials each over the entire study sample. These missing data were given the group mean value for the corresponding condition. Ankle angle at impact varied between participants as a percent of their maximum dorsiflexion angle (MDA). A significant main effect for ankle angle [F (3, 75) = 477.242, $p < 0.05$] indicated that a 20% increase in targeted dorsiflexion angle corresponded with an increase in actual ankle angle between 2.0 degrees and 4.4 degrees across participants (Figure 23).

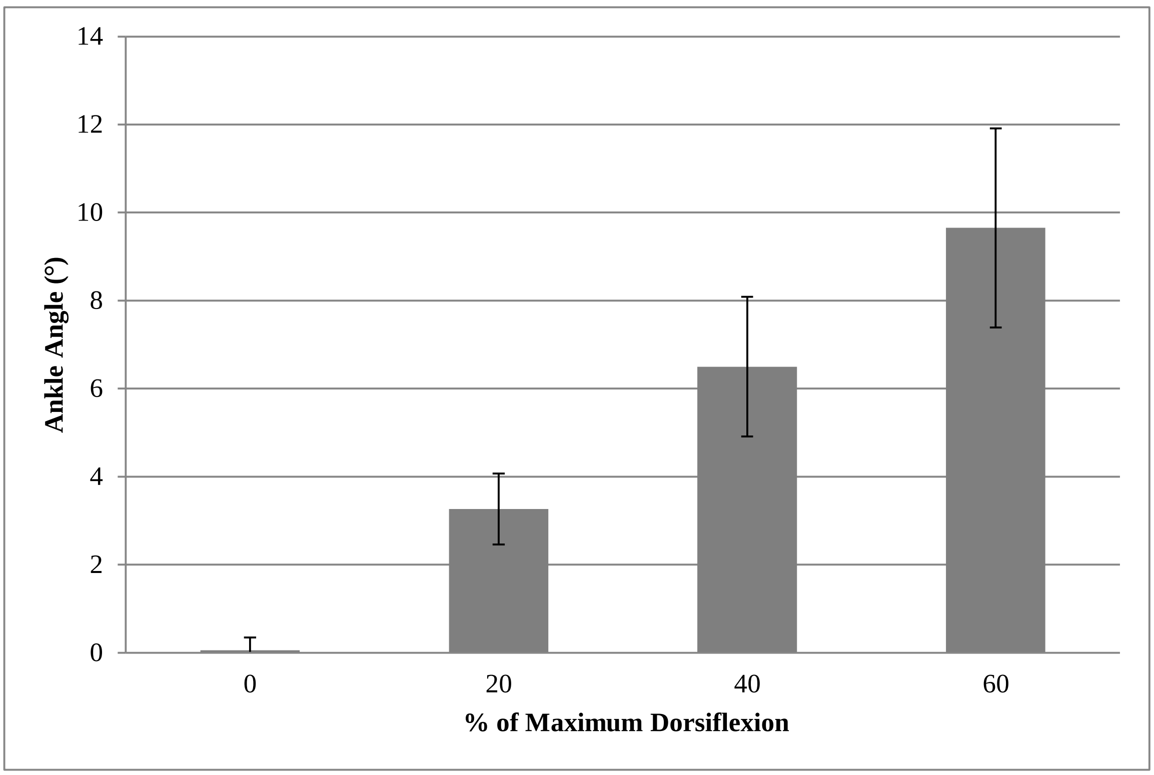

Figure 23. Mean (SD) ankle angle as a function of targeted dorsiflexion angle (% of maximum dorsiflexion angle). Mean ankle angles at all target angles were found to be significantly different from one another (n = 26). * $p < 0.05$

Although the participant's leg was restrained in a straight-legged orientation during impact, there was some knee joint motion. The knee joint flexed on average 4.6

(1.9) degrees across participants at impact. No significant differences for knee angle were revealed between male and females participants, therefore, the knee angle data were collapsed across sex. No significant main effects were found for either fatigue or ankle angle.

4.3 Tibial Response

In the current study, no significant main effects of sex were found for tibial response variables (PA, TPA, AS). Therefore, tibial response variables were collapsed across sex, and a 2-way repeated measures ANOVA (2 x 4: fatigue x ankle angle) was performed for each dependent variable.

4.3.1 Peak Acceleration (PA)

A significant main effect was revealed for ankle angle at impact [F (3, 75) = 6.139, $p < 0.05$], such that PA was generally found to decrease as dorsiflexion angle increased (Figure 24).

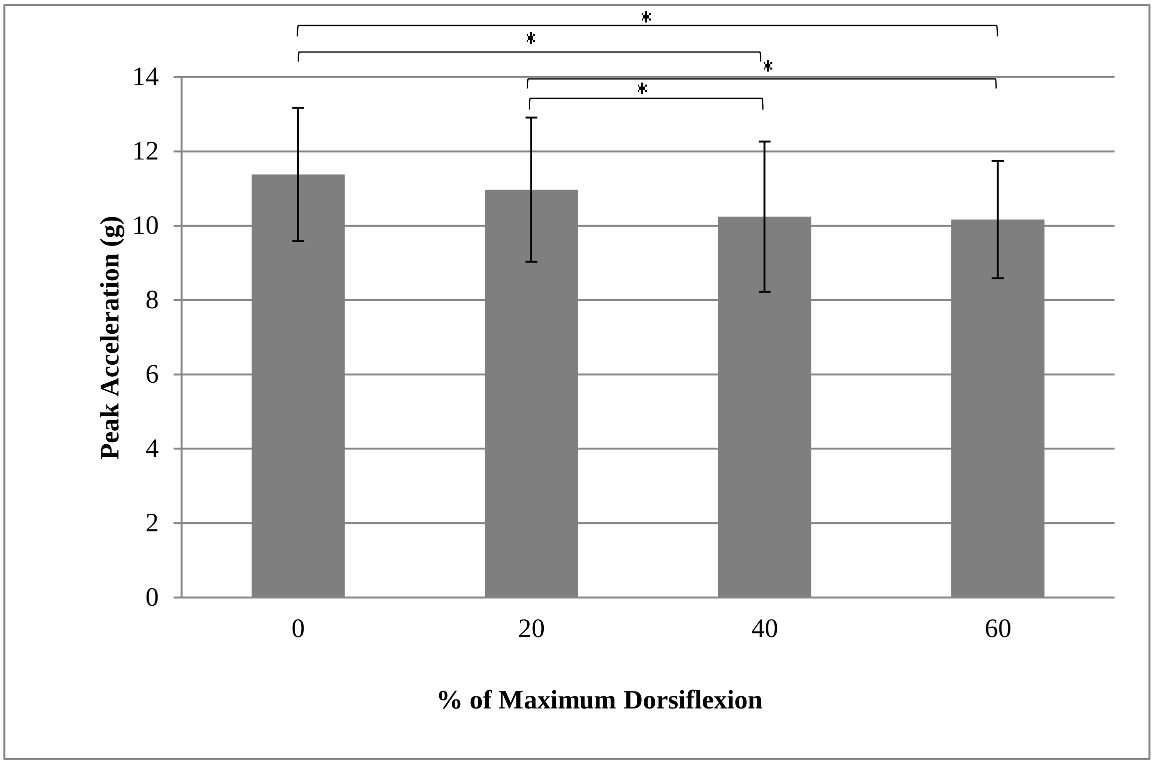

Figure 24. Mean (SD) peak acceleration as a function of targeted dorsiflexion angle (% of maximum dorsiflexion angle) (n = 26). * p < 0.05

4.3.2 Time to Peak Acceleration (TPA)

Mean TPA values did not vary significantly across ankle angles and between the fatigue conditions. The range of values for TPA was 15.8 – 20.3 ms across conditions. No significant main effects or interactions were revealed.

4.3.3 Acceleration Slope (AS)

Similar to TPA, no significant main effects or interactions were revealed for AS values across all levels of ankle angle or between fatigue conditions. The range of values for AS was 857 – 1243 g/s across conditions.

4.4 Fatigue

4.4.1 Time to Fatigue and Mean Power Frequency

No significant differences were found between sexes for TTF or MPF values. The overall mean TTF across all participants was 57.6 (14.0) seconds and the average percent drop in MPF was 26.1 (6.9) percent (Table 5). One participant was removed from this analysis because his z-score for percent drop in MPF was 2.74 standard deviations below the mean. Although he only displayed a 2.7% drop in MPF, his TTF was 71.2 seconds and he exhibited all other signs of fatigue. The MPF trace for this participant was highly variable and an initial stable baseline could not be established. Consequently, the percent drop in MPF could not be determined. The overall average EMG data for TA across all ankle angles of this participant was slightly higher (25.7 (12.4) % MVE) than the average of all other participants (16.5 (9.7) % MVE), but was not outlying; they were therefore not removed from further EMG analyses.

Table 5. Mean (SD) values for TTF and MPF (n = 25).

Sex	# of participants	TTF (seconds)	Drop in MPF (%)
Female	11	62.9 (11.7)	25.1 (5.7)
Male	14	53.5 (14.7)	26.9 (7.9)
Overall	25	57.6 (14.0)	26.1 (6.9)

4.5 Electromyography (EMG)

Significant main effects of sex, time period, fatigue, and ankle angle at impact on EMG were revealed from the statistical analysis. Main effects were subjected to post-hoc analysis, as none of the following interactions accounted for at least 1% of the variance: TA (time and ankle angle [$F(6,144) = 18.673$, $p < 0.05$ ($\omega^2 = 0.006$)]), LG (ankle angle and sex [$F(3,72) = 3.625$, $p < 0.05$ ($\omega^2 = 0.0009$)], time and ankle angle [$F(6,144) =$

3.913, $p < 0.05$ ($\omega^2 = 0.002$)]), SOL (time and ankle angle [$F(6,144) = 2.883$, $p < 0.05$ ($\omega^2 = 0.002$)]), FL (time and ankle angle [$F(6,144) = 14.669$, $p < 0.05$ ($\omega^2 = 0.005$)], and fatigue and ankle angle [$F(3,72) = 2.935$, $p < 0.05$ ($\omega^2 = 0.001$)]).

4.5.1 Main Effect of Sex

The mean EMG over all time periods was greater for females than for males for all muscles evaluated, but differences between the sexes were only significant for two muscles, LG [$F(1,24) = 15.183$, $p < 0.05$] and FL [$F(1,24) = 18.884$, $p < 0.05$] (Figure 25). The percent difference in EMG for the LG and FL was 52.1% and 53.5% greater for females than for males, respectively.

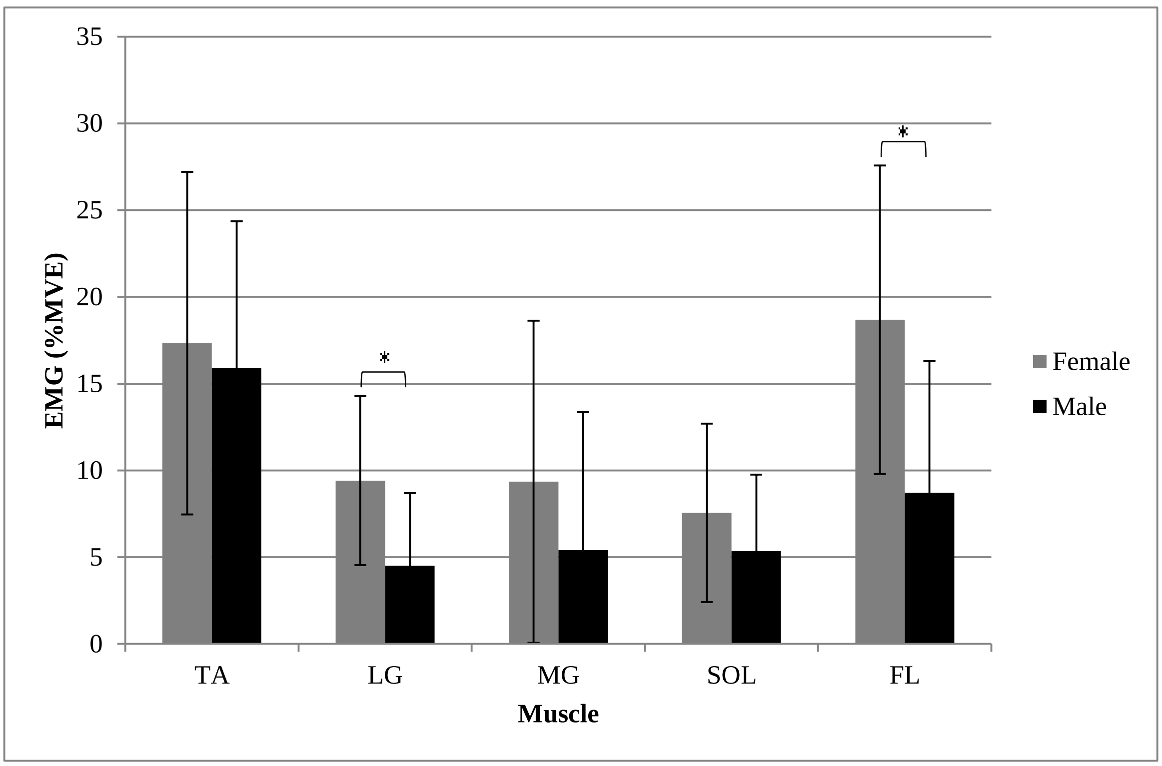

Figure 25. Main effect of sex for EMG (n = 26). * p < 0.05

4.5.2 Main Effect of Time Period

The mean EMG increased for all muscles between baseline and pre-impact periods on average, but significant main effects for time period were only found for the TA [$F(2,48) = 10.275$, $p < 0.05$], LG [$F(2,48) = 6.817$, $p < 0.05$], MG [$F(2,48) = 4.960$, $p < 0.05$], and SOL [$F(2,48) = 7.057$, $p < 0.05$] (Figure 26). Muscle activation of the plantarflexors increased significantly by a percent difference of 10.8% for the LG, 31.8% for the MG, and 22.6% for the SOL, but not for TA (dorsiflexor) between the baseline and pre-impact periods. Significant decreases were seen compared to post-impact for the TA between both the baseline (11.1 % difference) and pre-impact (17.5 % difference). Between the baseline and post-impact conditions, significant increases in mean EMG were seen for the LG (11.6 % difference) and SOL (27.2 % difference).

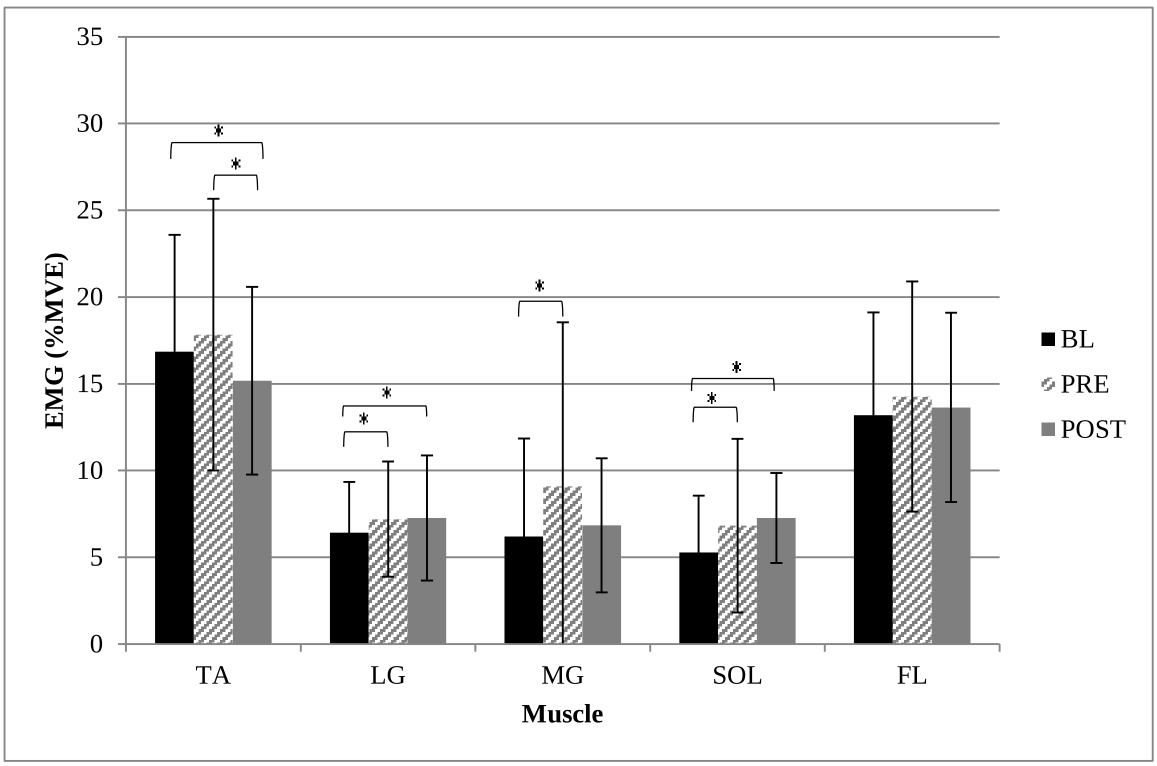

Figure 26. Main effect of time period for EMG. Average EMG was measured for each muscle at baseline (BL), pre-impact (PRE), and post-impact (POST) intervals (n = 26). * p < 0.05

4.5.3 Main Effect of Fatigue

After the fatigue protocol, the mean EMG amplitude decreased for all muscles. However, significant decreases were only seen for TA [$F(1,24) = 13.016$, $p < 0.05$], SOL [$F(1,24) = 7.455$, $p < 0.05$], and FL [$F(1,24) = 10.197$, $p < 0.05$] (Figure 27). EMG activity decreased by a percent difference of 18.5%, 11.7%, and 10.7% for TA, SOL and FL, respectively.

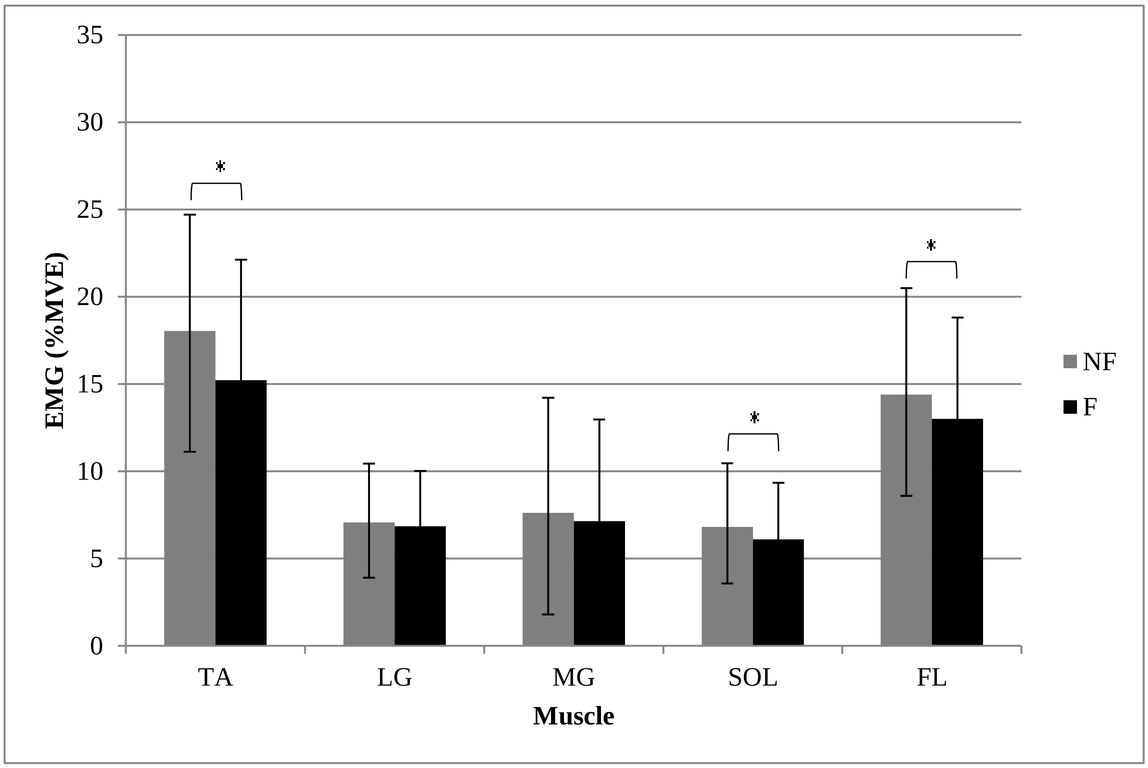

Figure 27. Main effect of fatigue for EMG. Average EMG was measured for each muscle in the non-fatigue (NF) and fatigue (F) conditions (n = 26). * p < 0.05

4.5.4 Main Effect of Ankle Angle at Impact

An increase in the mean EMG was seen for the TA as the dorsiflexion angle increased. EMG of the TA was shown to increase by a percent difference of 23.9 (5.9) %, on average, for every 20% increase in ankle angle (Figure 28). EMG of the FL also increased significantly by a percent difference of 15.2 (6.4) %, on average, as dorsiflexion angle increased between the following pairs: 0%/40%, 0%/60%, 20%/40%, 20%/60%, 40%/60%. The LG exhibited an increase in EMG activity from 0% to 40% MDA (4.8% difference) and 0% to 60% MDA (6.4% difference). Also, the % MVE for the MG decreased by 35.6% between 0% and 40% MDA. Overall, main effects for ankle angle were revealed for the TA [$F(3,72) = 89.547$, $p < 0.05$], MG [$F(3,72) = 5.387$, $p < 0.05$], SOL [$F(3,72) = 2.811$, $p < 0.05$], and FL [$F(3,72) = 24.143$, $p < 0.05$] (Figure 28).

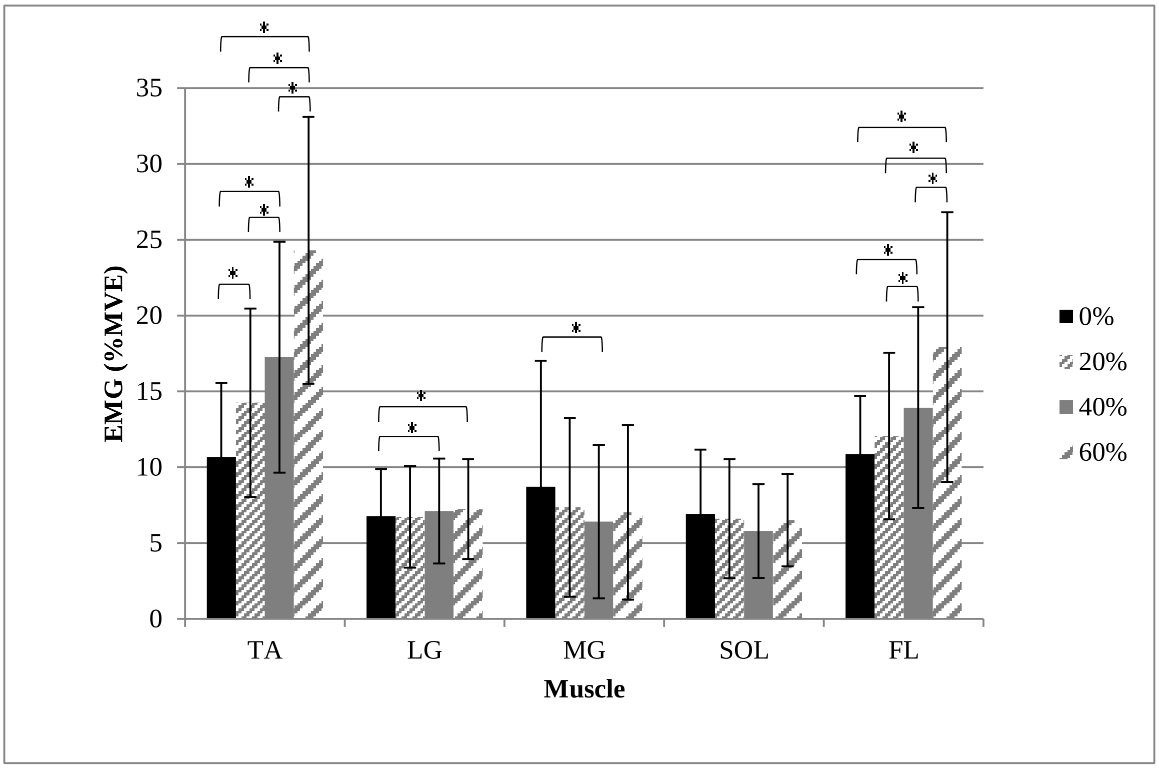

Figure 28. Main effect of ankle angle for EMG. Average EMG was measured for each muscle at 0%, 20%, 40%, and 60% of maximum dorsiflexion angle (n = 26). * p < 0.05

4.6 Individual Muscles' Contribution to Joint Rotational Stiffness (MJRS)

On average, across all conditions, the relative contributions of the individual muscles to AJRS were: TA 18.9 (9.5) %, LG 6.3 (2.8) %, MG 19.2 (5.1) %, SOL 51.7 (11.1) %, and FL 4.9 (2.5) % (Figure 29). The contribution of each muscle crossing the ankle joint to its joint rotational stiffness (MJRS) was analyzed to determine if any main effects or interactions for sex, time, fatigue, and ankle angle took place. A significant interaction that accounted for more than 1% of the variance ($\omega^2 > 0.01$) in JRS was found for time and ankle angle for the TA [$F(6,144) = 26.503$, $p < 0.05$ ($\omega^2 = 0.02$)]. Because time and ankle angle were incorporated into a higher-order interaction, post-hoc analysis was not performed on their main effects (see below). Additional interactions were found for time and ankle angle for the following muscles: LG [$F(6,144) = 5.495$, $p < 0.05$($\omega^2 = 0.003$)], MG [$F(6,144) = 8.305$, $p < 0.05$ ($\omega^2 = 0.002$)], SOL [$F(6,144) = 9.024$, $p < 0.05$ ($\omega^2 = 0.002$)], and FL [$F(6,144) = 8.597$, $p < 0.05$ ($\omega^2 = 0.003$)], and for time and fatigue for the MG [$F(2,48) = 3.876$, $p < 0.05$ ($\omega^2 = 0.0003$)], however these interactions did not account for more than 1% of the variance, and thus were not subjected to post-hoc testing.

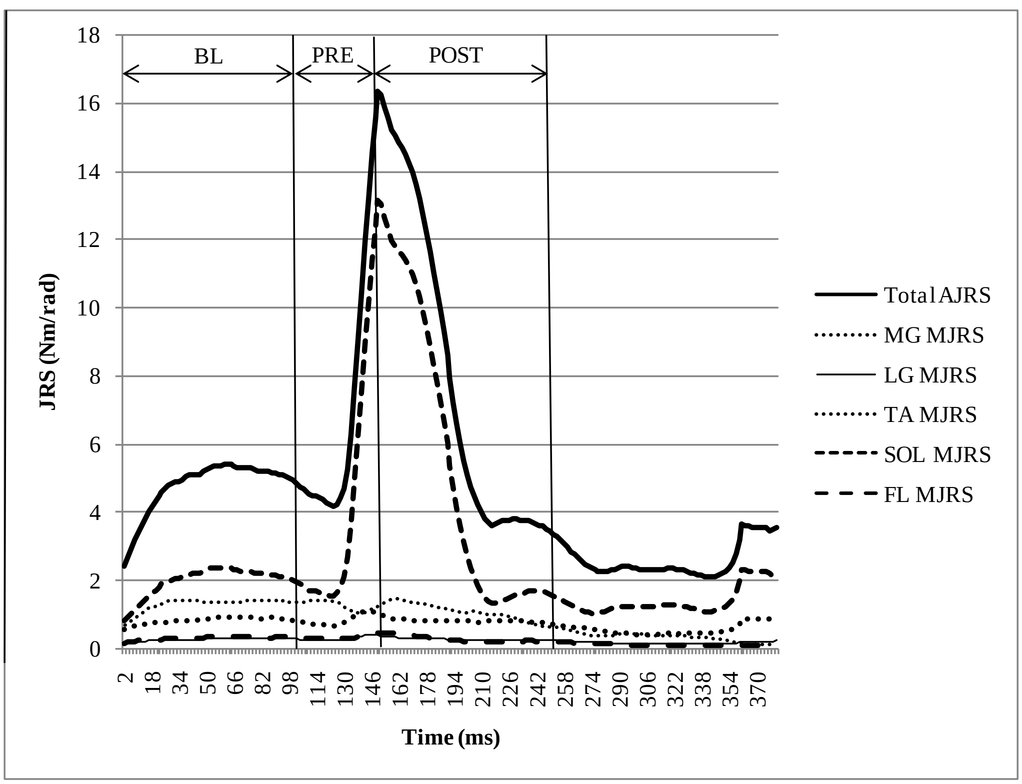

Figure 29. Changes in muscle joint rotational stiffness (MJRS) and ankle joint rotational stiffness (AJRS) with time. Note that the FL and LG appear very close together in the figure, but are distinguished by a thin solid line and a large dashed line. Baseline (BL), pre-impact (PRE) and post-impact (POST) time periods are labeled.

4.6.1 Main Effect of Sex

No significant differences in mean MJRS were found between sexes for the muscles investigated.

4.6.2 Main Effect of Fatigue

Main effects for fatigue were revealed only for the TA [$F(1,24) = 5.440$, $p < 0.05$] and the LG [$F(1,24) = 5.176$, $p < 0.05$] (Figure 30). After the fatigue protocol, the mean MJRS of the TA significantly decreased by a percent difference of 9.4%, while the MJRS of the LG increased by a percent difference of 6.0%.

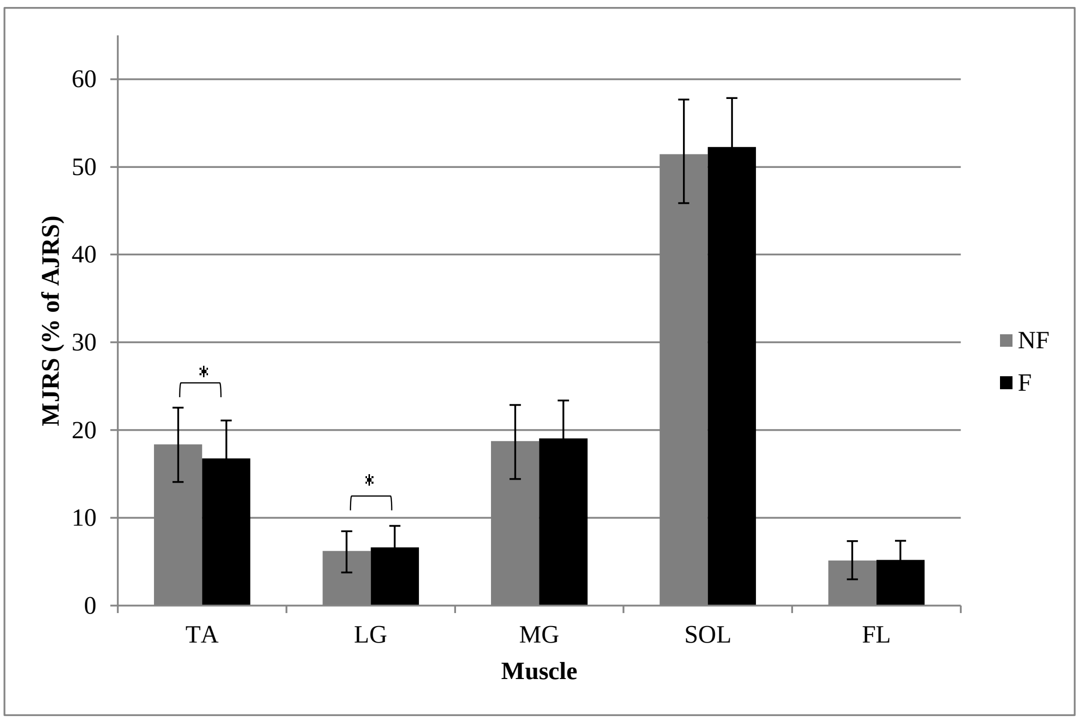

Figure 30. Main effect of fatigue for MJRS. Average MJRS was measured for each muscle in the non-fatigue (NF) and fatigue (F) conditions (n = 26). * p < 0.05

4.6.3 Time Period-Ankle Angle Interaction for Tibialis Anterior

A significant interaction between time period and ankle angle for the TA was revealed. Contributions of the TA to AJRS increased with ankle angle at a similar rate for the baseline and pre-impact time periods, but at a slower rate for the post-impact period (Figure 31).

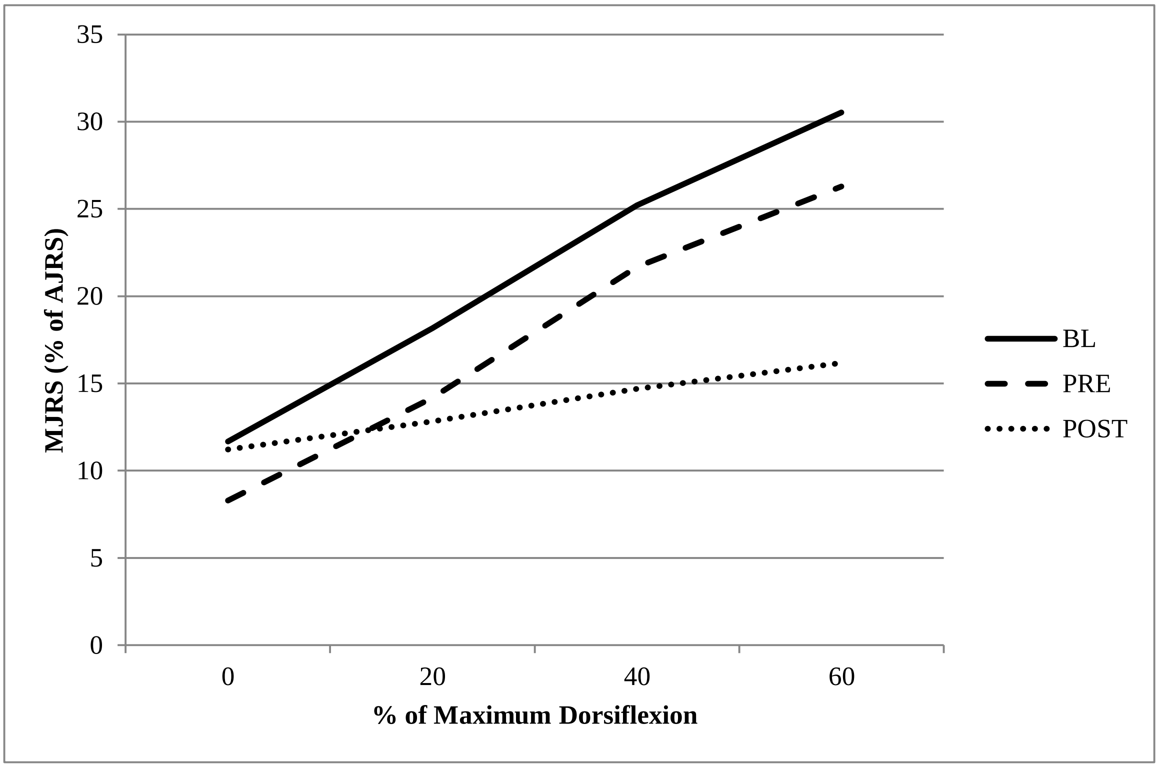

Figure 31. MJRS interaction between time period and ankle angle for the tibialis anterior (TA). Average MJRS was measured for all muscles at baseline (BL), pre-impact (PRE), and post-impact (POST) intervals across 0%, 20%, 40%, and 60% of maximum dorsiflexion angle (MDA). All comparisons are significantly different ($p < 0.05$) except for the following % of maximum dorsiflexion pairs: 0% MDA BL/POST and 20% MDA POST/PRE (n = 26).

4.7 Ankle Joint Rotational Stiffness (AJRS)

Significant main effects of sex, time period, and fatigue on AJRS were revealed from the statistical analysis. Significant interactions were revealed for time and fatigue [$F(2,48) = 3.887$, $p < 0.05$ ($\omega^2 = 0.0003$)] and time and ankle angle [$F(6,144) = 2.594$, $p < 0.05$ ($\omega^2 = 0.001$)]. However, since neither of the interactions accounted for at least 1% of the variance, all main effects were subjected to post-hoc analysis.

A main effect was seen for sex [F(1,24) = 4.829, $p < 0.05$], with the mean overall AJRS for males being 35.5% greater than females (Figure 32). A significant main effect for time was also found [F(2,48) = 25.254, $p < 0.05$], with AJRS increasing by 20.8% on average from baseline to pre-impact (Figure 33). Lastly, a main effect for fatigue was revealed [F(1,24) = 6.038, $p < 0.05$], with mean AJRS decreasing by 7.5% on average after the fatigue protocol (Figure 34).

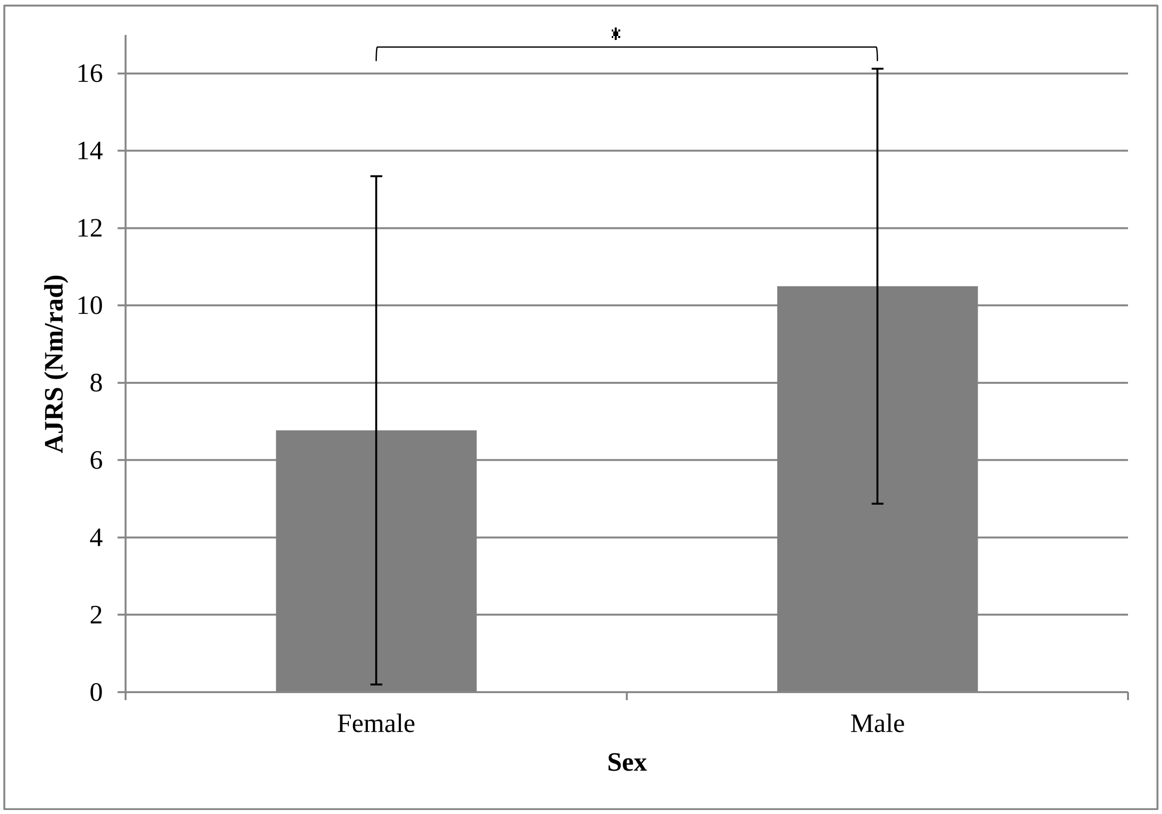

Figure 32. Main effect of sex for ankle joint rotational stiffness (AJRS) (n = 26). * p < 0.05

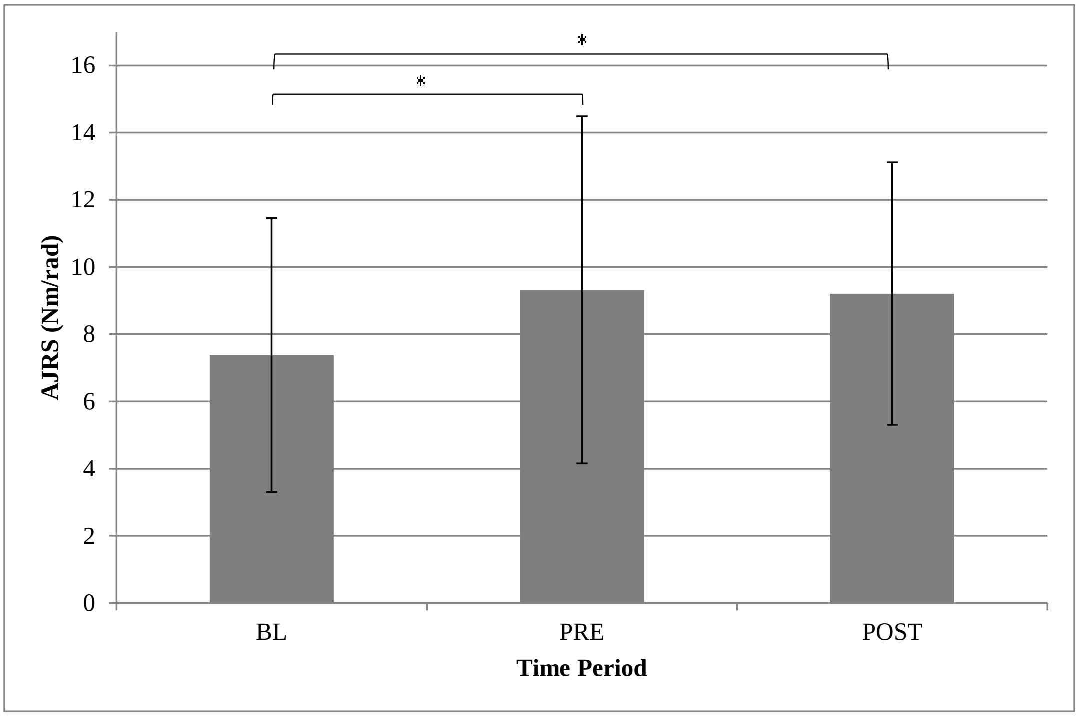

Figure 33. Main effect of time period for ankle joint rotational stiffness (AJRS). AJRS was measured at baseline (BL), pre-impact (PRE), and post-impact (POST) intervals (n = 26). * p < 0.05

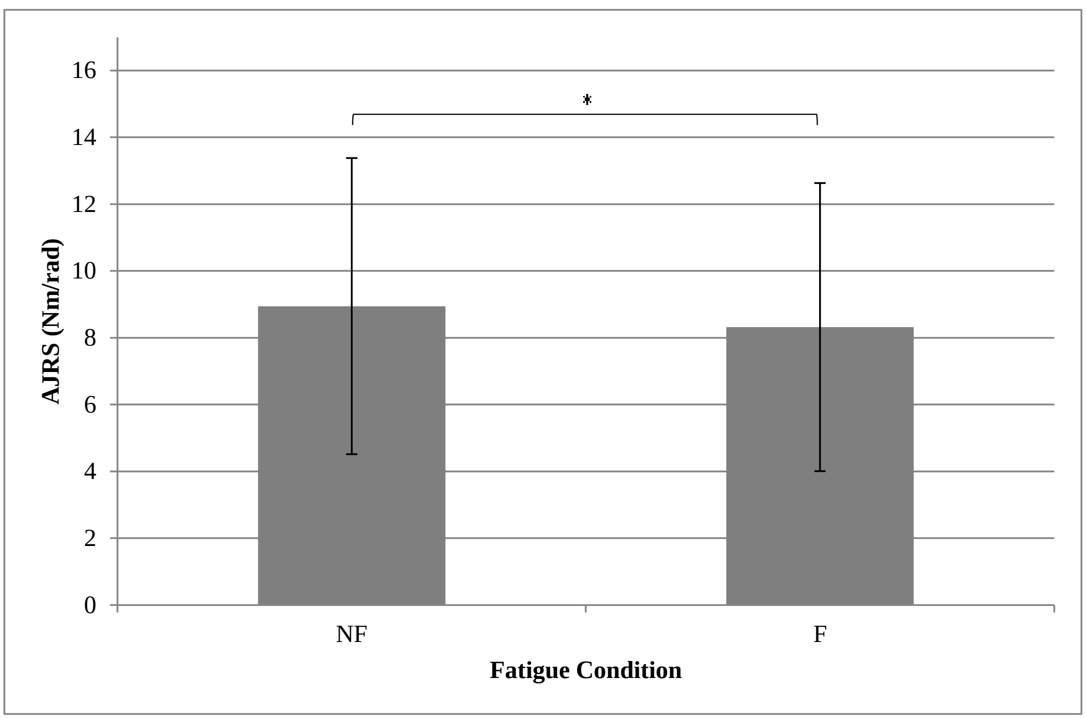

Figure 34. Main effect of fatigue for ankle joint rotational stiffness (AJRS). AJRS was measured in the non-fatigue (NF) and fatigue (F) conditions (n = 26). * p < 0.05

4.7.1 AJRS-Tibial Response Parameter Relationship

Pearson product-moment correlation coefficient (r) and coefficient of determination (r^2) calculations were performed between the AJRS and TRPs (PA, TPA, and AS) across the range of dorsiflexion angles for each of the sexes (male and female) and fatigue conditions (non-fatigue and fatigue) for the three time periods of interest (Tables 6-8). Significant correlations were seen for five of 36 conditions. When collapsed across fatigue and sex, no evident trends were revealed across the TRPs, thus the coefficients are not presented or described here.

During the pre-impact time period, both positive and negative relationships were revealed, and thus no consistent trend between PA and AJRS was found (Table 6). By contrast, during the post-impact phase, the relationship between PA and AJRS was consistently positive and strong, with a near-large effect size (>0.466) found for all conditions.

Table 6. Correlation coefficients and coefficients of determination between peak acceleration (PA) and ankle joint rotational stiffness (AJRS) collapsed across a range of 0% to 60% of maximum dorsiflexion angle (n = 26). * $p < 0.05$

		Correlation Coefficient (r)			**Coefficient of Determination (r^2)**		
Condition		Time Period			Time Period		
Fatigue	**Sex**	**Baseline**	**Pre-Impact**	**Post-Impact**	**Baseline**	**Pre-Impact**	**Post-Impact**
Non-fatigue	**Female**	-0.598	-0.858	0.682	0.357	0.736	0.466
	Male	-0.852	0.417	0.831	0.727	0.174	0.691
Fatigue	**Female**	0.605	0.985*	0.997*	0.366	0.970	0.994
	Male	-0.461	-0.259	0.801	0.213	0.067	0.642

The relationship between TPA and AJRS showed more consistent trends in terms of direction (Table 7). At baseline, an overall negative relationship between TPA and AJRS can be seen, with a large effect size for three of the four conditions. During the pre-impact period, a small to medium effect size, along with a nearly consistent negative relationship, was revealed between TPA and AJRS.

Table 7. Correlation coefficient and coefficients of determination between time to peak acceleration (TPA) and ankle joint rotational stiffness (AJRS) collapsed across a range of 0% to 60% of maximum dorsiflexion angle (n = 26). * p < 0.05

		Correlation Coefficient (r)			**Coefficient of Determination (r^2)**		
Condition		Time Period			Time Period		
Fatigue	**Sex**	**Baseline**	**Pre-Impact**	**Post-Impact**	**Baseline**	**Pre-Impact**	**Post-Impact**
Non-fatigue	**Female**	-0.203	-0.584	0.599	0.041	0.341	0.359
	Male	-0.977*	0.118	0.570	0.954	0.014	0.325
Fatigue	**Female**	-0.993*	-0.419	-0.580	0.985	0.175	0.337
	Male	-0.890	-0.793	0.265	0.793	0.630	0.070

During the pre-impact and post-impact periods, AS and AJRS demonstrated a positive relationship for seven of the eight conditions analyzed (Table 8). A small effect size was generally seen during the pre-impact period, while a medium to large effect size was revealed during the post-impact period.

Table 8. Correlation coefficients and coefficients of determination between acceleration slope (AS) and ankle joint rotational stiffness (AJRS) collapsed across a range of 0% to 60% of maximum dorsiflexion angle (n = 26). * p < 0.05

		Correlation Coefficient (r)			**Coefficient of Determination (r^2)**		
Condition		Time Period			Time Period		
Fatigue	**Sex**	**Baseline**	**Pre-Impact**	**Post-Impact**	**Baseline**	**Pre-Impact**	**Post-Impact**
Non-fatigue	**Female**	-0.369	-0.706	0.626	0.136	0.499	0.392
	Male	-0.824	0.137	0.709	0.678	0.019	0.502
Fatigue	**Female**	0.991*	0.457	0.615	0.982	0.209	0.378
	Male	-0.104	0.074	0.913	0.011	0.005	0.834

CHAPTER V

DISCUSSION

5.1 Participant Details

As expected, male participants exhibited significantly greater body mass, height and foot length values than females. Otherwise, groups were statistically similar for all personal variables. Because of the special criterion for this study (i.e. specific running distance per week, which resulted in a physically fit population), it is not surprising that participants had similar average values for body mass index (BMI) and weekly running distance.

5.2 Impact Parameters

The magnitudes of the impact forces (2.2 (0.3) BW) and impact velocities (1.03 (0.04) ms^{-1}) experienced by participants were similar to the values presented by previous researchers. This was expected, given that the same protocol and impact parameter targets were utilized in this study (Duquette & Andrews, 2010a; Flynn et al., 2004; Holmes & Andrews, 2006; Schinkel-Ivy et al., 2010 in press).

It has been assumed in past studies that employing a straight-legged orientation using a human pendulum restricts the knee from flexion during the impact, due to the restrained nature of the apparatus (Duquette & Andrews, 2010a; Flynn et al., 2004; Holmes & Andrews, 2006; Schinkel-Ivy et al., 2010 in press). Knee joint motion was limited to an average value of 4.6 (1.9) degrees across all participants and conditions in the current study. This finding shows that the human body will work against physical restraint to cushion itself from impact by way of changing the joint orientation (Derrick, 2004; Gerritsen et al., 1995; McMahon et al., 1987; Milliron & Cavanagh, 1990). Given the other limitations of the human pendulum (see 2.7.4), and the resolution of the electrogoniometer, this relatively small amount of knee flexion is not functionally significant in the opinion of the researcher.

5.3 Tibial Response Parameters (TRPs)

No sex differences were found for the TRPs. Although height, mass and foot segment lengths were statistically different between the sexes, the participants in this study had similar somatotypes and BMI values given the population drawn from. However, because body composition was not assessed, it cannot be employed as a reason for the similar findings.

A sheet of ethylene and vinyl acetate (EVA) foam was placed over the force plate to simulate the effect of a shod impact condition while maintaining full ankle range of motion. The EVA foam sheet was similar in density to that of a running shoe and acted to dampen the impact forces and resulting tibial acceleration values through greater deformation of the surface at impact. Because of the dampened impact, the PA and AS values from this study were at the lower end of the range of those previously seen during a similar protocol (e.g. Lafortune et al., 1996a), while values for TPA were greater than those seen in previous studies as it took longer for the peak acceleration to reach the proximal tibia (Table 9).

Table 9. Comparison of the means (SD) of the tibial response parameters in the current study with previously reported results. † = Use of time instead of amplitude to calculate acceleration slope.

Reference	Peak Acceleration (g)		Time to Peak Acceleration (ms)		Acceleration Slope (g/s)	
	NF	F	NF	F	NF	F
Current Study	10.0 (2.0) - 11.5 (2.1)	10.4 (1.8) - 11.8 (1.8)	16.8 (4.0) - 18.4 (6.6)	16.8 (4.2) - 18.1 (5.3)	879 (274) - 1106 (408)	970 (320) - 1111 (399)
Duquette & Andrews (2010a)	10.9 (2.5) - 13.7 (2.4)	9.5 (2.4) - 11.8 (3.5)	9.8 (1.7) - 10.9 (1.1)	10.5 (1.4) - 11.5 (1.8)	1313 (528) - 1764 (355)†	1081 (332) - 1307 (538)†
Schinkel-Ivy et al. (2010) Overall % body fat	10 (2) - 10 (4)	---	14 (0.3) - 14 (0.4)	---	1374 (767) - 2205 (1003)	---
Holmes & Andrews (2006) Session 1	12.1 (1.4)	9.6 (1.7)	9.0 (2.2)	9.4 (2.7)	1703 (549)	1423 (679)
Holmes & Andrews (2006) Session 2	12.7 (1.7)	13.0 (1.8)	8.4 (1.9)	8.9 (2.0)	2095 (801)	1790 (757)
Flynn et al. (2004) Session 1	13.3 (3.7)	12.1 (3.1)	10.1 (5.0)	10.9 (6.0)	3067 (1488)†	2416 (1363)†
Flynn et al. (2004) Session 2	13.2 (4.5)	12.0 (3.5)	9.7 (2.0)	10.2 (4.0)	2843 (1883)†	2589 (1759)†
Lafortune et al. (1995)	6.4 (0.7)	---	16.1 (3.0)	---	671 (220)	---

5.3.1 Peak Acceleration (PA)

Significant decreases were seen in PA as dorsiflexion angle increased. This result was also seen by Duquette and Andrews (2010a); however, no suggestions were offered to explain this unexpected trend. It is thought that altered joint orientation at the ankle may explain the reduced PA values in the current study, as it has been found that changes in joint orientation affect the transmission of forces through the upper limbs (Burkhart & Andrews, 2010; Wake, Hashizume, Nishida, Inoue & Nagayama, 2004). In addition, bone is the primary structure responsible for the transmission of shock waves through the body during running (Valiant, 1990), so changes in joint orientation are thought to influence force transmission to a major extent.

The ankle joint is a hinge joint formed by the articulation of the distal ends of the tibia (medial malleolus) and fibula (lateral malleolus) and the talus. In a standing posture, the ankle is oriented with the foot being at 90° to the leg (corresponding to 0% of MDA in the current study). As the dorsiflexion angle increases, there is reduced bony contact between these ankle bones. Less contact between the bones would result in a decreased ability of the ankle joint to transmit the shock wave, ultimately resulting in reduced PA at the knee. In support of this concept, when investigating the influence of knee angle on the transmission of accelerations through the leg, Potthast, Bruggemann, Lundberg and Arndt (2010) found that a more extended knee posture allowed for more bony contact at the articulation of the tibia and femur, which consequently led to increased acceleration values across the knee joint.

Studies that employed running shoes or a covered force plate reported overall decreased PA values with softer impacting interfaces, which resulted from the force of impact being applied over a greater period of time during the deformation of the foam (Gerritsen et al., 1995; Lafortune et al., 1996a; Ly et al., 2010). The results of the current study agree with these previous studies in this regard.

5.3.2 Time to Peak Acceleration (TPA)

TPA was not significantly altered as a function of the changes in ankle angle or fatigue level. Overall, values for TPA were longer than those typically found in the literature; however, in agreement with the current study, Lafortune et al. (1996a) found that softer interfaces resulted in longer TPA. Longer TPAs are consistent with the impact force being spread out over a longer amount of time as a result of the EVA foam used in the current study.

5.3.3 Acceleration Slope (AS)

Overall, values of AS were at the lower end of the range of those previously found in the literature (Table 9). AS represents the rate of change of acceleration, and is associated with how quickly PA is reached. A greater mean TPA was seen in the current study compared to previous work (Table 9), due in part to the EVA foam interface. It is important to note that AS was calculated as the slope of the linear portion of the acceleration waveform between 30% and 70% of PA. Duquette & Andrews (2010b) showed that calculating AS based on amplitude instead of the time interval can result in AS values that are larger in magnitude. Therefore, it is important to specify the method used for calculating AS so that comparisons between studies are facilitated.

5.4 Fatigue

5.4.1 Time to Fatigue and Mean Power Frequency

The fatiguing protocol used in this study allowed a relationship between MPF and fatigue to be established. MPF was shown to decrease by 26% on average in the current study. Comparable decreases in MPF following similar localized muscle fatigue (LMF) protocols have been previously reported in the literature (Duquette & Andrews, 2010a; Flynn et al., 2004; Holmes & Andrews, 2006). In addition, other indicators of fatigue were noted including visible changes in ankle joint angle, muscle trembling, groaning, and facial expressions of great discomfort.

Although not statistically significant, female participants had longer TTFs than male participants (62.9 (11.7) s vs. 53.5 (14.7) s). Hunter and Enoka (2001) found that females were able to exhibit longer endurance times (by 118%) over their male counterparts; a difference that was replicated exactly in the current study. EMG activity of all muscles evaluated was also found to be greater for females in both of these studies. The study by Hunter and Enoka (2001) found that endurance time was inversely related to absolute force, and in order to sustain a target force, an increased rate of motor unit recruitment was required. Females have greater endurance times because of their decreased muscle mass and inability to generate as much absolute force as compared to their stronger male counterparts, who have shorter endurance times.

5.4.2 Tibial Response to Fatigue

LMF induced in the TA did not result in the same tibial response as previously seen in the literature, as past studies involving LMF have shown decreases in AS with fatigue (Table 8). The results of the current study indicated that the tibial impact parameters tested were not significantly different between the non-fatigue and fatigue conditions. Coventry et al. (2006) had similar results in a single-leg impact study, where a fatigued leg did not attenuate impact shock waves to a greater extent than a non-fatigued leg. Their study, however, used drop landings whereby the ankle, knee and hip joint angles could be altered to decrease the overall stiffness of the whole leg (see Section 2.5.2). The effect of LMF has typically been found to result in decreased PA, increased TPA and decreased AS values (Flynn et al., 2004; Holmes & Andrews, 2006), even when controlling for ankle angle (Duquette & Andrews, 2010a). In the current study, no such trends between non-fatigue and fatigue conditions were found, however a couple of reasons should be considered.

The lack of difference between the non-fatigue and fatigue conditions could first be due to the fact that the aforementioned studies used various populations of participants including younger and older adults (Flynn et al., 2004) and those that were described as right-leg dominant, and healthy (Duquette & Andrews, 2010a; Holmes & Andrews, 2006). It is proposed that, since recreationally trained runners were used in this study, perhaps the effect of running training influenced the fatigue response of the tibia to impacts in a different way than previously studied populations. It has been hypothesized (Flynn et al., 2004; Holmes & Andrews, 2006) that a decrease in PA and AS and an increase in TPA are due to increased shock dissipation capabilities of the TA in a fatigued state. In the current study, although it was not found to be statistically significant, the MJRS of the plantarflexors (LG, MG, and SOL) were found, on average, to increase after the fatigue protocol. The plantarflexors are a very large muscle group relative to the dorsiflexor action of the TA, and even a non-significant increase in MJRS from the plantarflexors may have been enough to compensate for the reduced MJRS and force-generating capability of the TA after fatigue. This would suggest that the ability of the plantarflexor group to compensate for the shock-dissipating effect of a fatigued TA during fatigued running is a strategy to maintain AJRS used by recreational runners. It is proposed that the AJRS has a significant role in determining shock propagation up the leg. The idea of maintaining AJRS is proposed to balance the stiffness requirements for preventing injury (i.e. maintaining a safe ankle range of motion) and improving running/jumping performance (i.e. a stiffer joint will return more energy and allow for faster running/higher jumping) (Kubo et al., 2000).

Another possible reason for why no apparent fatigue effects were found is that fatigue was not experienced during all impacts in the fatigue condition. On average, participants were subjected to approximately 16 impact trials in the fatigued condition after the fatiguing protocol in order to get 12 trials that had impact parameters (impact force and velocity) that fell within the proscribed ranges. Although participants had to dorsiflex during most of these impacts, which would help to extend the fatigue effect after the fatiguing protocol, the fatigue effect may have diminished in some participants due to the length of time taken to complete these trials. The training of the population studied may have also provided them with the ability to recover from fatigue at a faster rate than the previously studied populations. This could be why no significant changes between fatigue conditions were found for the tibial acceleration parameters in the current study. To verify this, future work should investigate the effect of LMF on tibial response to isolated impacts in trained vs. untrained populations. To ensure that fatigue actually decreased over this time period, MPF could be monitored in the fatigued state.

5.5 Electromyography (EMG)

5.5.1 Main Effect of Sex

Female participants exhibited greater mean EMG values than male participants for all muscles investigated. On average, females have less muscle mass than males, which would result in less muscle force contributing to the ankle joint rotational stiffness (AJRS). If a minimum AJRS (as an absolute or relative value) is required to prevent injury, then it is a logical finding that females would have to exhibit greater % MVE to generate enough force to obtain the same AJRS values as men, due to their smaller musculature. Of the five muscle groups investigated, it was found that the LG and FL muscles were the only muscles that differed significantly between sexes. The percent difference in % MVE was more than 50% greater for females than males for both of these muscles.

5.5.2 Main Effect of Time Period

EMG activity increased from baseline to pre-impact for all muscles monitored. However, this increase was only significant for the plantarflexors of the superficial posterior compartment of the leg (LG, MG and SOL). The increase in EMG activity prior to impact suggests that the muscles of the lower extremity are experiencing pre-activation, or muscle tuning (Wakeling et al. 2003; Wakeling & Nigg, 2001b; Wakeling et al., 2001), in anticipation of the impact. The TA (dorsiflexor) did not exhibit the muscle tuning effect, which could be due to its voluntary involvement in maintaining a target dorsiflexion angle prior to impact.

5.5.3 Main Effect of Fatigue

Decreases in EMG were seen for all muscles after the fatigue protocol, however significant decreases were revealed only for the TA, FL, and SOL. Since the TA is the primary dorsiflexor, after the fatigue protocol it would have been less capable of firing at the same rate as pre-fatigue (Winter, 2005). Also, the FL appeared to be activated to a high % MVE during dorsiflexion. It may be that FL was activated this extent to prevent inversion of the foot during dorsiflexion at impact. SOL may have demonstrated a reduction in EMG after the fatigue protocol because during the fatiguing it may have been co-contracting in order to serve as a stabilizing muscle against the TA contraction.

5.5.4 Main Effect of Ankle Angle at Impact

The EMG of the TA and FL increased for every increase in targeted dorsiflexion angle. In order to increase the % of MDA, the TA was required to increase its activation to produce dorsiflexion (TA) at the ankle. The TA is the primary dorsiflexor, and thus an increase in % MVE with each 20% increase in MDA is expected. The FL exhibited an increase in % MVE with increased dorsiflexion as well. This is probably due to the eversion action that was observed to prevent inversion of the foot during dorsiflexion at impact.

5.6 Individual Muscles' Contribution to Joint Rotational Stiffness (MJRS)

5.6.1 Main Effect of Sex

No significant differences in MJRS were found between the sexes for the muscles investigated. Thus, the muscles that contributed to AJRS, contributed in the same proportions regardless of sex.

5.6.2 Main Effect of Fatigue

After fatiguing the TA, its contribution to AJRS significantly decreased by 9.4%. In contrast, the MJRS of the LG significantly increased by 6.0% after fatigue. Given this apparent tradeoff, it may be that the two muscles were working together to balance each other's contributions, in order to maintain a consistent level of AJRS. A minimum amount of AJRS may be required to prevent damage to the ankle joint at impact. The MG, SOL and FL also remained consistent in their contributions to AJRS, supporting the notion that there may be an optimal amount of AJRS that must be maintained as an injury prevention strategy.

5.6.3 Time Period-Ankle Angle Interaction for Tibialis Anterior

A significant interaction was revealed between time period and ankle angle for the TA. During the baseline and pre-impact periods, the MJRS of the TA increased in a similar manner, while during the post-impact period the MJRS of the TA increased at a slower rate. Even though there was a similar trend in increasing the TA MJRS with ankle angle for all time periods, this interaction suggests that after the impact, the TA contributed less to the AJRS, compared to the baseline and pre-impact time periods.

The current study was not particularly interested in the post-impact reaction of the ankle to impact and did not have participants control their ankle angle after the heel impact. This lack of control over ankle angle after impact could have lead to differences in AJRS after impact. Therefore, this interaction was not functionally relevant to the current analysis.

5.7 Ankle Joint Rotational Stiffness (AJRS)

Overall, the AJRS for males was 35.5% higher than for females. It was hypothesized (Hypothesis 4) that males would exhibit greater MJRS and AJRS prior to and after fatigue, compared to females. Although MJRS of the individual muscles investigated (as a percent contribution to AJRS) did not differ between the sexes, males were found to have significantly greater overall AJRS values than females. No significant interaction was found for sex and fatigue, nor did the TTF differ significantly between the sexes, indicating that males and females fatigued at similar rates.

Increased EMG activity in females resulted in increased active stiffness of the leg muscles. The increased muscle activity in females might have helped to compensate for their lower muscle mass, although muscle mass was not quantified in the current study.

Greater force output and PCSA have been observed in males compared to females for muscles of the lower extremities (Staron et al., 2000). Therefore, the greater force capacity as a function of greater muscle mass likely plays an important role in the active resistive capabilities of the musculotendinous unit. Because participants were not matched for muscle mass in this study, it would not be possible to comment on any sex differences found for structural stiffness. Blackburn et al. (2006) found differences in the structural stiffness values of the triceps surae muscles (SOL, MG, and LG) between sexes, while controlling for anthropometric measurements. In order to determine if sex differences do exist, male and female participants would have to have the same PCSA for the muscles crossing the ankle joint, in addition to other similar anthropometric measurements.

It was found that AJRS increased significantly between baseline and pre-impact and between baseline and post-impact. An increase in AJRS prior to impact supports the idea that the muscles of the leg are tuned in response to the impending impact (Wakeling et al. 2003; Wakeling & Nigg, 2001b; Wakeling et al., 2001). Also, it supports the idea that the ankle joint must have a minimum amount of AJRS to optimize joint stability and prevent injury at impact (Butler et al., 2003; Granata et al., 2002; McMahon & Cheng, 1990).

It was hypothesized (Hypothesis 3) that AJRS would decrease when TA was fatigued. This was supported by the results, as AJRS decreased by 7.5% on average. With the onset of fatigue, the force-generating capacity of a muscle is reduced (Kent-Braun et al., 2002), and thus, the muscles contributing to AJRS would have reduced their ability to maintain the AJRS established in the non-fatigue state. This may have implications in terms of the susceptibility to injury, as the ankle joint appears to be less stable in a fatigued state.

The force plate used in the current study was covered with a sheet of EVA foam similar to that used in running shoe construction. Researchers agree that leg stiffness is adjusted to the impacting conditions, in order to maintain the intensity of the shock wave that is allowed to reach the head (Farley & Morgenroth, 1999; Ferris & Farley, 1997; Hamill et al., 1995; Shorten & Winslow, 1992). Consistent with this conclusion, it is likely that, if the current study was replicated without foam covering the force plate, the magnitudes of the AJRS achieved in absolute terms may not coincide with those presented herein.

5.7.1 AJRS-Tibial Response Parameter Relationship

It was hypothesized (Hypothesis 1) that there would be a positive relationship between AJRS and PA and AS, but a negative relationship with TPA. The strongest relationships between AJRS and the TRPs were expected to be during the pre-impact and post-impact time periods, as it is during these times that muscles are preparing themselves for the impact and attempting to control their recovery from the impact. However, based on the correlational analyses, a specific time period did not appear to yield the expected relationship more consistently than any other.

Generally speaking, the hypothesized relationships could be seen for all of the TRPs, however the time period in which these relationships occurred were not consistent. Post-impact, a large effect size for nearly all conditions suggests that after impact, increased AJRS is associated with an increase in PA. It was hypothesized (Hypothesis 1) that an increase in AJRS would be positively correlated with PA as dorsiflexion angles increased, because the shock wave would be travelling up a more rigid structure caused by the increased TA activation (Pain & Challis, 2002). During both the baseline and pre-impact periods, the hypothesized negative relationship (Hypothesis 1) between TPA and AJRS was revealed for seven of the eight conditions across fatigue and sex. As hypothesized (Hypothesis 1), a positive relationship between AS and AJRS was revealed for the pre-impact and post-impact periods.

Contrary to past studies (Flynn et al., 2004; Holmes & Andrews, 2006; Duquette & Andrews, 2010a), the current study did not find that the fatiguing of the TA resulted in an increased ability of the leg to attenuate impact shock. Thus, the relationship between AJRS and the TRPs before and after fatigue could not be analyzed as hypothesized (Hypothesis 2).

5.8 Functional Significance and Application

The current study investigated the effect of AJRS and LMF on TRPs across a range of ankle angles. The human body appears to compensate for fatigue to protect the joints at impact, which would practically relate to the later phases of running. An optimal level of stiffness has been suggested to exist to balance performance enhancement characteristic of increased stiffness (Granata et al., 2002; Kubo et al., 2000) with the injury potential (Butler et al., 2003; Granata et al., 2002; McMahon & Cheng, 1990) and reduced economy (Dutto & Smith, 2002; Kuitunen et al., 2002; McMahon & Cheng, 1990; Stefanyshyn & Nigg, 1998) associated with too little stiffness.

The current study suggested that when the TA muscle was fatigued and decreased its muscle activity and subsequent contribution to AJRS, other leg muscles compensated to some degree by increasing their muscle activity. This strategy could have implications for runners, as injury to any of the leg muscles could seriously affect ankle stability and the ability of muscles surrounding the ankle to compensate for altered fatigue states and ankle angles. By identifying the stabilizing potential of individual ankle muscles, applications could prove useful in injury prevention and rehabilitation, as strengthening treatment and training protocols can be applied to targeted muscles.

5.9 Limitations and Future Directions

The human pendulum method has certain limitations in replicating a running impact, as previously described (Section 2.7.4). Most notably, the horizontal orientation and constrained nature of the pendulum reduces the relevance of the results to running. However, this method of impact delivery can limit certain external and inter-participant sources of variability in kinematic adaptations. Because the body was restricted from responding to impact by changing joint angles (Derrick, 2004; Gerritsen et al., 1995; McMahon et al., 1987; Milliron & Cavanagh, 1990), the shock experienced by the body may not have been entirely representative of what occurs during running impacts. Consequently, if the impact was not entirely representative of running, then relating the AJRS to what might be experienced during running lacks some relevance as well. In addition, the fatigue protocol used in this study is not completely representative of the fatigue incurred in running. In this study, fatigue was incurred through an isometric contraction at 50 percent of a maximum exertion, and only for a relatively short time. In long distance running, or jogging, fatigue occurs over a longer time interval, and the TA is working at a lower percentage of maximum exertion. Thus, directly applying the results of the LMF protocol used in this study to running should be done with some consideration. Regardless of these limitations, it was the goal of the current study to investigate whether the AJRS played a role in describing the effect of fatigue on TRPs, while controlling for the effect that ankle angle has on tibial response to impact. The use of a human pendulum to deliver the impacts allowed for kinematic variables to be controlled, which is not possible during treadmill running.

Although the human pendulum method allows for very good control over impact conditions, the way in which participants impacted the force plate was not consistent. Some participants were observed to consistently ‘slap’ their forefoot forward towards the force plate after heel contact, while others consistently kept their ankle in a rigid, dorsiflexed position after the heel contacted the plate. The variability with which participants struck the plate would have created variability in muscle activation patterns and the moment curves produced. In addition, the small amount of knee flexion measured in this study during impact would help to absorb some of the shock wave being transmitted through the leg. Future research using the human pendulum should consider controlling, to a greater extent, the postures of the foot and knee at impact.

Surface EMG (sEMG) is a measure of the activity of a muscle that reaches the electrodes that are placed over the muscle. The JRS model employed in this study uses the relationship between muscle activity and force output in order to estimate the internal EMG moment (Mo_{EMG}), to which the external reaction moment (Mo_{JtRxn}) is compared. The EMG signal is the result of many physiological, anatomical and technical factors that cannot all be controlled entirely. Therefore, EMG only provides an estimate of the force produced in the muscle.

The model used in this study was also limited in terms of its applicability to the population being evaluated. For example, the model used herein was based on anthropometric measurements from cadavers (Delp et al., 1990). Cadaveric tissues do not respond the same way as living tissues and are typically from older populations. Consequently, the use of the anatomical muscle origin and insertion data of the lower extremity, as well as the three-dimensional path of the muscle movement put forth by Delp et al. (1990), could lead to inaccurate values being calculated for the changes in muscle lengths and velocities during a perturbation. Thus, some aspects of the structural model are not representative of the young, active sample studied here.

There were a few other limitations associated with using the JRS model for the leg. The goal of the model is to match the EMG-based moment (Mo_{EMG}), as determined by the model, to the external joint reaction moment (Mo_{JtRxn}) to an applied perturbation, as measured by kinematic values. When modeling the Mo_{EMG}, it was apparent that not enough EMG data were taken from dorsiflexor muscles, in order to match the Mo_{JtRxn} that was calculated using kinematic measurements. The result of this limitation is that the gain factor applied to the Mo_{EMG} may not have been as accurate as it could have been.

Only one trial per impact condition was used in the analysis, even though three were collected. This was because some participants were not capable of activating their leg musculature consistently for every impact, resulting in a number of incomplete data sets. Therefore, the decision was made to analyze only one representative trial within a condition in order to increase the number of participants evaluated in the study. Although important to maintain the sample size, this reduced the variability of the data, and possibility the generalizability of the results. The impact that this had on the final results is thought to be small, given that an analysis involving the calculation of the average coefficient of variability (CV=SD/mean*100) was performed on the ankle angle

(CV = 14.2%), TRP (CV_{PA} = 8.5%, CV_{TPA} = 7.1%, CV_{AS} = 16.0%), impact parameter ($CV_{impact\ force}$ = 4.3%, $CV_{impact\ velocity}$ = 1.2%), and EMG (CV = 16.4%) data prior to the selection of representative trials based on the JRS model output. The CV values calculated for these variables are relatively small in general, indicating that in this study taking only one trial is acceptable.

CHAPTER VI

CONCLUSIONS

Based on the results of the current study, the following conclusions can be made:

- Consistent relationships between the tibial response parameters (TRPs) and AJRS were found for some of the time periods, although the effect size ranged from small to large. Thus, a positive relationship exists between AJRS and PA, as well as AJRS and AS. A negative relationship exists between AJRS and TPA.
- The soleus (SOL) muscle was the single greatest contributor to AJRS (of the individual muscles studied), regardless of the fatigue condition or participant sex.
- Males exhibited greater AJRS values than females, due to their increased muscle mass (assumed and not measured).
- AJRS decreased following fatigue. However, because fatigue did not impose the expected effect on the TRPs, their relationship with AJRS could not be investigated as a function of fatigue.
- It is proposed that an optimal amount of AJRS is needed when regulating the transmission of impact shock. In addition, it appears that the ankle joint requires a minimum amount of AJRS to optimize joint stability and possibly to prevent injury resulting from impact. Changes in muscle contributions to AJRS that were observed may be a way of altering shock propagation through the leg in situations where changes to segment and joint positions have been restricted (e.g. when using the human pendulum).

REFERENCES

Ament, W., Bonga, G. J. J.. Hoff, A. L., Verkerke, G. J., 1993. EMG median power frequency in an exhausting exercise. *Journal of Electromyography and Kinesiology 3*, 214-220.

Blackburn, J. T., Padua, D. A., Weinhold, P. S. & Guskiewicz, K. M. (2006). Comparison of triceps surae structural stiffness and material modulus across sex. *Clinical Biomechanics, 21*, 159-167.

Bobbert, M. F., Yeadon, M. R. & Nigg, B. M. (1992). Mechanical analysis of the landing phase in heel-toe running. *Journal of Biomechanics, 25*, 223-234.

Bowerman, W. J. & Harris, W. E. (1967). *Jogging*. New York: Grosset & Dunlap.

Boyer, K. A. & Nigg, B. M. (2006). Muscle during running: implications of an un-tuned landing. *Journal of Biomechanical Engineering, 128*, 815-822.

Boyer, K. A. & Nigg, B. M. (2007). Changes in muscle activity in response to different impact forces affect soft tissue compartment mechanical properties. *Journal of Biomechanical Engineering, 129*, 594-601.

Buckwalter, J.A., & Lane, N.E. (1997). Does participation in sports cause osteoarthritis? *Iowa Orthopaedic Journal, 17*, 80-89.

Burkhart, T. A. & Andrews, D. M. (2010). The effectiveness of wrist guards for reducing wrist and elbow accelerations resulting from simulated forward falls. *Journal of Applied Biomechanics, 26*, 281-289.

Butler, R. J., Crowell III, H. P. & Davis, I. M. (2003). Lower extremity stiffness: implications for performance and injury. *Clinical Biomechanics, 18*, 551-517.

Cavanagh, P. R. & Lafortune, M. A. (1980). Ground reaction forces in distance running. *Journal of Biomechanics*, *13*, 397-406.

Cavanagh, P. R., Valiant, G. A. & Misevich, K. W. (1984). Biological aspects of modeling shoe/foot interaction during running. In E. C. Frederick (Ed). *Sport Shoes and Playing Surfaces* (pp. 24-46). Champaign, IL: Human Kinetics.

Chavet, P., Lafortune, M. A. & Gray, J. R. (1997). Asymmetry of lower extremity responses to external impact loading. *Human Movement Science, 16*, 391-406.

Christina, K. A., White, S. C. & Gilchrist, L. A. (2001). Effect of localized muscle fatigue on vertical ground reaction forces and ankle joint motion during running. *Human Movement Science, 20*, 257-276.

Chu, M. L., Yazdani-Ardakani, S., Gradisar, I. A. & Askew, M. J. (1986). An in vitro simulation study of impulsive force transmission along the lower skeletal extremity. *Journal of Biomechanics, 19*, 979-987.

Clarke, T. E., Frederick, E. C. & Cooper, L. B. (1983). Effects of shoe cushioning upon ground reaction forces in running. *International Journal of Sports Medicine, 4*, 247-251.

Cohen, B. (1988). *Statistical Power Analysis for the Behavioral Sciences (2nd Edition).* Hillsdale, New Jersey: Lawrence Erlbaum Associates, Inc.

Cole, G. K., Nigg, B. M., van den Bogert, A. J. & Gerritsen, K. G. M. (1996). Lower extremity joint loading during impact in running. *Clinical Biomechanics, 11*, 181-193.

Cole, G. K., Nigg, B. M., Fick, G. H. & Morlock, M. M. (1995). Internal loading of the foot and ankle during impact in running. *Journal of Applied Biomechanics, 11*, 25-46.

Cort, J. A. & Potvin, J. R. (2008). Neuromuscular contribution of the leg flexor muscles to knee joint rotational stiffness following a sudden leg perturbation. *Proceedings of the North American Congress on Biomechanics (NACOB) Conference*, Ann Arbor, MI.

Coventry, E., O'Connor, K. M., Hart, B. A., Earl, J. E. & Ebersole, K. T. (2006). The effect of lower extremity fatigue on shock attenuation during single-leg landing. *Clinical Biomechanics, 21*, 1090-1097.

de Leva, P. (1996). Adjustments to Zatsiorsky-Seluyanov's segment inertia parameters. *Journal of Biomechanics, 29*, 1223-1230.

Delp, S. L., Loan, P. J., Hoy, M. G., Zajac, F. E., Topp, E. L. & Rosen, J. M. (1990). An interactive graphics-based model of the lower extremity to study orthopaedic surgical procedures. *IEEE Transactions on Biomedical Engineering, 37*, 757-767

Derrick, T. R. (2004). The effects of knee contact angle on impact forces and accelerations. *Medicine & Science in Sports & Exercise, 36*, 832-837.

Derrick, T. R., Dereu, D. & Mclean, S.P. (2002). Impacts and kinematic adjustments during an exhaustive run. *Medicine & Science in Sports & Exercise, 34*, 998-1002.

Derrick, T. R., Hamill, J. & Caldwell, G.E. (1998). Energy absorption of impacts during running at various stride lengths. *Medicine & Science in Sports & Exercise, 30*, 128-135.

Duquette, A. M. & Andrews, D. M. (2010a). Tibialis anterior muscle fatigue leads to changes in tibial axial acceleration after impact when ankle dorsiflexion angles are visually controlled. *Human Movement Science, 29,* 567-577.

Duquette, A. M. & Andrews, D. M. (2010b). Comparing methods of quantifying tibial acceleration slope. *Journal of Applied Biomechanics, 2,* 229-233.

Dutto, D. J., Levy, M., Lee, K. K., Sidthalaw, S. & Smith, G. A. (1997). Effect of fatigue and gender on running mechanics. *Medicine & Science in Sport & Exercise, 29,* S82.

Dutto, D. J. & Smith, G. A. (2002). Changes in spring-mass characteristics during treadmill running to exhaustion. *Medicine & Science in Sports & Exercise, 34*, 1324-1331.

Farley, C. T., Houdijk, H. H. P., van Strien, C. & Louie, M. (1998). Mechanism of leg stiffness adjustment for hopping on surfaces of difference stiffnesses. *Journal of Applied Physiology*, *85*, 1044-1055.

Farley, C. T. & Morgenroth, D. C. (1999). Leg stiffness primarily depends on ankle stiffness during human hopping. *Journal of Biomechanics, 32,* 267-273.

Ferber, R., McClay Davis, I. & Williams III, D. S. (2003). Gender differences in lower extremity mechanics during running. *Clinical Biomechanics, 18*, 350-357.

Ferris, D. P. & Farley, C. T. (1997). Interaction of leg stiffness and surface stiffness during human hopping. *Journal of Applied Physiology, 82*, 15-22.

Ferris, D. P., Liang, K. & Farley, C. T. (1999). Runners adjust leg stiffness for their first step on a new running surface. *Journal of Biomechanics, 32*, 787-794.

Flynn, J. M., Holmes, J. D. & Andrews, D. M. (2004). The effect of localized leg muscle fatigue on tibial impact acceleration. *Clinical Biomechanics, 19*, 726-732.

Fong, D. T., Hong, Y. & Li, J. X. (2007). Cushioning and lateral stability functions of cloth sport shoes. *Sports Biomechanics, 6,* 407-417.

Gajdosik, R. L., Vander Linden, D. W., McNair, P. J., Williams, A. K. & Riggin, T. J. (2005). Effects of an eight-week stretching program on the passive-elastic properties and function of the calf muscles of older women. *Clinical Biomechanics, 20*, 973-983.

Gefen, A., Megido-Ravid, M. & Itzchak, Y. (2001). In vivo biomechanical behaviour of the human heel pad during the stance phase of gait. *Journal of Biomechanics, 34*, 1661-1665.

Gerritsen, K. G. M., van den Bogert, A. J. & Nigg, B. M. (1995). Direct dynamics simulation of the impact phase in heel-toe running. *Journal of Biomechanics, 28,* 661-668.

Granata, K. P., Padua, D.A. & Wilson, S.E. (2002). Gender differences in active musculoskeletal stiffness. Part II. Quantification of leg stiffness during functional hopping tasks. *Journal of Electromyography and Kinesiology, 12*, 127-135.

Gruber, K., Denoth, J., Stuessi, E. & Ruder, H. (1987). The wobbling mass model. In B. Jonsson (Ed.), Biomechanics X-B (pp. 1095-1099), Champaign, IL: Human Kinetics.

Gruber, K., Ruder, H., Denoth, J. & Schneider, K. (1998). A comparative study of impact dynamics: wobbling mass model versus rigid body models. *Journal of Biomechanics, 31*, 439-444.

Gunther, M. & Blickhan, R. (2002). Joint stiffness of the ankle and the knee in running. *Journal of Biomechanics, 35*, 1459-1474.

Hamill, J., Derrick, T. R. & Holt, K. G. (1995). Shock attenuation and stride frequency during running. *Human Movement Science, 14*, 45-60.

Hamill, J., Derrick, T. R. & McClay, I. (2000). Joint stiffness during running with different footfall patterns. *Proceedings of the Canadian Society for Biomechanics (CSB) conference*, Montreal, Canada.

Hennig, E. M., Milani, T. L. & Lafortune, M. A. (1993). Use of ground reaction force parameters in predicting peak tibial accelerations in running. *Journal of Applied Biomechanics, 9*, 306-314.

Hicks, A. L, Kent-Braun, J., & Ditor, D. S. (2001). Sex differences in human skeletal muscle fatigue. *Exercise and Sports Sciences Reviews, 29*, 109-12.

Hill, D. K. (1968). Tension due to interaction between the sliding filaments in resting striated muscle. The effect of stimulation. *Journal of Physiology, 199*, 637-684.

Holmes, A. M. & Andrews, D. M. (2006). The effect of leg muscle activation state and localized muscle fatigue on tibial response during impact. *Journal of Applied Biomechanics, 22*, 275-284.

Hreljac, A., Marshall, R. N. & Hume, P.A. (2000). Evaluation of lower extremity overuse injury potential in runners. *Medicine & Science in Sports & Exercise, 32*, 1635-1641.

Hunter, S. K. & Enoka, R. M. (2001). Sex differences in the fatigability of arm muscles depends on absolute force during isometric contractions. *Journal of Applied Physiology, 91*, 2686-2694.

Kellis, E. & Liassou, C. (2009). The effect of selective muscle fatigue on sagittal lower limb kinematics and muscle activity during level running. *Journal of Orthopaedic and Sports Physical Therapy*, 39, 210-220.

Kent-Braun, J. A., Ng, A. V., Doyle, J. W. & Towse, T. F. (2002). Human skeletal muscle responses vary with age and gender during fatigue due to incremental isometric exercise. *Journal of Applied Physiology, 93*, 1813-1823.

Keppel, G. (1982). Design and Analysis: A Researcher's Handbook (2nd ed.). New Jersey: Prentice-Hall Inc.

Kubo, K., Kanehisa, H., Kawakami, Y. & Fukunaga, T. (2000). Elastic properties of muscle-tendon complex in long-distance runners. *European Journal of Applied Physiology, 81*, 181-187.

Kuitenen, S., Komi, P. V. & Kyrolainen, H. (2002). Knee and ankle joint stiffness in sprint running. *Medicine & Science in Sports & Exercise, 34*, 166-173.

Lafortune, M. A. & Lake, M. J. (1995). Human pendulum approach to simulate and quantify locomotor impact loading. *Journal of Biomechanics, 28*, 1111-1114.

Lafortune, M. A., Henning, E. & Valiant, G. A. (1995). Tibial shock measured with bone and skin mounted transducers. *Journal of Biomechanics, 28*, 989-993.

Lafortune, M. A., Hennig, E. M. & Lake, M. J. (1996a). Dominant role of interface over knee angle for cushioning impact loading and regulating initial leg stiffness. *Journal of Biomechanics, 29*, 1523-1529.

Lafortune, M. A., Lake, M. J. & Hennig, E. M. (1996b). Differential shock transmission response of the human body to impact severity and lower limb posture. *Journal of Biomechanics, 29*, 1531-1537.

Lake, M. J. & Lafortune, M. A. (1998). Mechanical inputs related to perception of lower extremity impact loading severity. *Medicine & Science in Sports & Exercise, 30*, 136-143.

Latash, M. L. & Zatsiorsky, V. M. (1993). Joint stiffness: myth or reality? *Human Movement Science*, *12*, 653-692.

Ly, Q. H., Alaoui, A., Erlicher, S. & Baly, L. (2010). Towards a footwear design tool: Influence of shoe midsole properties and ground stiffness on the impact force during running. *Journal of Biomechanics*, *43*, 310-317.

MacLean, C. L., Davis, I. S. & Hamill, J. (2009). Influence of running shoe midsole composition and custom foot orthotic intervention on lower extremity dynamics during running. *Journal of Applied Biomechanics, 25*, 54-63.

McMahon, T. A. & Cheng, C. G. (1990). The mechanics of running: How does stiffness couple with speed? *Journal of Biomechanics*, *23*, S1, 65-78.

McMahon, T. A., Valiant, G. & Frederick, E. C. (1987). Groucho running. *Journal of Applied Physiology*, *62*, 2326-2337.

Mercer, J. A., Bates, B. T., Dufek, J. S. & Hreljac, A. (2003). Characteristics of shock attenuation during fatigued running. *Journal of Sports Sciences, 21*, 911-919.

Milliron, M. J. & Cavanagh, P. R. (1990). Sagittal plane kinematics of the lower extremity during distance running. In P. R. Cavanagh (Ed), *Biomechanics of Distance Running* (pp. 65-99). Champaign, IL: Human Kinetics.

Milner, C. E., Ferber, R., Pollard, C. D., Hamill, J. & Davis, I. S. (2006). Biomechanical factors associated with tibial stress fracture in female runners. *Medicine & Science in Sports & Exercise*, *38*, 323-328.

Mizrahi, J. & Susak, Z. (1982). Analysis of parameters affecting impact force attenuation during landing in human vertical free fall. *Engineering in Medicine*, *11*, 141-147.

Mizrahi, J., Verbitsky, O. & Isakov, E. (2000a). Fatigue-related loading imbalance on the shank in running: a possible factor in stress fractures. *Annals of Biomedical Engineering*, *28*, 463-369.

Mizrahi, J., Verbitsky, O., Isakov, E. & Daily, D. (2000b). Effect of fatigue on leg kinematics and impact acceleration in long distance running. *Human Movement Science, 19*, 139-151.

Munro, C. F., Miller, D. I. & Fuglevand, A. J. (1987). Ground reaction forces in running: A reexamination. *Journal of Biomechanics, 20*, 147-155.

Nichols, T. R. (1987). The regulation of muscle stiffness. *Medicine and Sport Science, 26*, 36-47.

Nigg, B. M. (1997). Impact forces in running. *Current Opinion in Orthopaedics, 8*, 43-47.

Nigg, B. M. & Liu, W. (1999). The effect of muscle stiffness and damping on simulated impact force peaks during running. *Journal of Biomechanics, 32*, 849-856

Nigg, B. M. & Wakeling, J. M. (2001). Impact forces and muscle tuning: a new paradigm. *Exercise & Sport Sciences Reviews, 29*, 37-41.

Pain, M.T.G. & Challis, J.H. (2001). The role of the heel pad and shank soft tissue during impacts: a further resolution of the paradox. *Journal of Biomechanics, 34*, 327-333.

Pain, M.T.G. & Challis, J. H. (2002). Soft tissue motion during impacts: their potential contributions to energy dissipation. *Journal of Applied Biomechanics, 18*, 231-242.

Potthast, W., Bruggemann, G. P., Lundberg, A. & Arndt, A. (2010). The influences of impact interface, muscle activity, and knee angle on impact forces and tibial and femoral accelerations occurring after external impacts. *Journal of Applied Biomechanics, 26*, 1-9.

Potvin, J. R. & Brown, S. H. M. (2005). An equation to calculate individual muscle contributions to joint stability. *Journal of Biomechanics, 38*, 973-980.

Radin, E. L., Paul, I. L. & Lowy, M. (1970). A comparison of the dynamic force transmitting properties of subchondral bone and articular cartilage. *The Journal of Bone and Joint Surgery, 52-A*, 444-455.

Reeves, N. P., Narendra, K. S. & Cholewicki, J. (2007). Spine stability: The six blind men and the elephant. *Clinical Biomechanics, 22*, 266-274.

Schinkel-Ivy, A., Burkhart, T. A. & Andrews, D. M. (2010, in press). Leg tissue mass composition affects tibial acceleration response following impact. *Journal of Applied Biomechanics*.

Schaffler, M. B. & Jepsen, K. J. (2000). Fatigue and repair in bone. *International Journal of Fatigue, 22*, 839-846.

Shorten, M. R. & Winslow, D. S. (1992). Spectral analysis of impact shock during running. *International Journal of Sport Biomechanics, 8*, 288-304.

Staron, R. S., Hagerman, F. C., Hikida, R. S., Murray, T. F., Hostler, D. P., Crill, M. T., Ragg, K. E. & Toma, K. (2000). Fiber type composition of the vastus lateralis muscle of young men and women. *Journal of Histochemistry and Cytochemistry, 48*, 623-629.

Stefanyshyn, D. J. & Nigg, B. M. (1998). Dynamic angular stiffness of the ankle joint during running and sprinting. *Journal of Applied Biomechanics, 14*, 292-299.

Taunton, J. E., Ryan, M. B., Clement, D. B., McKenzie, D. C., Lloyd-Smith, D. R. & Zumbo, B. D. (2002). A retrospective case-control analysis of 2002 running injuries. *British Journal of Sports Medicine, 36*, 95-101.

Teramoto, K., Dufek, J. S. & Mercer, J. A. (2006). The effects of local muscle fatigue on shock attenuation for female runners. *Proceedings of the American Society of Biomechanics (ASB) Conference*, Blacksburg, VA.

Valiant, G. A. (1990). Transmission and attenuation of heelstrike accelerations. In P. R. Cavanagh (Ed), *Biomechanics of Distance Running* (pp.). Champaign, IL: Human Kinetics.

Verbitsky, O., Mizrahi, J., Voloshin, A., Treiger, J. & Isakov, E. (1998). Shock transmission and fatigue in human running. *Journal of Biomechanics, 14,* 300-311.

Voloshin, A. S. (1988). Shock absorption during running and walking. *Journal of the American Podiatric Medicine Association, 78,* 295-299.

Voloshin, A. S., Mizrahi, J. Verbitsky, O. & Isakov, E. (1998). Dynamic loading on the human musculoskeletal system - effect of fatigue. *Clinical Biomechanics, 13,* 515-520.

Wake, H., Hashizume, H., Nishida, K., Inoue, H. & Nagayama, N. (2004). Biomechanical analysis of the mechanism of elbow fracture dislocations by compression force. *Journal of Orthopaedic Science, 9*, 44-50.

Wakeling, J. M., Liphardt, A. & Nigg, B. M. (2003). Muscle activity reduces soft-tissue resonance at heel-strike during walking. *Journal of Biomechanics, 36*, 1761-1769.

Wakeling, J. M. & Nigg, B. M. (2001a). Soft-tissue vibrations in the quadriceps measured with skin mounted transducers. *Journal of Biomechanics, 34*, 539-543.

Wakeling, J. M. & Nigg, B. M. (2001b). Modification of soft tissue vibrations in the leg by muscular activity. *Journal of Applied Physiology, 90*, 412-420.

Wakeling, J. M., von Tscharner, V., Nigg, B. M. & Stergiou, P. (2001). Muscle activity in the leg is tuned in response to ground reaction forces. *Journal of Applied Physiology, 91*, 1307-1317.

Whittle, M. W. (1999). Generation and attenuation of transient impulsive forces beneath the foot: a review. *Gait and Posture, 10*, 264-275.

Williams, K. R., Snow, R. & Agruss, C. (1991). Changes in distance running kinematics with fatigue. *Journal of Applied Biomechanics, 7,* 138-162.

Winter, D. A. (2005). Biomechanics and motor control of human movement, third ed. New Jersey: John Wiley & Sons.

Wolff, I., van Croonenborg, J. J., Kemper, H. C. G., Kostense, P. J. & Twisk, J. W. R. (1999). The effect of exercise training programs on bone mass: a meta-analysis of published controlled trials in pre- and postmenopausal women. *Osteoporosis International, 9,* 1-12.

Yue, Z. & Mester, J. (2001). A model analysis of internal loads, energetics, and effects of wobbling mass during the whole-body vibration. *Journal of Biomechanics, 35*, 639-647.

APPENDICES

APPENDIX A
General Health Questionnaire (GHQ)

Please answer the following questions.

1. Have you had any prior surgeries to your feet, legs, or back?

   [ ] YES [ ] NO

2. Do you suffer from constant soreness in your feet, legs, or lower back?

   [ ] YES [ ] NO

3. Have you had any recent trauma (spring, strain, major bruising, stitches, etc.) to your feet, legs, or lower back?

   [ ] YES [ ] NO

4. Do you suffer from arthritis or any congenital abnormalities concerning your feet, legs, or lower back?

   [ ] YES [ ] NO

5. Do you have any current health conditions that may exclude you from this study (i.e. high blood pressure, pregnancy)?

   [ ] YES [ ] NO

Please note that this questionnaire will be kept confidential. If you answered 'YES' to any of these questions, or if you do not wish to disclose this information, it is your right to not answer or withdraw from the study.

APPENDIX B

CONSENT TO PARTICIPATE IN RESEARCH

Title of Study: **The Effect of Ankle Joint Rotational Stiffness and Localized Muscle Fatigue on Tibial Response During Impact**

You are asked to participate in a research study conducted by **Nikki Nolte and Dr. David Andrews**, from the Department of Kinesiology at the University of Windsor. The results will be contributed to a master's thesis project. Funding for this work is provided by NSERC.

If you have any questions or concerns about the research, please feel to contact Nikki Nolte (519-253-3000 x2468; nolte@uwindsor.ca); or Dr. David Andrews, Associate Professor, Department of Kinesiology, University of Windsor (519-253-3000 x2451; Room 120 Human Kinetics Building; dandrews@uwindsor.ca).

PURPOSE OF THE STUDY

The primary purpose of the proposed project is to investigate the relationship between the ankle joint rotational stiffness (AJRS) and the shock attenuating ability of the leg upon impacts that are similar in magnitude to those seen during running.

PROCEDURES

If you volunteer to participate in this study, we would ask you to do the following things:

- To participate in one testing session, approximately 60-75 minutes in length, in the Biomechanics and Ergonomics Laboratory on the second floor in the Human Kinetics Building. Measurements of your weight and height will be recorded during the data collection session, as well as your age and weekly running mileage.
- Your foot length will also be taken using a flexible tape measure. General health questions will be asked to ensure that you have no leg or back injuries or pain that might put you at additional risk during the study.
- Impacts of a magnitude similar to those found during running will be applied to the heel of your right foot while you lie on your back on a human pendulum (a lightweight structure similar to a cot, suspended from the ceiling by cables). You will be secured to the apparatus with straps to prevent any unwanted movement during testing. Your foot will be impacted into a wall mounted force platform three times at four different ankle angles.
- Your knee and ankle angles will be monitored using an electrogoniometer that will be attached to the skin on the outer side of your knee joint and inner side of your ankle joint using double sided tape. You will be asked to hold the required ankle angle, which will be presented to you on a computer screen in your field of view, as you lie on the pendulum.
- An accelerometer will be placed just below your knee and will be held in place with an elastic strap to prevent any movement relative to the underlying skin.
- Surface electromyography electrodes will be applied to the following muscles: tibialis anterior, fibularis longus, medial gastrocnemius, lateral gastrocnemius, and soleus, to monitor each muscle's electrical activity. Electrodes and accompanying wires will be secured using a cloth-like adhesive bandage to prevent any unwanted wire movement.
- Your tibialis anterior will be fatigued. This will be done by having you dorsiflex against a provided resistance until you are fatigued. Additional impacts similar to before fatigue will be applied in the fatigued state.

POTENTIAL RISKS AND DISCOMFORTS

The impacts that you will experience in this study will be comparable to those encountered during running and have been studied in a number of similar projects in the past, without incident. You may experience some mild tenderness in the heel following the testing session; however, this tenderness generally does not last longer than a day. Should you require it, you may apply ice to the affected area to help alleviate any discomfort you may be experiencing. If further medical attention is required, you may contact the Green Shield Clinic at 519-253-3000 ext. 2426 or Student Health Services at 519-973-7002.

Minor redness of the skin may occur in the areas located underneath the accelerometer and EMG electrodes, which generally disappears within a day following the testing session.

POTENTIAL BENEFITS TO PARTICIPANTS AND/OR TO SOCIETY

You will learn about how a biomechanics research study is conducted in the Department of Kinesiology. This study considers the response of the leg to impacts similar to running, at a range of dorsiflexion angles. Data collected from this study may be used in future studies that model the leg during impacts similar to running.

PAYMENT FOR PARTICIPATION

You will receive a complimentary Kinesiology Research t-shirt as compensation for your participation.

CONFIDENTIALITY

Any information that is obtained in connection with this study and that can be identified with you will remain confidential and will be disclosed only with your permission.

All data from your trials will be number or letter coded so that a third party would be unable to identify individual results. Only the investigators working on the project will have access to the codes associated with your trials. Computer files will be kept on secured computers.

PARTICIPATION AND WITHDRAWAL

You can choose whether to be in this study or not. If you volunteer to be in this study, you may withdraw at any time without consequences of any kind. You may also refuse to answer any questions you don't want to answer and still remain in the study. The investigator may withdraw you from this research if circumstances arise which warrant doing so.

FEEDBACK OF THE RESULTS OF THIS STUDY TO THE PARTICIPANTS

Should you desire feedback regarding the results of the study, you may access a summary of the results on the University of Windsor Research Ethics Board (REB) website at:

Web address: www.uwindsor.ca/reb

Date when results are available: December 31, 2010

SUBSEQUENT USE OF DATA

These data may be used in subsequent studies.

Do you give consent for the subsequent use of the data from this study?

RIGHTS OF RESEARCH PARTICIPANTS

You may withdraw your consent at any time and discontinue participation without penalty. If you have questions regarding your rights as a research participant, contact: Research Ethics Coordinator, University of Windsor, Windsor, Ontario, N9B 3P4; Telephone: 519-253-3000, ext. 3948; e-mail: ethics@uwindsor.ca

SIGNATURE OF RESEARCH PARTICIPANT/LEGAL REPRESENTATIVE

I understand the information provided for the study **The Effect of Ankle Joint Rotational Stiffness and Localized Muscle Fatigue on Tibial Response During Impact** as described herein. My questions have been answered to my satisfaction, and I agree to participate in this study. I have been given a copy of this form.

____

Name of Participant

_____________________________________ __________________

Signature of Participant Date

SIGNATURE OF INVESTIGATOR

These are the terms under which I will conduct research.

____________________________________ ___________________

Signature of Investigator Date

APPENDIX C

Office of the Research Ethics Board

University of Windsor
thinking forward

Today's Date:	May 20, 2009
Principal Investigator:	Nikki Nolte
Department/School:	Kinesiology
REB Number:	09-090
Research Project Title:	The Effect of Ankle Joint Rotational Stiffness and Localized Muscle Fatigue on Tibial Response During Impact
Clearance Date:	May 15, 2009
Project End Date:	December 31, 2009
Progress Report Due:	
Final Report Due:	December 31, 2009

This is to inform you that the University of Windsor Research Ethics Board (REB), which is organized and operated according to the *Tri-Council Policy Statement* and the University of Windsor *Guidelines for Research Involving Human Subjects*, has granted approval to your research project on the date noted above. This approval is valid only until the Project End Date.

A Progress Report or Final Report is due by the date noted above. The REB may ask for monitoring information at some time during the project's approval period.

During the course of the research, no deviations from, or changes to, the protocol or consent form may be initiated without prior written approval from the REB. Minor change(s) in ongoing studies will be considered when submitted on the Request to Revise form.

Investigators must also report promptly to the REB:
a) changes increasing the risk to the participant(s) and/or affecting significantly the conduct of the study;
b) all adverse and unexpected experiences or events that are both serious and unexpected;
c) new information that may adversely affect the safety of the subjects or the conduct of the study.

Forms for submissions, notifications, or changes are available on the REB website: www.uwindsor.ca/reb. If your data is going to be used for another project, it is necessary to submit another application to the REB.

We wish you every success in your research.

Pierre Boulos, Ph.D.
Chair, Research Ethics Board

cc: Dr. David Andrews, Kinesiology
Mark Curran, Research Ethics Coordinator

This is an official document. Please retain the original in your files.

401 Sunset Avenue, Windsor, Ontario, Canada N9B 3P4 . tel: 519.253.3000 ext. 3948 . web: www.uwindsor.ca/reb

VITA AUCTORIS

NAME	Nikki Leigh Nolte
PLACE OF BIRTH	Windsor, Ontario
YEAR OF BIRTH	1985
EDUCATION	Sandwich Secondary School LaSalle, Ontario 1999-2003
	University of Windsor Windsor, Ontario 2003-2007 BHK (Honours Movement Science)
	University of Windsor Windsor, Ontario 2007-2010 MHK (Applied Human Performance)